

MICRORNA EXPRESSION IN REGULATORY T CELLS  
IN CHRONIC OBSTRUCTIVE PULMONARY DISEASE

---

A Dissertation  
Submitted to  
the Temple University Graduate Board

---

In Partial Fulfillment  
of the Requirements for the Degree  
DOCTOR OF PHILOSOPHY

---

by  
Wissam M. Chatila  
July 2015

Examining Committee Members:

Marc Monestier, MD, PhD, Department of Microbiology and Immunology  
Philip Cohen, MD, Department of Medicine, Section of Rheumatology  
Stefania Galluci, MD, Department of Microbiology and Immunology  
Thomas Rogers, PhD, Department of Pharmacology  
Alexander Tsygankov, PhD, Department of Microbiology and Immunology  
Bassel Sawaya, PhD, Fels Institute for Cancer Research and Molecular Biology

## ABSTRACT

COPD is characterized by an abnormal regulatory T cell (Treg) response with a shift towards a Th1 and Th17 cell responses. However, it is unclear if the function of Treg cells is impaired by smoking and in COPD. In addition, the miRNA profile of Treg cells in COPD is unknown and whether miRNA deregulation contributes to COPD immunopathogenesis. We set the objective to study Treg cell function isolated from peripheral blood of patients with COPD versus controls and to compare their miRNA profiles. We also were interested in exploring the function of some of the differentially expressed Treg cell miRNAs. We assessed the Treg cell function by observing their suppressive activity on autologous effector T cells and analyzed their miRNA expression initially by microarray analysis then conducted real time RT-PCR validation for selected miRNAs. *In Silico* target gene analysis for the validated miRNAs suggested that miR-199-5p is particularly relevant to Treg cell physiology so its function was investigated further using CCD-986Sk and MOLT-4 cells. We found no difference in Treg cell function between COPD and controls but we were able to identify 6 and 96 miRNAs that were differentially expressed in COPD versus control Treg cells. We confirmed that miR-199a-5p was repressed by approximately 4 fold in Treg cells of COPD patients compared to cells in healthy smokers. Importantly, miR-199a-5p had significant overrepresentation of its target genes in the Treg cell transcriptome, with many targets associated with the TGF- $\beta$  activation pathway. We also confirmed the function of miR-199a5p in an in-vitro loss-of-function cell model running TaqMan<sup>®</sup> arrays of the Human TGF- $\beta$  Pathway. These findings suggest that the abnormal repression of miR-199a-5p in patients with COPD compared to unaffected smokers may be involved in modulating the adaptive immune balance in favor of a Th1 and Th17 response.

I dedicate this work to my wife  
Mona and the rest of my family.

## ACKNOWLEDGMENT

First, I would like to express with humbleness my gratitude to my wife Mona who has endured for many years and supported me with astounding patience and sacrifice. Second, I offer my appreciation to the members of the advisory committee for their guidance and devoted commitment to my project and scholarly activities. I'm in debt for their extremely helpful advices and constructive criticisms throughout the past five years with special appreciation to Dr. Rogers for his remarkable mentorship. Dr. Rogers' great insight, understanding, patience, and intricate knowledge were key to the success of this project. I am also grateful to many other individuals for helping me to complete this work as they contributed in different ways: Drs. Ezoubi and Chaudhry worked hard to learn some of the techniques and volunteered valuable time to generate part of the T cell functional data; JK Chang and Bill Cornwell helped with several technical aspects of particular experiments; Dr. Moldover spent long hours analyzing the bioinformatics data; and Dr. Hancock who graciously opened the door of his laboratory and introduced me to Dr. Akimova who taught me techniques to study the regulatory T cells. Finally, I could not have devoted myself to this career were it not for the exceptional support of Dr. Jerry Criner, chairman of the Division of Pulmonary and Critical Care Medicine.

## TABLE OF CONTENTS

	Page
ABSTRACT	iii
ACKNOWLEDGMENTS	v
LIST OF FIGURES	ix
LIST OF TABLES	xi
CHAPTER	
1. INTRODUCTION	1
Inflammation in COPD: Triggers and Perpetuating Factors	1
Cigarette Smoke, Particulate Material, and Oxidants	1
Disruption of Lung Maintenance and Premature Lung Aging	4
COPD, and Autoimmune Disease	5
The Adaptive Immune Response in COPD	6
B cells	8
CD8+ and CD4+ Effector Cells (Th1, Th2, and Th17)	9
Regulatory CD4+T (Treg) Cells in COPD	11
Subsets of Treg Cells	13
Regulation of Treg Cells	16
MicroRNAs in Treg Cells	20
MicroRNAs in COPD	30
Significance	35
Aims	36

	Page
2. METHODS AND MATERIALS	38
Reagents and Drugs	38
Kits	40
Subject Selection	40
Tissue Immunohistochemical Staining	42
Quantitative Analysis of Lung Tissue CD4+ and FoxP3+ Cells	43
Isolation and Purification of Peripheral Blood Mononuclear Cells (PBMCs) and CD4+ Cells	44
Isolation of Peripheral CD4+ Cells	45
Isolation of Peripheral CD4+CD25- Teff and CD4+CD25+ Treg Cells	46
Treg Suppression Assay	49
Flow Cytometry for Treg Suppression Assay	53
Isolating and Analyzing the CD4+CD25+CD127-CD49- Treg Cells	53
RNA Purification	57
miRNA Microarray Analysis and TaqMan <sup>®</sup> miRNA Gene Expression	59
<i>In Silico</i> Analysis: Identifying miRNA targets in the Treg Cell Transcriptome and Analyzing their Potential Function	62
Validating the Results of the <i>In Silico</i> Functional Analysis in Cell Lines	62
CCD-986Sk Cell Culture, LNA transfection, and Treatment with TGF- $\beta$ 1	63
MOLT-4 Cell Culture, miR-Mimic Transfection, and Treatment with EGCG	65
Western Blot Analysis	66
Preparation of Solutions and Reagents	67

Taqman <sup>®</sup> Single Gene RT-PCR and Taqman <sup>®</sup> Array Analysis	68
Bioinformatics and Statistical Analysis	73
3. RESULTS	74
FoxP3 <sup>+</sup> T Cells are Increased in the Lungs of Patients with COPD and Correlate with Disease Severity	74
Non-Specific Suppressive Function of Peripheral CD4 <sup>+</sup> CD25 <sup>+</sup> Treg Cells is not Impaired in COPD	81
Cigarette Smoke Alters the Treg Cell Function in COPD but not in Healthy Controls	84
Improving Treg Cell Purity	86
Extracting RNA for miRNA Analysis	87
COPD Affects Expression of miRNA in Peripheral Treg Cells but not Teff Cells	87
miR-199a-5p and HIF-1 $\alpha$ Are Downregulated in COPD Treg Cells	94
<i>In Silico</i> Analysis Identifies the TGF- $\beta$ Pathway and Putative Target Genes of miR-199a-5p	100
Knockdown of miR-199a-5p Upregulates the Expression of Some of Its Predicted Target Genes	107
Overexpressing miR-199a-5p Downregulates BMP4 Gene Expression in MOLT-4 Cells	110
4. DISCUSSION	113
REFERENCE CITED	133
APPENDIX	169

## LIST OF FIGURES

Figure	Page
1. Treg Cell Differentiation	19
2. miRNA Biogenesis	21
3. miRNAs Regulating the Differentiation of CD4+ Cell Subsets	23
4. miRNA-mediated Regulation of Treg Cell Homeostasis and Function	24
5. Role of miR-199a-5p in Regulating the UPR	34
6. Protocol for Isolating CD4+ Cells and Treg Cells for the Suppression Assay	48
7. Plate Set Up for Treg Cell Suppression Assay Using CFSE Dilution	51
8. Histograms of Treg Cell Suppression Assay	52
9. Double Staining of PBMCs and CD4+ Cells	54
10. The TaqMan <sup>®</sup> TGF- $\beta$ pathway Array Plate	72
11. FoxP3 Immunohistochemical Staining of Lung Tissue	77
12. FoxP3+ Cells Density in Small Airways and BALTs	79
13. Teff Cell Proliferation Graphs in our Three Groups of Subjects	83
14. Treg Cell Suppression with Exposure to CSE	85
15. Clustering Based on Principal Component Analysis of the miRNome	89
16. Differential Expression of Treg-Teff Cell miRNAs	90
17. Differential miRNA Expression in Treg Cells by Real Time RT-PCR	96
18. HIF-1 $\alpha$ Expression	99
19. TGF- $\beta$ Signaling Network	104
20. TGF- $\beta$ and PPAR $\alpha$ Signaling Pathways	105
21. Growing the Signaling Network	106

22. Transfection of CCD-986Sk Cells with LNA	108
23. Effects of miR-199a-5p Inhibition on TGF- $\beta$ Pathway in CCD-986Sk Cells	109
24. Effect of miR-199a-5p Overexpression on BMP4 in MOLT-4 Cells	112
25. A Schematic of the Proposed Function of miR-199a-5p in Treg Cells	130

## LIST OF TABLES

Table	Page
1. Taqman <sup>®</sup> miRNA Primers	61
2. Characteristics of Subjects Having Immunohistochemical Analysis of FoxP3+ Cells	76
3. Correlations of Foxp3+ and CD4+ Cells with Disease Severity	80
4. Demographics of Subjects Having Functional Treg Cell Assays	82
5. Differential Expression of miRNAs in Treg Cells in the 3 Subject Groups	91
6. Demographics of Subjects Having miRNA Validation (n=12/group)	97
7. Treg Cell Genes That Are Predicted miR-199a-5p Targets	101
8. Top Networks of miR-199a-5p Targets	102
9. Top Canonical Pathways Associated with Predicted Targets of miR-199a-5p	103
10. Select miRNAs That Are Involved in COPD	122

# CHAPTER 1

## INTRODUCTION

### **Inflammation in COPD: Triggers and Perpetuating Factors**

COPD is a heterogeneous and progressive disease characterized by local and systemic inflammation(1). Exposure to smoking and toxic particles induces a neutrophilic inflammatory response but with progression to airflow obstruction and lung destruction the inflammatory response fails to resolve(2). The characteristic pathological changes in COPD are then accompanied by increased numbers of macrophages and other components of the adaptive immune response, including increased formation of lymphoid follicles(2;3;4). Recently, several pathogenic mechanisms have been proposed to explain the development and progression of COPD(5;6). These mechanisms involve pathobiological processes related to abnormal oxidative stress and unfolded protein responses that eventually maintain the chronic inflammatory state and possibly contribute to deregulation of the lung maintenance programs. The end result of these interacting and overlapping responses eventually lead to the characteristic airway remodeling and lung destruction observed in COPD(7).

#### *Cigarette Smoke, Particulate Material, and Oxidants*

COPD is a smoking-related disease but its progressive nature and the presence of low-grade inflammation in ex-smokers likely reflects an ongoing

injury, which is poorly understood and may not be caused solely by smoking(8). Smoking has significant immunomodulatory effects both locally and peripherally(9;10), on innate and adaptive immune responses(9;11;12), and on cellular and humoral immune function(13). Smoking components activate aryl hydrocarbon receptors, which are ligand-activated transcription factor involved in reactivation of xenotoxic metabolism(14). In animal models activation of the aryl hydrocarbon receptor on both CD4+ and CD8+ cells leads to suppression of the cytotoxic T cell response(15) and various cigarette components have been shown to reduce T cell proliferation and activation(16;17;18). Many of the cigarette components were found to affect IL-2 production and its dependent activation thus causing a reduction of CD25 expression in both peripheral CD4+ and CD8+ cells(17;18;19;20). Suppression of IL-2 production in T cells by smoking was also reported in lung-derived T cells(21).

Occupational exposures are also well known risk factors for COPD. In fact, chronic bronchitis has been reported in 4-22% of never smokers(22;23). Indoor and outdoor air pollution from organic and inorganic dust, chemical agents, and fumes from biomass fuel combustion coupled with poor ventilation could be harmful and have been associated with decrements of lung function and COPD(24;25;26). The NHANES III survey done in the U.S. population aged 30-75 years estimated the fraction of work-related COPD to be approximately 19%, and 31% among never-smokers(27). Similar to cigarette smoking, inhaled pollutants from biomass fuels cause lung inflammation and destruction with some degree of fibrosis, resulting in two well-defined COPD phenotypes, chronic

bronchitis and emphysema. Smoke, whether from cigarettes, biomass fuel combustion, or other pollutants, affects many pulmonary cellular components via repeated oxidative stress. Oxidative stress is associated with lung inflammation and is one of the major factors contributing to the amplification of inflammation in COPD and to resistance to the anti-inflammatory effects of corticosteroids(28). There is abundant evidence that oxidative stress is increased in the lungs of patients with COPD. Studies demonstrated increased concentrations of hydrogen peroxide, 8-isoprostane, and ethane in exhaled breath(29;30;31) and increased lipid peroxidation in lung tissue(32). Oxidative stress is generated also by positive feedback loops from activated neutrophils and macrophages, providing a mechanism which accounts for a sustained and unrelenting presence of an increased oxidative stress in patient with COPD even after quitting smoking(30). Taking in consideration the complexity and heterogeneity of COPD, it is likely that the same feedback loops may be involved in other processes as well including enhanced senescence/aging and tissue destruction with alveolar cell apoptosis and excessive extracellular matrix proteolysis(33). Consequently, alveolar tissue damage further amplifies the inflammatory processes potentially leading to autoimmunity and self-perpetuating stimuli for enhanced influx of inflammatory cells in the damaged COPD lung(34).

### *Disruption of Lung Maintenance and Premature Lung Aging*

A growing body of evidence indicates that certain aging mechanisms may have a critical role in the pathogenesis of COPD(35). Aging is characterized by a decline in structure and function due to a gradual loss of homeostatic mechanisms responsible for the maintenance and regeneration of adult tissues. At a cellular level, aging is associated with senescence, stem cell exhaustion, and apoptosis, all could be potentially driven by a stress-deregulated inflammatory response and oxidative response(36;37). In the aging lungs, there are emphysema-like changes and gradual subtraction of airways but this attrition is much steeper in COPD(38). The observed loss of lung tissue with aging and COPD has been attributed to increased cellular senescence and apoptosis(39;40). Muller et al. have found that the proliferation rate and number of population doublings of parenchymal lung fibroblasts from patients with emphysema are reduced suggesting that some disruption in the lung maintenance program exist in emphysema(41). In addition, findings of increased cellular senescence markers in epithelial and endothelial cells in emphysema lungs also suggest that the loss of lung tissue is in part related to senescence(40;42). Importantly, both oxidative stress and inflammation have a close relationship with cellular senescence. Oxidative stress has been linked to enhanced telomere shortening(43) and senescent cells demonstrate activation of NF- $\kappa$ B and release of numerous inflammatory cytokines resulting in enhanced inflammatory state which is thought to be part of the “inflammaging” processes(44;45).

### *COPD, an Autoimmune Disease*

Many of the classic features of autoimmune diseases have been reported in patients with COPD. Several studies have confirmed the presence of various IgG autoantibodies with avidities for lung antigens in patients with COPD. Fegahli-Bostwick et al. demonstrated the presence of pulmonary anti-epithelial cell IgG antibodies and intrapulmonary immune complexes in their COPD patients. In addition, they observed evidence of increased cytotoxicity of pulmonary epithelial cells by allogeneic mononuclear cells after incubation with COPD plasmas, which is suggestive of autoimmune/humoral induced lung injury(46). In support of the autoimmune paradigm Nunez et al. also found that anti-tissue antibody titers were associated with severity of airflow limitation and gas exchange impairment after adjusting for potential confounders(47). Although prior reports don't imply direct causality between the presence of the autoantibodies and COPD but their potential pathogenic relevance was tested in a study that injected rats with human umbilical vein endothelial cells(48). Antibodies against the endothelial cells were produced in the injected rats and emphysema developed in association with apoptosis of alveolar cells and accumulation of CD4+ T cells in their lungs(48). This study also showed that the antibodies against human endothelial cells in these rats induced endothelial cell apoptosis in vitro and caused emphysema when transferred to mice. Finally, the transfer of T cells isolated from the spleens of rats that were immunized with human endothelial cells also caused emphysema in immunocompetent rats(48). The current discoveries of anti-elastin(49), pulmonary anti-epithelial(46) and

anti-endothelial antibodies(50) however have not led so far to the identities of the antigens that induce these aforementioned antibodies. Moreover, several mechanisms are likely to be involved in generating some of these autoantigens. Exposure to infectious or environmental insults, tissue trauma, oxidative stress, or cell death could release sequestered antigens, modify proteins(51), damage mitochondria, and release DNA from apoptotic cells that result in neo/autoantigens. The adaptive immune system can recognize these products as foreign antigens and trigger autoimmune responses that are self-perpetuating since the immunogenic neoantigens are continually renewed despite smoking cessation and removal of the inciting injury.

### **The Adaptive Immune Response in COPD**

Recurrent exposure to noxious agents, including smoking and infections, activate the epithelial cells and the innate response with influx of neutrophils and macrophages producing inflammatory mediators such as TNF $\alpha$ , IL-1b, GM-CSF, and IL-8(52), which in turn trigger the adaptive immune response after repeated exposures(53). The association between the inflammatory reaction, involving the adaptive immune response, and COPD has been established decades ago but more recent evidence demonstrated that the progression of COPD is associated with increasing infiltration of the airways by CD8 cells, B cells, and lymphoid follicles(54). The role of the adaptive immune response is further supported in smoking animal models that demonstrated similar increase in inflammatory

cellular organization into lymphoid follicles that accompanied the development of emphysema(3). The increase in lymphocytes and their organization into follicles are consistent with increased immune surveillance of mucosal surfaces in the airways of patients with COPD leading the way to close collaboration among the epithelium, antigen-presenting cells, and lymphoid follicles to facilitate antigen presentation and modulation of the adaptive immune response. The cascade of events that follows this collaboration to cause lung tissue remodeling is not fully elucidated but transgenic animal models have shown that overexpression of particular cytokines and proteinases may be sufficient to cause emphysema and peribronchiolar fibrosis(55). Experiments in transgenic mice have shown that overexpression of IL-13 results in emphysema with mucus hyperplasia and inflammation while inducing multiple metalloproteinases and cathepsins(55). Taraseviciene-Stewart et al showed that humoral and CD4+ cell dependent mechanisms are alone sufficient to cause alveolar cell apoptosis and activation of matrix metalloproteinases (MMP) leading to the development of centrilobular emphysema(48). Nonetheless, and keeping in mind the limitations of studying animal models, the same cytokines may not be always identified in humans as is the case for IL-13(56). Di Stefano et al colleagues found instead an increased number of IFN- $\gamma$  producing cells in bronchial biopsies from COPD patients compared with controls(57). They also demonstrated a significant association between the presence of IFN- $\gamma$  expressing cells with the degree of airflow limitation in smokers(57).

## B Cells

Several groups have demonstrated the presence of B-cell aggregates in the lungs of COPD patients(3;54;58). Peribronchial lymphoid follicles are tertiary lymphoid organs with specialized structures that form under chronic inflammatory processes and are composed of defined B- and T-cell areas, and follicular dendritic cells with development of lymphatics and high endothelial venules. In adults these lymphoid follicles are absent in healthy individuals but they are induced in pathologic conditions such as COPD. The neogenesis of the follicles involves activation of lymphocytes to express the cytokine lymphotoxin  $\alpha 1\beta 2$  on their membrane. Signaling through the lymphotoxin on stromal cells triggers the release of chemokines that orchestrate lymphocyte homing and compartmentalization in the follicles. CCL19 and CC21 regulate homing of CCR7+ naive T cells and mature dendritic cells, while CXCL13 attracts CXCR5+ B cells into the lymphoid follicles. Additionally, CXCL13 induces lymphotoxin  $\alpha 1\beta 2$  resulting in a positive feedback loop(59). In a recent study, Litsiou et al. demonstrated that B cells were the main source of CXCL13 in COPD lungs and that lymphoid follicle formation are driven by the CXCL13-dependent mechanism involving the toll-like receptor and lymphotoxin receptor signaling. The same mechanism was shown to be induced by cigarette smoke extract, H<sub>2</sub>O<sub>2</sub>, and LPS exposure(60). In addition, Bracke et al. showed that both CXCL13 mRNA and protein levels were increased in lungs of cigarette smoke-exposed mice and patients with COPD, and administration of anti-CXCL13 antibodies completely prevented the cigarette smoke-induced formation of pulmonary lymphoid follicles

in mice(4). Intriguingly, absence of tertiary lymphoid organs attenuated destruction of alveolar walls and inflammation in bronchoalveolar lavage (BAL) but did not affect airway wall remodeling.

So far the role of the tertiary lymphoid follicles in COPD and their impact on disease progression remain controversial. It is possible that lymphoid follicle formation is associated with the development of protective responses during infections or may be detrimental if directed against lung auto- and neoantigens with the development of pathogenic autoantibodies and persistent inflammation. Hogg et al demonstrated that the number of lymphoid follicles present in small airways is increased in patients with severe COPD when compared with those with mild COPD or healthy control subjects(54). Van der Strate et al. reported also the same observation, correlating lymphoid B follicles and the extent of alveolar destruction(3). The investigators also extended their observation to document a clonal process in all lymphoid follicles thus suggesting that antigen-specific responses may be involved in lymphoid neogenesis(3).

#### *CD8+ and CD4+ Effector Cells (Th1, Th2, and Th17)*

Cigarette smoke-driven neoantigens, bacterial or viral agents, and breakdown products from extracellular matrix can modulate the adaptive immune responses in the lungs of COPD patients with the participation of CD4+ and CD8+ T cells(34;54;61). The number of pulmonary CD8+ cells increases substantially with progression of COPD(61) and when activated they release proteolytic enzymes, e.g. perforin and granzymes, which cause apoptosis and

necrosis thus contributing to the lung destruction in COPD(62). Furthermore, phagocytosis of apoptotic cells by alveolar macrophages is deficient in COPD and this can increase the amount of antigenic material, which may contribute to the autoimmune response.

CD4+ T cells are also increased in the airways and parenchyma of smokers with COPD(54). The lung CD4+ cells are activated and are oligoclonal suggesting that their accumulation is the result of stimulation by antigens distributed throughout the lung(63). Initially, the CD4+ cell phenotype was reported to be Th1 because these cells expressed STAT4 and IFN- $\gamma$  and they correlated with disease severity(57). The effector functions of the Th1 cell are mediated by their characteristic cytokines (IL-1, IL6, INF- $\gamma$ )(64;65), promoting transendothelial migration of inflammatory cells to the site of injury; however, a Th1 response is not always observed in COPD and it does not explain all the pathologic changes(55). More recently, and with discovery of other T cell phenotypes, interest revolved around studying Th17 cells because of their inflammatory functional activities. These cells were designated Th17 and are characterized by expression of IL-18 and IL-23 receptors (cytokines typically produced by monocytes, macrophages, and dendritic cells) and by production of IL-17A and IL-17F(66;67) to regulate tissue inflammation. Th17 cells are believed to be involved in mediating host defensive mechanisms to extracellular bacterial infections and they have been implicated in the pathogenesis of many autoimmune diseases(67). Of interest, Th17 cytokines have been reported to be increased in COPD lung(68;69); however, their involvement may be more related

to smoking per se rather than to COPD because the increase in IL-17A+ cells was also observed in control smokers with normal lung function and in the asthmatic lungs(70). In support of the role of Th17 in COPD, Chen et al observed in a murine model that cigarette smoke augmented in vitro and in vivo Th17 cell differentiation via the aryl hydrocarbon receptor(71). The effector functions of Th17 are also mediated via interactions between their cytokines and other chemokines/chemokine receptors(CXCL10, CXCL9, CXCR3) to upregulate the production of matrix metalloproteinase-12 (MMP-12) in macrophages thereby facilitating lung destruction(71;72;73).

### **Regulatory CD4+ T (Treg) Cells in COPD**

Regulatory T cells have a significant role in autoimmune disorders, transplant rejection, allergic diseases, and asthma(74;75). In the Th2 model of asthma, Treg cells may interfere with the development of asthma at different levels, such as allergic sensitization, airway remodeling, and airway hyperresponsiveness(74). The role of Treg cells in COPD is starting to be characterized(49;76;77;78) but it is yet to be well defined or agreed upon. Three studies that examined the Treg cells in BAL fluid showed a decrease of these cells in COPD compared to smokers and nonsmokers(77;78;79), but the results are inconsistent in lung tissue. Plumb et al. showed increased Treg cells in the lungs of COPD patients(80) whereas Lee et al. reported the opposite(49) and Isajevs et al reported that the Treg cells are decreased in small airways and are increased in large airways(81). Similarly, studies that addressed Treg cell

function in COPD cells reported conflicting results(49;82;83);Lee et al. reported no difference in peripheral Treg cell function between COPD and controls(49), Tan et al. found impaired Treg suppression in COPD(83), whereas Kalathil et al. found the COPD Treg cells to be excessively suppressive(82). Of note, the suppressive assays in the three aforementioned studies were performed using different stimulation protocols on autologous effector T cells. The discrepancy in the results may be related to methodological differences, dysfunction in Teff cells rather than Treg cells, or due to underlying demographic and/or clinical variables. Therefore, it is difficult to conclude if Treg cell function in COPD is overly or inadequately suppressive causing recurrent infection versus persistent and uncontrolled lung inflammation based on the available human data. In addition, the aforementioned functional studies were done on peripheral Treg cells and may not reflect the lung tissue Treg cell phenotype and function.

Functional experiments in mice models, however, favor the concept of a defective tissue Treg cell response rather than having an overactive response that lead to COPD(84;85). Wang et al. reported a marked shift of the Th17/Treg balance that occurred in mice with chronic but not subacute cigarette smoke exposure. The investigators observed a significant increase of Th17 cells that was accompanied with a significant decrease in Treg cells in lung tissue (85).Interestingly, the same trend was observed in peripheral blood CD4+ cells(85). This paradigm of an attenuated Treg cell generation/function seems to be in agreement with that of other autoimmune diseases(86;87;88;89) and may also explain the increase in bronchus-associated lymphoid tissue (BALT)

because lung homing of functional Treg cells is essential in controlling BALT formation(84). Several studies reported that BALTs have an important role in the development of airflow limitation and are associated with severity of disease(3;4;60;90). Future studies will be needed to confirm if a similar Treg cell dysfunction can explain the increased BALTs in COPD patients.

### Subsets of Treg Cells

Regulatory T cells are neither homogeneous nor static in nature, having multiple possible origins and functional profiles(91) but the nomenclature and defining markers of these profiles remain non-standardized. The FoxP3+ transcription factor was assumed to be a master regulator and a specific marker for the so-called natural Treg thymically-derived (nTreg) cells but recent evidence proved otherwise. It is now believed that FoxP3+ CD4+ cells are composed of two distinct subsets of Treg cells originating from either the thymus (tTreg or nTreg) or the periphery (pTreg) that are derived from mature CD4+ cells. The nTreg cells, however, are the major Treg population, which appear sufficient for the control of systemic and tissue-specific autoimmunity(91) while the pTreg cells may broaden the antigen specificity of Treg cells and promote immune tolerance to environmental antigens(92).

In addition to distinctions based on the location of induction (thymic versus peripheral), Treg cells have been divided into functional subsets(93). These include: 1. “central” Treg cell population, which has circulatory characteristics that are similar to naive conventional CD4+ T cells; 2. several “effector” Treg cell

populations, which have enhanced function and signs of recent antigen encounter; and 3. the polarized “tissue-resident” Treg cell populations, which are present in most non-lymphoid organs. The central Treg cells constitute the majority of Treg cells in the circulation and secondary lymphoid organs, and have been referred to as “resting or naïve” Treg cells in some studies. These central Treg cells share phenotypic features with naive and memory conventional T cells, yet they are not quiescent, with baseline suppressive function, being CD62L<sup>hi</sup>CCR7<sup>+</sup> or CD45RA<sup>hi</sup>CD25<sup>low</sup> T cells, and most often collected from the secondary lymphoid organs. In contrast, the effector Treg cells make up a minor fraction of the Treg population in the circulation and secondary lymphoid organs and are referred to as “activated” Treg cells in some studies. This population shares phenotypic features with activated conventional T cells and is defined as CD62L<sup>low</sup>CCR7<sup>low</sup>CD44<sup>hi</sup>KLRG1<sup>+</sup>CD103<sup>+</sup> or CD45RA<sup>low</sup>CD25<sup>hi</sup>, depending on the study. These effector Treg cells likely have encountered antigens more recently than central Treg cells and show enhanced migration through non-lymphoid tissues. Last, the tissue-resident Treg cells are those Treg cells that have long-term residence in non-lymphoid tissues, in contrast to the short-term migration through non-lymphoid tissues observed by effector Treg cells. Potentially, each organ might harbor a distinct population of tissue-resident Treg cells such as the adipose tissue Treg cells that are marked by the expression of PPAR- $\gamma$ (93).

The role of Treg cell subpopulations in containing the inflammatory response in COPD was only addressed in one study(78). Prior studies that

investigated peripheral blood Treg cells in COPD did not reveal differences between COPD patients and controls, smokers and nonsmokers, but all these studies did not examine the various Treg cell subpopulations(76;77;81). More recently, however, Hou et al separated the CD4+ Foxp3+ cells in peripheral blood into three different subsets: resting Treg cells (CD25++CD45RA+), activated Treg cells (CD25+++CD45RA-), and a pro-inflammatory (IL-17 and IFN- $\gamma$ ) secreting Treg subset (CD25++CD45RA-)(78). In this study, an imbalance between the subpopulations of Treg cells was found in COPD versus smokers without COPD, with a decrease in both resting and activated Treg cells (the suppressive phenotypes) and an increase in the cytokine-secreting Treg cells (the pro-inflammatory phenotype). Interestingly, the imbalance in Treg cell populations, which favors the pro-inflammatory Treg cell in COPD, was also found in local Treg cells (obtained from BAL) and was significantly associated with severity of airflow obstruction and enhanced CD8 cell activation(78). Therefore, and in view of the perpetual antigenic milieu found in COPD (as discussed in previous sections, possibly from smoking and its degradation byproducts, latent viral pathogens, and repeated exacerbations), it seems that local and systemic immune activation prevail in conjunction with Treg cell disturbances. For now, it is unclear if the immune activation is caused by the Treg dysfunction or if both are driven by overlapping mechanisms that underlie the persistent inflammation in COPD.

### Regulation of Treg Cells

Regulatory T cell population has a high turnover and fine sensitivity to a range of signals from its environment. Their lineage commitment is controlled by genetic and epigenetic imprinting and is modulated by milieu-driven transcriptional programs(93). These properties allow for the rapid adjustment in Treg cell number, location, and function that are required for a balanced and effective immune response. In fact, the capacity of Treg cells for immune suppression depends on the maintenance of a stable population size which is achieved by having a high basal proliferation rate (50% undergo division every 10 days in humans and mice) which is offset by a high apoptosis rate(94;95). The mechanism for the Treg cells high proliferation rate is currently unknown and may be driven by TCR-self reactivity or by the FoxP3 transcriptional program, their key lineage-specifying factor. On the other hand, more is known about mechanisms involved in their apoptosis and that these mechanisms are different in the various Treg cell subsets. Apoptosis of the central Treg cells (circulating and in lymphoid organ) was reported to be induced by FoxP3-dependent phosphorylation of BCL-2 interacting mediator (BIM)(96) which can be negated by IL-2. IL-2 upregulates the pro-survival protein myeloid leukemia cell differentiation 1 (MCL1) (94) which in turns antagonizes the pro-apoptotic function of BIM. The effector Treg cell population, however, seems to be restricted by a different factor, B lymphocyte-induced maturation protein(BLIMP-1), directing a transcriptional program that is required for optimal IL-10 and ICOS expression and causes the downregulation of the pro-survival protein

BCL-2(97;98). As for tissue-resident Treg cells, they may have additional distinguishing homeostatic circuitry that are tissue-specific and are driven by host-environment interaction(94;95;99).

Regulatory T cells play an important role in the adaptive immune response becoming specialized for different environmental contexts and tailored not only by their homeostatic controls but also by their function and diversity. Among the pivotal functions of Treg cells is the control of immune tolerance as demonstrated by constitutive or inducible depletion of FoxP3(91). While expression of FoxP3 is required to maintain the Treg cell program and suppressive function in the periphery, recent evidence suggests that it is neither a distinct marker of Treg cells nor a sole regulator of their function. Expression of FoxP3 does not define the transcriptional landscape of Treg cells, rather, several other transcriptional factors and feedback loops cooperate with FoxP3 to stabilize expression of the Treg cell signature(100;101)which is characterized by IL2RA (IL-2R  $\alpha$ -chain, also known as CD25), CTLA4 (cytotoxic T lymphocyte antigen 4), GITR (known as tumor necrosis factor receptor superfamily member 18, TNFRSF18), and ICOS (inducible T cell co-stimulator). These feedback loops reinforce the expression of FoxP3 and its cofactors, such as GATA3 (GATA-binding 3), RUNX1 (runt-related transcription factor 1) and STAT3 (signal transducer and activator of transcription 3), and ensure that the Treg cell population is maintained in a stable differentiated state(102); however, there are modifications of this state that give rise to Treg cell heterogeneity and several different transcription factors seem to be capable of driving further diversification of Treg cell function on the basis of

tissue localization and inflammatory milieu. This heterogeneity of effector Treg cells is also linked to altered homing and homeostatic properties via upregulation of key transcription factors and alterations in migration pattern (Figure 1). Interferon regulatory factor 4 (IRF-4) was found to have a non-redundant role in the differentiation of central Treg cells to effector Treg cells(97). Direct TCR ligation with CD28 +/- IL-2 co-stimulation induces the upregulation of expression IRF4, which in turn orchestrates the differentiation of central Treg cells into effector Treg cells(97). The effector Treg cell differentiation involves also BACH-2 (BTB and CNC homologue 2) downregulation and BLIMP-1 upregulation. Eventually other unknown stimuli induce the polarization of Treg cells by upregulating transcription factors that can act together with FoxP3 to induce the expression of chemokine and homing receptors that mediate their recruitment to specific tissues (or sites of inflammation) where specific mediators become involved in their homeostasis or suppressive function (Figure 1).

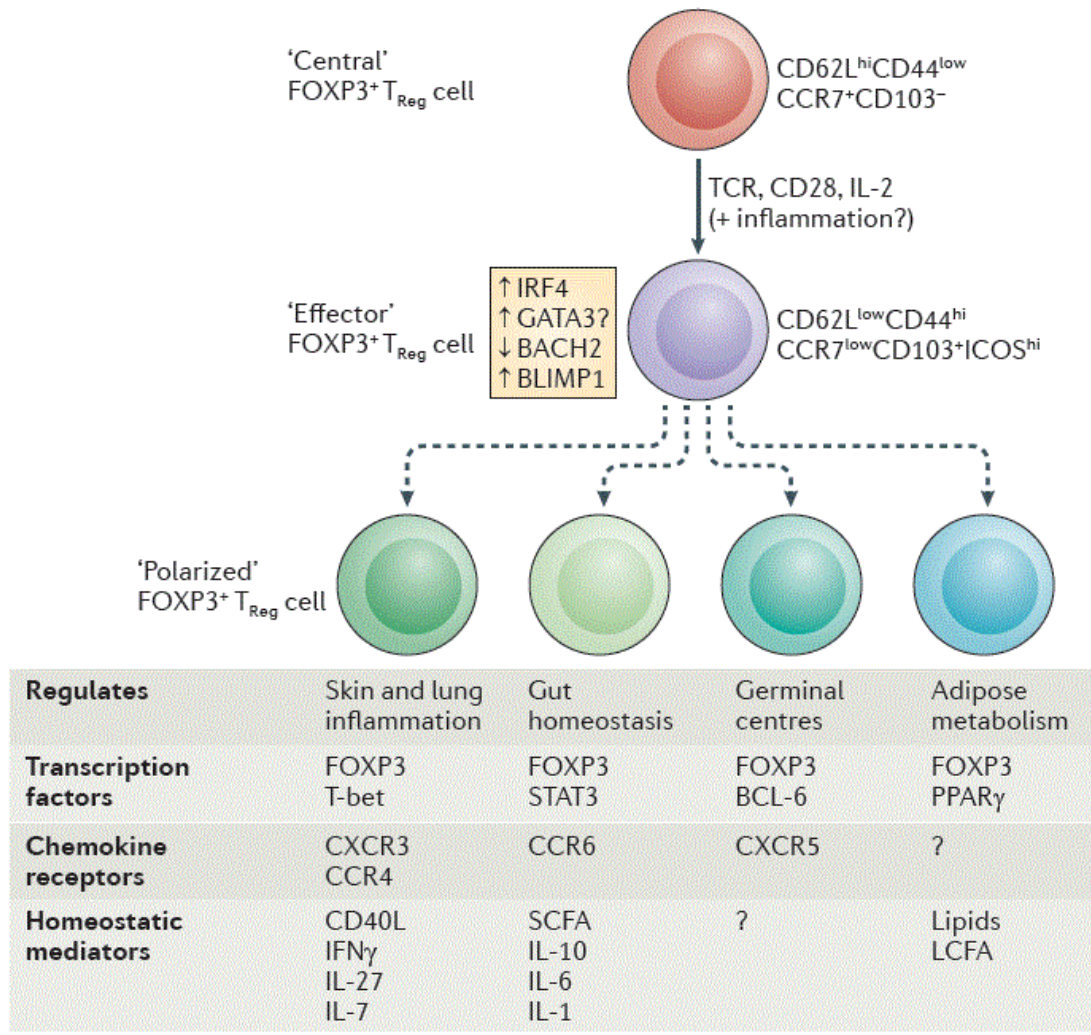


**Figure 1:** Treg Cell Differentiation. FoxP3<sup>+</sup>Treg cells are exported from the thymus and recirculate through secondary lymphoid tissues as ‘central’ Treg cells. Activation of the central Treg cells upregulates IRF-4 and modulates other transcription factors to differentiate into effector Treg cells. Dashed lines indicate uncertainty over the reversibility of differentiation. (BCL-6, B cell lymphoma 6; CCR, CC-chemokine receptor; CXCR, CXC-chemokine receptor; GATA3, GATA-binding 3; ICOS, inducible T cell co-stimulator; IFN $\gamma$ , interferon- $\gamma$ ; LCFA, long-chain fatty acid; PPAR $\gamma$ , peroxisome proliferator-activated receptor- $\gamma$ ; SCFA, short-chain fatty acid; STAT3, signal transducer and activator of transcription 3).

[Reprinted by permission from Macmillan Publishers Ltd: Nature Reviews Immunology. Liston A and Gray D. Homeostatic control of regulatory T cell diversity.14: 154–165 (2014)]

### MicroRNAs in Treg Cells

Mature microRNAs (miRNA) are small single stranded RNA molecules, typically 22 nucleotides in length, originally transcribed as a larger RNA species hundreds or thousands of bases long termed primary miRNA (pri-miRNA). The pri-miRNA is trimmed in the nucleus by the microprocessor comprised of a Drosha family member into a roughly 70 nucleotide hairpin, termed precursor miRNA (pre-miRNA), then exported to the cytoplasm. The RNase III enzyme, Dicer in collaboration with RNA-binding proteins further cleaves the pre-miRNA into the shorter RNA duplexes generating a double-stranded RNA (19–24 nucleotides long) with one strand being loaded in a protein complex called RNA-induced silencing complex (RISC). Mature miRNAs finally guide the complex to their target mRNAs typically base pairing imperfectly to its 3'-UTR. The recruitment of this complex to a target mRNA inhibits its translation but it can also induce degradation of the mRNA target (Figure 2). The imperfect nature of the base-pairing, formed from a 7-nucleotide seed region within the miRNA, allows a single miRNA to control multiple genes with homologous sequences in the target region. As such, miRNAs have been identified as key regulators of gene expression and subsequently shown to participate in the regulation of the immune response.

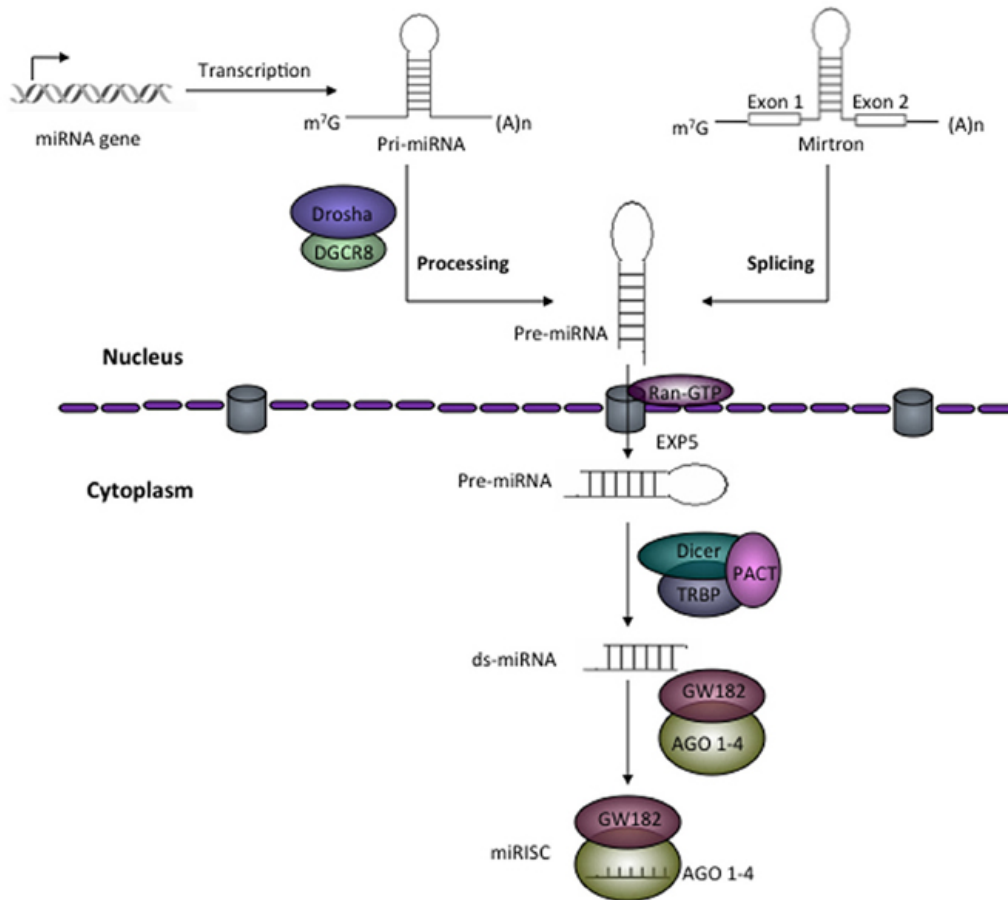


**Figure 2:** miRNA Biogenesis. RNA polymerase II transcribes the miRNA gene and produces hairpin structured pri-miRNA that contains 5' cap and 3' poly-A tail. In the nucleus, Drosha in association with DGCR8, a ds-RNA-binding protein generates about 55–70 nt long precursor miRNA (pre-miRNA). In eukaryotes, some pre-miRNAs are generated from mirtrons as a product of splicing reaction. With the help of Ran-GTP bound exportin-5 pre-miRNAs are exported from the nucleus to cytoplasm. In the cytoplasm, Dicer together with TAR RNA-binding protein (TRBP) or PACT removes the loop and generates miRNA duplex from pre-miRNAs. The miRNA duplex (ds-miRNA) is then loaded into Argonaute (AGO) proteins (in the case of humans AGO 1–4). One of the strands of ds-mRNA called guide strand retained in the AGO and with other effector protein factors forms miRNA-induced silencing complex (miRISC)

[Reprinted by permission from *Frontiers: Frontiers in Genetics*. Role of miRNAs in CD4 T cell plasticity during inflammation and tolerance. Volume 4, article 8, Jan 2013. <http://journal.frontiersin.org/Journal/10.3389/fgene.2013.00008/abstract>]

Currently there is ample evidence that supports the role of miRNAs in regulating the development, homeostasis, and function of the adaptive immune cells, including Th17 cells, NK cell, B cells, and Treg cells(103). In T cells,miR-181 was found to regulate the antigen response by modulating their TCR signaling strength(104) and miR-155 was found to be involved in their differentiation and activation(105;106). As for Treg cells, and under certain conditions, they downregulate their FoxP3 expression, attenuate suppressor functions, and manifest some of the functions of effector T cells (Th1, Th2, and Th17 cells)(107). In addition to the aforementioned networks of transcription factors that are involved in regulation of the fate and function of Treg cells (Figure 1) depletion of specific overexpressed miRNAs results in altering particular aspects of CD4+ cell development and function (Figure 3). Pan-miRNA depletion in murine models, which is done by knocking out Dicer, results in autoimmune pathology similar to FoxP3 deficiency with notable reduction in Treg cell numbers and function(108;109;110). The miRNA-deficient Treg cells fail to remain stable with downregulated FoxP3 and altered marker expression consistent with their impaired suppressive activity(108).Deletion of Drosha in Treg cells led to a similar loss of suppressive activity and defective FoxP3 induction as well(111). These earlier investigations confirmed the pivotal role of miRNAs in the regulation of Treg cell differentiation and function but did not identify the individual miRNAs that are relevant to these processes. This is an area of active research and more recent investigations started to discover the members of the miRNA network that regulate the Treg cell biology (Figure 4).

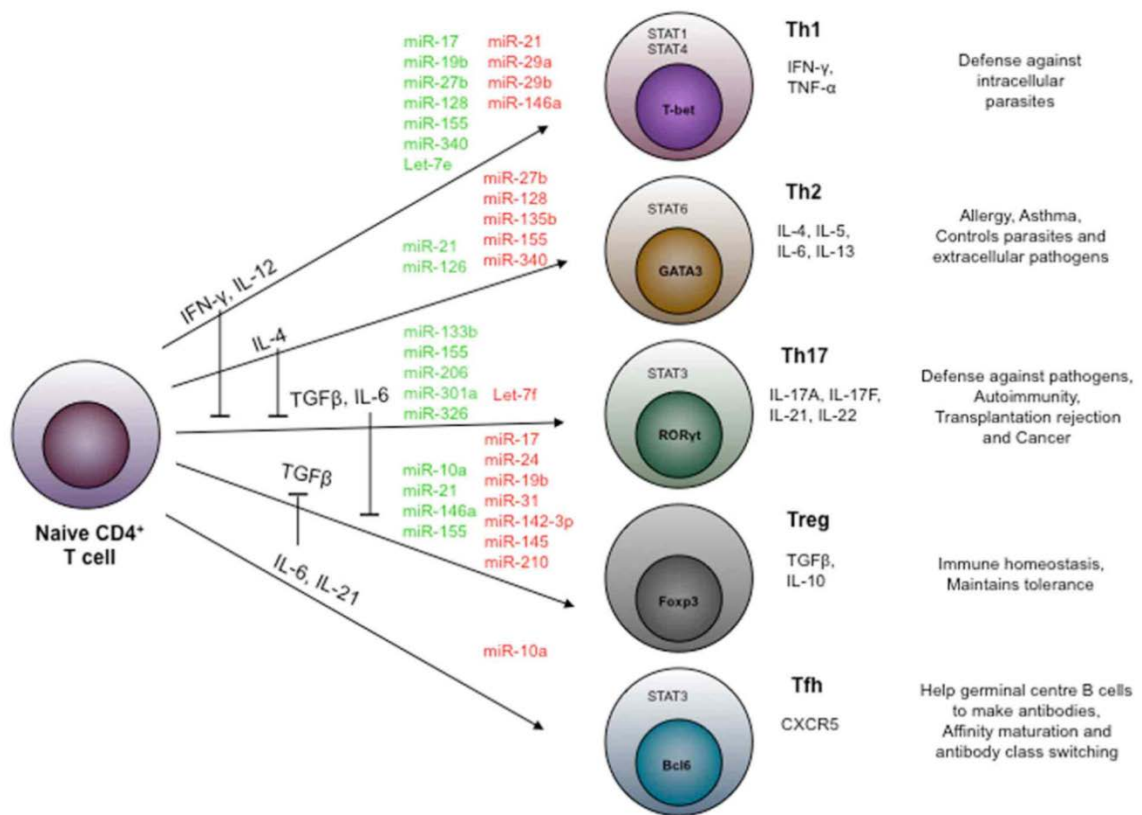


**Figure 3:** miRNAs Regulating the Differentiation of CD4<sup>+</sup> Cell Subsets. miRNAs regulate the differentiation of different effector (Th1, Th2, Th17, and Tfh) and Treg sub-population of CD4<sup>+</sup> cells. miRNAs shown in green color are reported to positively regulate whereas those in red color negatively regulate their differentiation

[Reprinted by permission from Frontiers: Frontiers in Genetics. Role of miRNAs in CD4 T cell plasticity during inflammation and tolerance. Volume 4, article 8, Jan 2013.

<http://journal.frontiersin.org/Journal/10.3389/fgene.2013.00008/abstract>

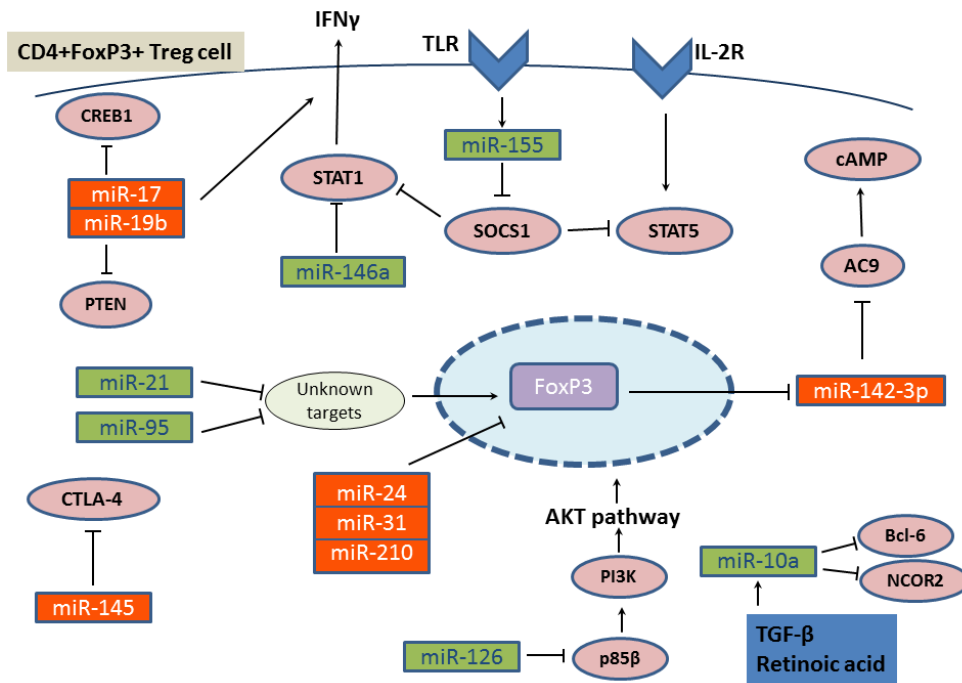


**Figure 4:** miRNA-mediated Regulation of Treg Cell Homeostasis and Function. Multiple miRNA-mediated pathways that contribute to the regulation of Treg cell homeostasis and function are shown. MiR-146a expression in Treg cells prevents IFN $\gamma$ -mediated Th1 cell pathology. MiR-155 promotes Treg cell maintenance. Retinoic acid-induced miR-10a expression suppresses the conversion of Treg cells into T follicular helper (Tfh) cells under certain conditions by the inhibition of Tfh cell-associated transcriptional repressor B cell lymphoma-6 (Bcl6) and the nuclear co-repressor 2 (Ncor2). MiR-17~92 cluster restrains different aspects of Treg cell biology with miR-19b and miR-17 (which are part of that cluster) being responsible for promoting a Th1 response. MiR-142-3p regulates the production of cAMP by targeting AC9 thus may be involved in regulating Treg cell suppressive function. Likewise miR-126 could impair the suppressive activity of Treg cells through targeting p85 $\beta$ . Other miRNAs may be involved in regulating FoxP3 directly by targeting its 3'UTR or indirectly via unknown targets. The miRNAs shown in red boxes are downregulated whereas those in green boxes are overexpressed in Treg cells. There are many other differentially expressed miRNAs that have been described in Treg cells but their function and role in Treg cell homeostasis and plasticity currently unknown.

[Modified from: microRNA networks in regulatory T cells. Tang et al. J Physiol Biochem, 70:869–875; 2014]

Several investigations reported on differentially expressed miRNA between Treg and effector non-Treg CD4+ cells with some focus on the interrelationship between the identified miRNAs and FoxP3. Cobb et al. showed in transgenic mice that Treg cells have a miRNA profile distinct from non-Treg CD4+ cells and a partial Treg cell-like miRNA profile is conferred by the enforced expression of FoxP3, suggesting that FoxP3 directly or indirectly contributes to miRNA expression in Treg cells(110). Rouas et al. studied human Treg cells obtained from umbilical cord blood and found 5 specific miRNAs that were differentially expressed in Treg cells; three were upregulated (miR-181c, miR-21, miR-374) and two were downregulated (miR-31 and miR-125a)(112). Two of the five miRNAs were shown to regulate FoxP3 expression, miR-31 and miR-21, however, miR-31 had a functional target sequence in the 3'UTR of FoxP3 to repress its expression whereas miR-21 indirectly upregulated it(112). The same group went on to investigate the Treg signature in healthy adults peripheral blood Treg cells and found 15 statistically differentially expressed miRNAs: miR-9, -18a, -24, -27b, -95, -126, -133a, -134, -145, -181b, -181d, -210, -224, -335, and -509(113). Of note, the Treg miRNA signature was characterized by mostly down-regulated miRNAs (13 of the 15 miRNAs) and only two miRNAs, miR-95 and miR-509, were overexpressed. They then investigated the functional role of 4 of the identified 15 miRNAs because FoxP3 and CTLA-4 were amongst their predicted targets. They found that miR-24 and miR-210 are negative regulators of FoxP3 through direct target sites in its 3'UTR. They demonstrated also that

miR-95 positively, but indirectly, regulated FOXP3 expression whereas miR-145 negatively regulated CTLA-4 expression by binding to its 3'UTR target site(113).

To elucidate the functional role of specific miRNA in Treg cells investigators resort to gain/loss of function of individual miRNA genes in murine models. Amongst these miRNAs, miR-155 has been studied most. MiR-155 expression is induced by TLR-mediated sensing and inflammatory cytokines such as antiviral cytokines IFN- $\beta$  and IFN- $\gamma$  suggesting that miR155 is a component of the innate immune response to a broad range of inflammatory mediators(114). MiR-155 is also essential for proper T cell response, B cell response, and for the interaction between dendritic cells and T cells. MiR-155-deficient Treg cells, however, attenuates IL-2 signaling through suppressor of cytokine signaling 1 (SOCS1)(115), which is a negative regulator of STAT5 (IL-2/signal transduction activation of transcription 5) signaling pathway. miR-155 promotes Treg cell maintenance by upregulating IL-2 expression via SOCS1 inhibition(115), thus miR-155 knockout mice have reduced number of Treg cells in both thymus and peripheral lymphoid but without any reduction in their suppression activity(105;115;116). These findings suggest that miR-155 is critical for Treg cell development and homeostasis but not for their suppressive function. Like miR-155, miR-146a is highly expressed in Treg cells, however, loss of miR-146a in these cells results in fatal Th1-mediated pathology(117) with increased production of IFN- $\gamma$  by both miR-146a-deficient and miR-146a-sufficient conventional T cells, whereas IL-17 production was unaffected(117). Therefore, miR-146a prevents acquisition of Th1-like properties by Treg cells by

restraining the production of IFN- $\gamma$  through targeting STAT1(117), a key transcription factor required for Th1 effector cell differentiation. Likewise, heightened STAT1 activation in Treg cells subjected to a selective ablation SOCS1, a negative regulator of STAT1 phosphorylation downstream of the IFN- $\gamma$  receptor, was associated with analogous Th1-mediated pathology(115). Mir-17 and miR-19b are also known to control the Th1 responses through promoting proliferation, suppressing inducible Treg cell differentiation, and reducing cell death(119) by targeting CREB1 and PTEN respectively. Both aforementioned miRNAs are members of the miR-17-92 cluster known to be required for the accumulation of activated antigen-specific Treg cells and for differentiation into IL-10- producing effector Treg cells. Mice with a Treg-specific loss of miR-17-92 expression develop more severe experimental autoimmune encephalitis and fail to establish clinical remission compared to control mice(120). The precise targets of these miRNAs are still unknown. Other Treg-enriched miRNAs (miR-17-3p, miR-19a-5p, and miR-19b-5p) are predicted to target numerous signaling molecules, transcription factors, and cell cycle regulators. It is likely that each miRNA in this cluster may recognize different targets and that the interplay of many interactions will ultimately control particular aspects of the differentiation and function of Treg cells(121).

Several other miRNAs expressed by Treg cells have been investigated as well. Huang et al. demonstrated that miR-142-3p regulates the production of cAMP by targeting AC9 (adenyl cyclase 9) in both non-Treg CD4<sup>+</sup> and Treg cells. Moreover, they showed that miR-142-3p limits the level of cAMP in non-

Treg cells by inhibiting AC9 production, whereas FoxP3 represses miR-142-3p to keep the AC9/cAMP pathway active in Treg cells(122). Interestingly, Treg cells contain a high level of a high level of cAMP for their suppressor function suggesting that miRNA-142-3p controlling AC9 expression may restrict the final level of cAMP thus regulating to some extent their suppressive function. It has been previously demonstrated that the suppressive activity of Treg cells is abolished by a cAMP antagonist as well as by a gap junction inhibitor(123).

MiR-126 and miR-10a have been reported to be highly expressed in Treg cells and have a significant impact on Treg cell function(124). Silencing of miR-126 could reduce the induction and impair the suppressive activity of Treg cells through targeting p85 $\beta$ , and subsequently altering PI3K/Akt pathway activity(125;126) and that of DNMT1(127;128). As for miR-10a, it may regulate the stability of Treg cells rather than their function. Takahashi et al. demonstrated that miR-10a limited the ability of Treg cells to acquire the features of follicular helper T cells by targeting Bcl-6 and the corepressor Ncor2(129). TGF- $\beta$  and all-transretinoic acid that promote the Treg phenotype are both required for maximal induction of miR-10a in induced Treg cells(124;129). Therefore, the expression of miR-10a in retinoic acid-treated induced Treg cells retains FoxP3 expression and enhances their stability.

It is increasingly recognized that miRNAs are essential in the differentiation, homeostasis, and function of different Treg cell subsets. Recent studies have clearly demonstrated that deregulation of individual miRNAs have a pivotal role in the development of significant immunopathology and autoimmune

diseases. The current state of our knowledge in this area (Figure 4) is far from being complete and continued investigations will be needed to reveal a better understanding of the miRNA network that is involved in gene regulation in Treg cells. Herein, I report that miR-199a-5p is differentially expressed in peripheral blood FoxP3+ Treg cells as compared to non-Treg CD4+ cells and that it is downregulated in COPD patients versus healthy smokers(130). I also demonstrate that miR-199a-5p could potentially modulate the Treg cell response through interference with the TGF- $\beta$  pathway. In peripheral blood leukocytes and leukocytic cell lines miR-199a-5a is downregulated and its locus is hypermethylated(131) but to my knowledge it has never been investigated in the context of Treg cell biology.

## MicroRNAs in COPD

The role of miRNAs in the altered immune responses and homeostatic mechanisms of COPD is beginning to emerge. MicroRNAs were found to be differentially expressed in induced sputum and lung tissue from subjects with and without COPD(132;133). Sputum levels of let-7c significantly and inversely correlated with protein levels of TNF receptor type II (TNFR-II) and were only reduced in current smokers with COPD but not ex-smokers with COPD(132). The tissue miRNA profiling was, however, different from that of sputum. MiR-223 and miR-1274a were most upregulated whereas miR-923 and miR-937 were most downregulated in COPD patients' lung tissue compared with smokers without COPD(133). Interestingly, miR-15b was found to be upregulated in COPD and localized to both areas of emphysema and fibrosis with its expression correlating with severity of COPD, based on degree of airflow obstruction(133). MiR-15b was also found to regulate components of the TGF- $\beta$  pathway, specifically SMAD7 which was reported to be decreased in bronchial epithelial cells in COPD suggesting that miR-15b may be involved in airway remodeling in COPD(133). When comparing studies that profiled miRNAs only miR-18a and miR-365 were common in datasets(134); however, the first study analyzed whole lung tissue whereas the second study examined bronchial airway epithelial cells of smokers and didn't include COPD patients. The lung tissue study also revealed increased expression of miR-146a in COPD patients versus those without COPD which is surprisingly opposite to another study that showed a reduced expression of miR-146a in cultured fibroblasts obtained from COPD

patients(135). In the latter study, downregulation of miR-146a led to disinhibition of cyclooxygenase (COX)-2 and subsequently increased production of prostaglandin E2 (PGE2)(135). PGE2 is an inflammatory mediator that is known to be increased in the lungs of patients with COPD and is also a potent inhibitor of lung fibroblast repair functions(30;136).

Differences between studies are likely related to COPD heterogeneity and site/cell-specific versus whole lung expression changes. Other investigators focused on identifying functional cell-specific miRNAs rather than whole lung miRNA profiling. Mizuno et al. studied miR-199-5p and miR-34a as potential biomarkers in COPD lung tissue(137) because these miRNAs have been previously shown to be involved in the control of HIF-1 $\alpha$  and VEGF protein expression(138)and are controlled by p53(139). Both miRNAs were found to be increased in COPD lung tissue and correlated with severity of airflow obstruction while inversely correlating with lung HIF-1 $\alpha$  protein expression. In addition, it was demonstrated in the pulmonary microvascular endothelial cells that transcriptional interactions exist between HIF-1 $\alpha$  and miR-34a and miR-199a-5p through AKT and p53. AKT is known to be involved in the regulation of HIF-1 $\alpha$  which suggests that these miRNAs play a role in the HIF-1 $\alpha$  -dependent lung structure maintenance program and COPD pathogenesis. Christensen et al., on the other hand, profiled global miRNA and mRNA expression within different regions of the lung of COPD and control subjects and reported that 63 miRNAs were altered with regional emphysema(140). However, only five miRNAs (miR-638, miR-18a-3p, miR-483-3p, miR-181d, and miR-30c) had greater than 50

positively or negatively correlated predicted targets. Importantly, the significantly associated pathways were almost all inversely correlated with upregulated miRNAs, suggesting that these miRNAs have an inhibitory role with increasing emphysema severity. The pathways that were mostly involved by the miRNA-gene interaction were involved in extracellular matrix (ECM) maintenance, oxidative stress response, and lung aging consistent with the concept that dysregulation of multiple miRNAs may contribute to disease severity. The function of miRNA-638 was then studied because it was amongst the most upregulated in the study and it is expressed in lung fibroblast and known to be associated with cellular senescence and DNA damage(141). miR-638 knock-down experiments in COPD lung fibroblasts led to upregulation of target genes involved in cell proliferation, autophagy, protein degradation, mitochondrial functioning, DNA damage response, oxidative stress response, and ECM remodeling, thus recapitulating the same emphysema-related patterns of gene expression. A somewhat similar study profiling both miRNAs and mRNAs was performed on resected lungs from patients with mild to moderate COPD by Savarimuthu Francis et al. but focused more on whole lung tissue differential expression of miRNAs between mild versus moderate COPD(based on diffusion capacity and not CT criteria)(142). Five miRNAs (miR-34c, miR-34b, miR-149, miR-133a and miR-133b) were significantly down-regulated in lungs of patients with moderate compared to mild emphysema, and three of these miRNAs (miR-149, miR-133a and miR-133b) correlated with emphysema severity. MiR-34c expression exhibited the greatest difference between groups with 0.3 fold lower

expression in the moderate severity group so it was over-expressed in BEAS-2B and HFL1 cell lines. Five genes (MAP4K4, SERPINE1, ALDOA, HNF4A and ZNF3) that were obtained from the miR-34c responsive genes were expressed at higher levels in lungs of patients with moderate or severe emphysema compared to normal subjects and mild emphysema. Of the five genes only SERPINE1 and HNF4A had higher expression in association with lower miR-34c expression; however, SERPINE1 was significantly more expressed in moderate than in mild emphysema(142).

In COPD, Kelsen et al. have shown that exposure to cigarette smoke adversely affects protein metabolism in the lung with activation of the unfolded protein response (UPR)(143). In chronic cigarette smokers, activated UPR is reflected by the up-regulation at the protein level of UPR chaperones including GRP78 in small airway epithelial cells and type II pneumocytes. Recent work by Hassan et al. identified miR-199a-5p as a key regulator of the UPR in  $\alpha$ -1 antitrypsin (ATT) deficient monocytes of COPD patients(144). In this study, the authors found that miR-199a-5p expression is lower in MM and ZZ monocytes isolated from individuals with COPD compared with asymptomatic MM or ZZ individuals. The authors also demonstrated that miR-199-5p repressed many components of the UPR and that miR-199a-2 promoter hypermethylation was responsible for miR-199a-5p inhibition in symptomatic ZZ COPD patients (Figure 5) hence leading to an exaggerated UPR and inflammatory response(144).

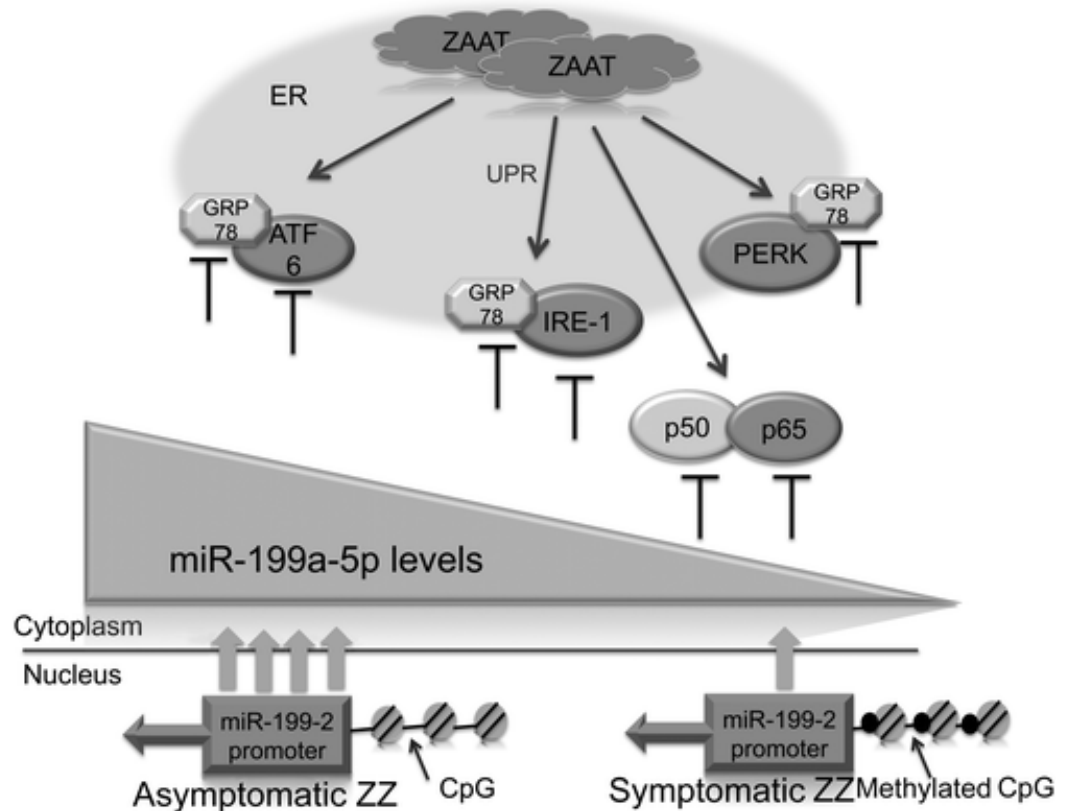


**Figure 5:** Role of miR-199a-5p in Regulating the UPR. Model showing the potential role of miR-199a-5p the unfolded protein response (UPR) in asymptomatic and symptomatic ZZ monocytes. The accumulation of the aberrant ZAA protein activates the UPR, which in turn induces miR-199a-5p expression. In asymptomatic ZZ, elevated miR-199a-5p could negatively regulate endoplasmic reticulum (ER) stress by targeting the 3' untranslated region (UTR) of the mRNAs encoding GRP78, activating transcription factor 6 (ATF6), nuclear factor- $\kappa$ B1 (p50), and RELA (p65). In symptomatic ZZ monocytes, hypermethylated CpG sites in the miR-199a-5p promoter attenuate the expression of miR-199a-5p, which in turn leads to intensification of the UPR. ERK = protein kinase RNA-like endoplasmic reticulum kinase; IRE-1 = inositol-requiring kinase 1.

[Reprinted with permission of the American Thoracic Society. Copyright © 2015 American Thoracic Society. Hassan T, et al. 2014. miR-199a-5p Silencing Regulates the Unfolded Protein Response in Chronic Obstructive Pulmonary Disease and  $\alpha$ 1-Antitrypsin Deficiency. *Am J Respir Crit Care Med*; Vol 189: 263–273]

## Significance

The current paradigm of COPD pathobiology highlights the interplay of dysregulated oxidative stress, protease/antiprotease imbalance, and aging/senescence(37). In this paradigm epigenetic modulation of the oxidative stress response is thought to have a significant impact on the innate immune response(5;145;146). However, much remain to be determined regarding the role of the adaptive immune response in COPD and little is known about the contribution of Treg cells to the pathogenesis of COPD. Both descriptive and functional investigations in this area have yielded conflicting results(49;80;81;82;83) and didn't fully explain the mechanism for the observed Th17/Treg cell imbalance(85). It is now well recognized that COPD is associated with deregulated miRNA expression(132;133;134;135;137;142;147) and that miRNAs are also critical to both adaptive and innate immunity, with regulatory effects on T cell function, plasticity, and homeostasis. Therefore, the potential to therapeutically regulate miRNA levels may offer new avenues for possibly regulating the immune system and prevent or attenuate disease progression (103). Currently, there is limited knowledge about the specific miRNAs that are involved in the regulation of these processes (118;148) and to what extent their deregulation contributes to COPD immunopathogenesis. Information regarding the miRNA profile of peripheral blood Treg cells has been limited to analysis of partially-purified Treg cells in a small cohort of adult subjects(113). There is yet much to be learnt about their functional targets and biological relevance in the T cell response and their complex roles in the development of (or protection from)

inflammatory diseases, including COPD. Identifying specific miRNAs with their key nodes and networks that are involved in regulating Treg cells and delineating their function are of great interest for not only COPD but also various inflammatory diseases that are associated with smoking.

### **Aims**

In view of the exaggerated T cell inflammatory response in COPD it is likely that Treg cells are impaired allowing for an unbalanced Th1, Th17, and CD8 response. However, available studies in this field have reported discrepant results most likely due to limitations in the techniques of performing functional assays in Treg cell populations and the complexities of isolating their subsets. Importantly, there is limited knowledge about the specific miRNAs that are involved in the regulation of the Treg cell population in disease states and to what extent their deregulation contributes to COPD immunopathogenesis. Therefore, we pursued an approach to investigate Treg cell function first then we analyzed their miRNA profile in the setting of COPD. Our main objective was to identify deregulated miRNAs in COPD that are involved in Treg cell function, differentiation, or homeostasis. MicroRNAs are small noncoding RNAs that interfere with gene expression and discoveries pertaining to their role may help in understanding pathogenic pathways that lead to the deregulated immunity found in COPD. Specifically, miRNAs were profiled in Treg and Teff cells in healthy subjects and COPD patients in an attempt to address the following aims:

1. To determine CD4+CD25+FoxP+3 Treg cell functional activity ex vivo from subjects with COPD and controls
2. To determine the effect of cigarette smoke extract ex vivo on function of peripheral blood CD4+CD25+FoxP+3 Treg cells of subjects with COPD versus controls
3. To identify particular Treg cell miRNAs that are altered by smoking and in COPD patients.
4. To explore the function of Treg-specific COPD miRNAs.
5. To identify potential targets of miR-199a-5p in Treg cells.

## CHAPTER 2

### MATERIALS AND METHODS

#### Reagents and Drugs

Xylene (Fisher Scientific, Cat # X3P-1GAL, Waltham, MA, USA), citrate buffer (Fisher Scientific, Cat # TA050CBX), 30% hydrogen peroxide stabilized with sodium stannate (Fisher Scientific, Cat # H323-500), hematoxylin counterstain (Fisher Scientific, Cat # H345-25), Cytoseal-Xyl (Fisher Scientific, Cat # 22-050-262), molecular biology grade tris base (Fisher Scientific, Cat # BP152-1, Waltham, MA, USA), ethylenediaminetetraacetic acid (EDTA) (Fisher Scientific, Cat # BP120-1), MACS buffer (DPBS 991ml, 5 ml FBS, 2 nM EDTA), CFSE buffer (DPBS 90ml and 5ml FBS), fetal bovine serum (FBS) (Fisher Scientific, Cat # 502300142), 50x tris acetic acid EDTA (TAE) buffer (242g tris base, 57 ml glacial acetic acid, 50 ml 0.5M EDTA pH 8.0 in 1L final volume pH 7.6), Ficoll-Paque Plus blood separation reagent (GE Healthcare, ThermoFisher Scientific, Cat # 45-001-749, Waltham, MA, USA), 1 x phosphate buffered saline (PBS) without  $\text{Ca}^{2+}/\text{Mg}^{2+}$  (Mediatech Inc, Cat # 21-040-CV, Manassas, VA, USA), Rosewell Park Memorial Institute (RPMI) 1640 medium (Mediatech Inc., Cat # 10-040-CV), trypan blue viability dye (Life Technologies, Cat # 15250-061), carboxyfluorescein succinimidyl ester (CFSE) (Invitrogen, Life Technologies, Cat # C34554), Human Treg Suppression Inspector beads (Miltenyi, Cat # 130-092-909), fixation/permeabilization concentrate (eBioscience, Cat #. 00-5521), the permeabilization buffer (10x Permeabilization buffer eBioscience, Cat # 00-8333-56), 2% normal rat serum (eBioscience, Cat # 24-5555-94), anti-human

FoxP3-PE antibody or PE rat IgG2a isotype control (eBioscience, Cat # 12-4776-42),

Lipofectamine 2000 (Invitrogen, Life Technologies, Cat # 11668-027), RNase-free molecular biology-grade water (Life Technologies, Cat # AM9937), Iscove's DMEM x1 medium (Fisher Scientific, Cat # 10-016-CV, Waltham, MA, USA), Opti-MeM Reduced serum Medium (Gibco, Thermo Fisher Scientific, Cat # 31985-062), TGF- $\beta$ 1 (Peprotech, Cat # 100-21, Rocky Hill, NJ, USA), Dharmacon 5X siRNA Buffer (GE, Dharmacon, # B-002000-ub-100, Lafayette, CO, USA), epigallocatechin gallate (EGCG) (Sigma- Aldrich, Cat # E4143, St. Louis, MO, USA), RIPA cell lysis buffer (Thermo Fisher Scientific, Cat # 1856210), halt protease and phosphatase 100x (Thermo Fisher Scientific, Cat # 78440), Pierce ECL Western Blotting Substrate (Thermo Fisher Scientific, Cat # 32106), 4x protein gel loading dye (Invitrogen, Life Technologies, Cat # NP0008), 1x 3-[N-morpholino]-propanesulfonic acid sodium dodecyl sulfate (MOPS SDS), gel running buffer (Invitrogen, Life Technologies, Cat # NP0001), nitrocellulose membrane (Thermo Fisher Scientific, Cat # PI-77010), positively charged nylon membrane (Thermo Fisher Scientific, Cat # PI-77015), 1 x Western blot transfer buffer (Invitrogen, Life Technologies, Cat # NP0006-1), Ponceau S solution (Sigma-Aldrich, Cat # P7170-1L, St. Louis, MO, USA), versene solution (Lonza, Cat # 17-711E, Basel, Switzerland).

## **Kits**

ImmPRESS Anti-Mouse Ig Polymer Detection Kit (Vector Laboratories, Cat # MP-7402, Burlingame, CA, USA) CD4CD25 Reg T Cell Isolation Kit (Miltenyi, Cat # 130-091-30, Cologne, Bergisch Gladbach, Germany), CD25+, CD49- T Cell Isolation Kit (Miltenyi, Cat # 130-094-551) and CD4+CD25+CD127dim/- Reg TC Kit II (Miltenyi, Cat # 130-094-775), eBioscience FoxP3 Staining Buffer Set (eBioscience, Cat # 00-5523, San Diego, CA, USA), mirVana miRNA Detection kit (Applied Biosystems, Life Technologies, Cat # AM1560, Carlsbad, CA, USA), TaqMan<sup>®</sup> MicroRNA Reverse Transcription Kit (Life Technologies, Cat # 4366596), SE cell line 4D-Nucleofactor X Kit L (Lonza, Cat # V4XC-1024, Basel, Switzerland), High-Capacity cDNA Reverse Transcription Kit with RNase inhibitor (Life Technologies, Cat # 4374966), Superscript III kit (Invitrogen, Thermo Fisher Scientific, Cat # 18080-400).

## **Subject Selection**

We included healthy non-smoking subjects, healthy current smokers, and COPD current smokers in our studies. We started by performing immunohistochemical staining on lung sections obtained from lung reduction surgery, transplantations, and resection surgeries (of COPD patients and smokers), and unused donor lungs (smokers and non-smokers). Functional assays of Treg cells and miRNA microarrays were performed on Treg and Teff

cells obtained from a different subset of subjects and patients who met our selection criteria for the 3 groups. Inclusion criteria for COPD patients were: age >40 and < 80 years old, currently smoking and with a history of cigarette smoking > 10 pack-years, and presence of airway obstruction ( $FEV_1/FVC < 70\%$ ) according to the GOLD criteria(149). The same criteria were applied to healthy current smokers except they didn't have evidence of airway obstruction. Inclusion criteria for nonsmokers were: age >40 and < 80 years old, never smoked tobacco products or they smoked approximately < 100 cigarettes during their lifetime (having had their last cigarette more than 10 years ago), and they didn't have a history of exposure to second-hand smoking (living with someone who smoked or work-related smoking exposure). We excluded patients and subjects with the following known morbidities: cardiac disease, cerebrovascular disease, connective tissue disease, malignancy, immune deficiency, active infectious conditions, and anyone on medications that may have an impact on the inflammatory/immune response including systemic steroids, aspirin, nonsteroidal anti-inflammatory medications, statins, narcotics, or using illicit drugs. Both COPD patients and the healthy smokers underwent spirometry according to the American Thoracic Society guidelines. All subjects who agreed to participate in the study signed informed consent according to a protocol that was approved by the IRB. As for the miRNA microarray analysis, we enrolled different subjects (12 subjects,4/group) with the same aforementioned criteria. The 3 groups were matched for age, sex, and race. We then increased the number of subjects to include 12 subjects/group for the RT-PCR validation. After

we increased the sample size per group, differences were noted between the groups in age and race.

### **Tissue Immunohistochemical Staining**

We used paraffin-embedded blocks from donor lungs and COPD patients to obtain several 5µm sections. Immunohistochemical staining was done as follows: sections were incubated at 57-60°C for 40 min, then placed in Xylene 3 times for 10 minutes each, followed by hydration in ethanol (100%, 90%, 70%, then water twice for 3 minutes each). For CD4, antigen retrieval was performed in heated Citrate Buffer for 20 minutes (HIER 20min @100°C in EDTA buffer, pH 8.0; LabVision – Ab-8; dilution 1:50) and for and FoxP3 (HIER 10min @100°C in citrate buffer, pH 6.0; Serotec – MCA2376; dilution 1:100). Remaining steps were similar for the 2 antibodies. We allowed cooling down for 30 minutes followed by washing 3 times in PBS, washing in 30% hydrogen peroxide for 20 minutes (diluted in methanol), washing 3 times in PBS, and blocking with 2.5% normal horse serum in PBS-BSA 0.1% for 1.5-2 hours. We used CD4 mouse mAb clone 4B12 (Thermo Fisher, LabVision, Cat # MS1528-S1) and FoxP3 rabbit pAB (BioLegend, Cat # 623802, San Diego, CA, USA).

Subsequently, we incubated with primary antibody diluted in 0.1% PBS-BSA for 60 minutes at room temperature, rinsed and washed 3 times in 1x PBS, then added secondary antibody (anti-Mouse IgG ImmPRESS kit ((Vector Labs, Cat # MP-7402, Burlingame, CA, USA) - adding 2 drops per slide at room

temperature for 30 min). Slides were washed 3 times in PBS and reincubated in DAB for 3-5 minutes. After incubation, we washed in tap water for 5 minutes, performed light Hematoxylin counter-staining (4-5 minutes), washed under running tap water for 30 seconds, dipped slides for seconds in Acid Alcohol, then washed under running tap water for 30 seconds. We re-blued slides in Ammonia Water or Bluing reagent (5-6 dips), washed under running water, dehydrate (70%, 90%, and 100% ethanol 2 times for 3 minutes each), cleared in Xylene 2 times for 10 minutes each, and finally mounted with Cytoseal-XYL ((Fisher Scientific, Cat 22-050-262, Waltham, MA, USA).

### **Quantitative Analysis of Lung Tissue CD4+ and FoxP3+ Cells**

Positively stained cells were counted with a laboratory counter in vivo in small airways and BALT (live microscopic imaging). This mechanism proved to be more effective and reliable in assessing strength and accuracy of stain positivity (important in distinguishing background staining and artifact). FoxP3 is a nuclear stains, hence cells were highlighted easily. Furthermore, the images were taken and studied through an NIH public domain imaging program, Image J 1.23p (Scion Corporation, Frederick, MD). We photographed full circumference airways and BALTs (Diagnostic Instruments, Inc., Spot Basic Image Capture Software, Sterling Heights, MI, USA). Each airway, including epithelial layer to adventitia, was divided into quadrants and digital photographs were taken at a magnification of 400X. The program was set to measure area and perimeter

(including 4 decimal points of both BALTs and airways). Parameters were set for pixel and distance value according to magnification used for each picture. Next step included using the freehand drawing tool to draw a line between two points to delineate the perimeters of BALTs whereas the drawing process for the airways involved two-steps consisting of an outer and inner perimeter. The outer line surrounded the smooth muscle layer, and the second one followed the inner aspect (lumen) of the respiratory epithelium. The program for tabulation automatically gave calculations for area and perimeter. We asked 2 pathologists to perform the morphometric airways assessments in order to quantify the number of cells per square millimeter in each quadrant. The pathologists were blinded to all demographic and clinical data of each patient as well as to the specific identification of any airway.

## **Isolation and Purification of Peripheral Blood Mononuclear**

### **Cells (PBMCs) and CD4+ Cells**

We obtained PBMCs by Ficoll-Paque centrifugation of 40-50 ml of blood from our consenting volunteers. Whole blood was collected in 4-5 10ml EDTA tubes then transferred into two 50ml centrifuge tubes containing 20ml PBS without  $\text{Ca}^{2+}/\text{Mg}^{2+}$  (Mediatech Inc., Cat # 21-040-CV, Manassas, VA, USA). Following blood transfer, 30ml of PBS and anticoagulated blood was gently layered onto 15 ml of Ficoll-Paque Plus (GE Healthcare, ThermoFisher Scientific, Cat # 45-001-749, Waltham, MA, USA) and centrifuged for 35 min at 1,300 rpm

at room temperature. The plasma was collected and banked and the PMBC cell layer was harvested via 5 ml serological pipette and transferred into two 50ml sterile centrifuge tubes. The collected PMBCs were washed twice in 30ml PBS without  $\text{Ca}^{2+}/\text{Mg}^{2+}$ , centrifuged at 1,250 rpm at 4°C for 10 min, then resuspended in 10ml MACS buffer (DPBS 991ml, 5 ml FBS, 2 nM EDTA). PBMCs were counted in order to proceed with CD4+ negative selection. Cells were counted using the Trypan blue (Invitrogen, ThermoFisher Scientific, Cat # 15250-061) staining with a hemocytometer. The CD4 cells were isolated using a CD4CD25 Reg T Cell Isolation Kit (Miltenyi, Cat # 130-091-30, Cologne, Bergisch Gladbach, Germany). The isolated CD4+ cells were then used for further isolation of CD4+CD25- and CD4+CD25+ cells, as Teff and Treg cells respectively, to perform the suppression assays. Two other Treg kits were used as well (Miltenyi, CD25+, CD49- T Cell Isolation Kit and CD4+CD25+CD127dim/- Reg TC Kit II, Cat # 130-094-551 and 130-094-775) in order to get a higher purity Treg cell population (CD4+CD49-CD127-CD25+ cells) for the microarray analysis.

### **Isolation of Peripheral CD4+ Cells**

The isolated PBMCs that were suspended in MACs buffer were labeled according to the CD4CD25 Reg T Cell Isolation Kit manufacturer's protocol. Specifically, the cell pellet was resuspended in 90µl of MACS buffer pre  $10^7$  cells, a Biotin-antibody cocktail added to the PBMCs (10µl per  $10^7$  cells, containing anti

CD8, CD14, CD16, CD19, CD36, CD56, CD123, TCR $\gamma/\delta$  and glycophorin A), incubated for 10 min at 4°C, then Anti-Biotin Microbeads were added (20  $\mu$ l per  $10^7$  cells) and re-incubated for 15min at 4°C. During the last few minutes of incubation, the LD column (Miltenyi, Cat # 130-042-901) in the magnetic field was prepared by rinsing it with 2x 1ml of MACS buffer. The Biotin/Anti-Biotin cell suspension was washed with 10ml of MACS buffer, centrifuged, and cell pellet resuspended in MACS 500 $\mu$ l per  $10^8$  cells. The cell suspension was applied to the LD column which was washed twice with 2ml of MACS buffer, to collect all the effluent containing the unlabeled pre-enriched CD4+ T cell fraction.

#### **Isolation of Peripheral CD4+CD25- Teff and CD4+CD25+ Treg Cells**

The isolated CD4+ cells were centrifuged at 1250 rpm at 4°C for 10 min then were resuspended in 90 $\mu$ l per  $10^7$  cells. 10 $\mu$ l per  $10^7$  of CD25 Microbeads were added to the cell pellet and incubated for 15 min at 4°C. Cells were then washed with 10ml MACs buffer and centrifuged at 1250 rpm for 10 min at 4°C. During the last 2 minutes of the cell centrifugation, the LS column (Miltenyi, Cat # 130-042-401) was rinsed with 2ml of MACS buffer. The cell pellet was resuspended in 500 $\mu$ l per  $10^8$  in MACS buffer then applied to the LS column that was placed in the magnetic field for positive selection. The CD4+CD25- Teff unlabeled cells that passed through the LS column while in the magnetic field were collected. The LS column was rinsed 3x 1ml MACS buffer to collect all the Teff cells. The LS column was then removed from the magnetic field and rinsed

with 2x 5ml MACS buffer to collect the labeled CD4+CD25+ Treg cells. These 2 cell populations were counted after each isolation, using the Trypan blue stain, then were used for flow cytometry analysis to assess their purity and for Treg cell suppression assays (Figure 6 and see next section).

PBMC → negative selection CD4+

CD4+CD25+ cells

CD4+CD25-

CD2, CD3, CD28  
ab-beads

CFSE

Serial dilution – culture RPMI 4 days

Stain and flow cytometry

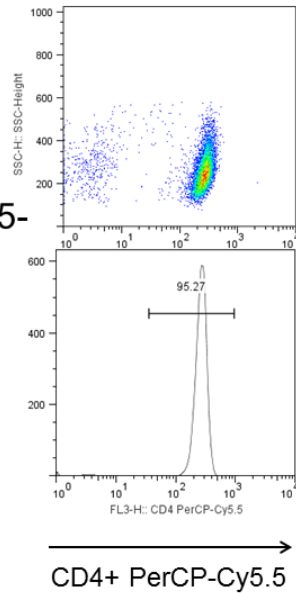


**Figure 6:** Protocol for Isolating CD4+ Cells and Treg Cells for the Suppression Assay. The negative selection of CD4+ cells yielded > 95% CD4+ population (right panel) that was used to isolate CD4+CD25- Teff cells and CD4+CD25+ Treg cells for the suppression assay.

## Treg Suppression Assay

Freshly isolated Teff cells were centrifuged for 8 min at 4°C then suspended in 5% CFSE (Invitrogen, Life Technologies, Cat # C34554) buffer, 1ml per  $10^7$  cells, at room temperature to be labeled with CFSE. The CFSE was prepared in the 5% CFSE buffer to yield a 1% CFSE dilution, using 110 $\mu$ l per  $10^7$  Teff cell, which were incubated for 3 min and washed x 3 with 15 ml of 5% CFSE buffer. After last wash, CFSE-labeled Teff cells were suspended in RPMI (Mediatech Inc., Cat # 10-040-CV, Manassas, VA, USA) at a concentration of  $10^6$ /ml. The freshly isolated Treg cells from previous separation procedures were re-suspended in RPMI at the same  $10^6$  cells/ml concentration and added to 96-well rounded-bottom plates in serial dilutions in order to give Treg/Teff ratios of 1/1, 1/2, 1/4, 1/8 and 1/16 (Figure 7). Each well contained  $50 \times 10^3$  Teff cells and Treg cells (starting with  $50 \times 10^3$  then serially diluting them as described). Wells without Treg cells, wells without Teff cells, and wells without CD3CD28 beads served as negative controls. After 4 days of incubation, Teff cell divisions were determined by CFSE dilution. All steps were performed while with cells suspensions maintained on ice. Human Treg Suppression Inspector beads (Miltenyi, Cat # 130-092-909) were prepared by washing in 1 ml of RPMI and centrifuged at 1500 rpm for 5 min. The Treg Suppression Inspector is made of  $5 \times 10^7$  AntiBiotin MACSiBead™ Particles preloaded with biotinylated CD2, CD3, and CD28 antibodies. The beads were then collected and added to the Teff cells at a ratio of 1:1 ( $5 \times 10^4$  beads/well), leaving one well without beads. Each

condition was set in duplicate (Figure 7) and after 4 days of incubation, we determined the Treg cell divisions by CFSE dilution (Figure 8).

To determine the effects of cigarette smoke extract (CSE) on Treg cells function we treated the isolated Treg cells with CSE (10 $\mu$ g/ml) for 2 hours or DMSO control then washed them with RPMI prior to the 4 days suppression assay. A commercially available CSE was used (Murty Pharmaceuticals, Lexington, KY, USA) prepared by smoking University of Kentucky 1R3F research cigarettes and extracting the condensate with DMSO to a final 40mg/ml solution.

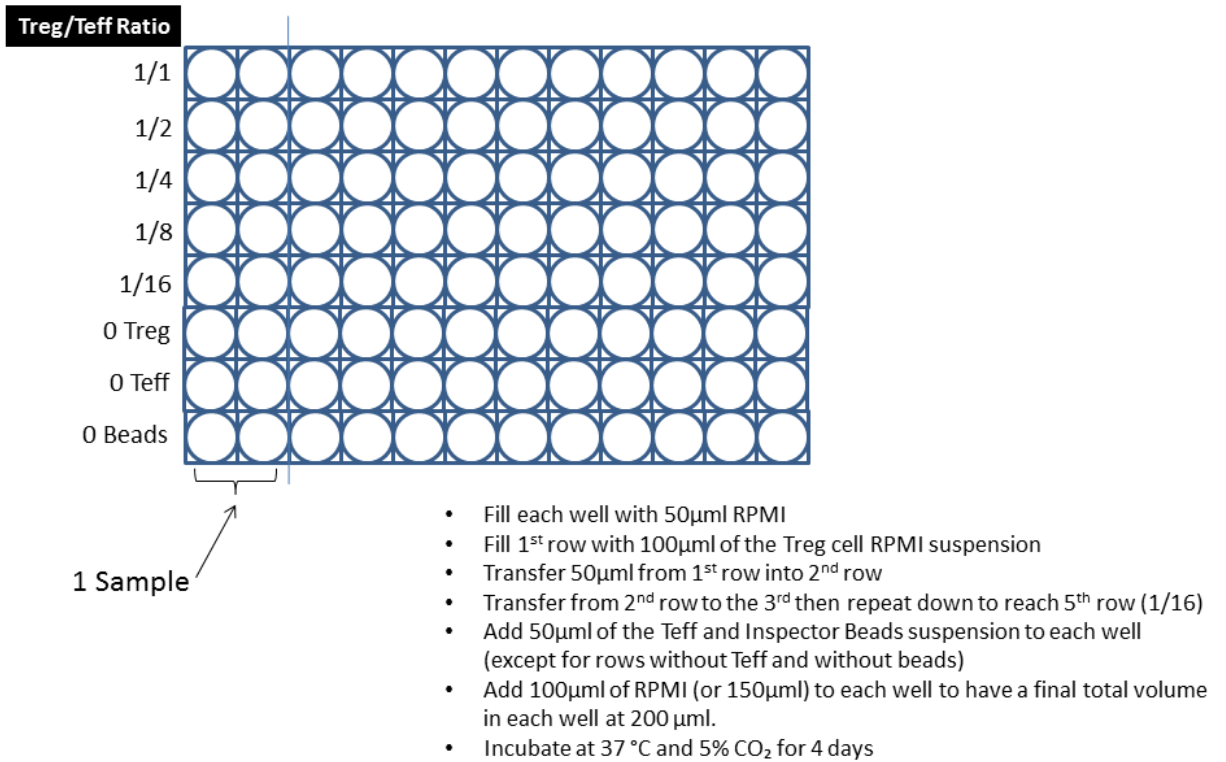


**Figure 7:** Plate Set Up for Treg Cell Suppression Assay Using CSFE Dilution.  
For cell and bead concentrations refer to text.

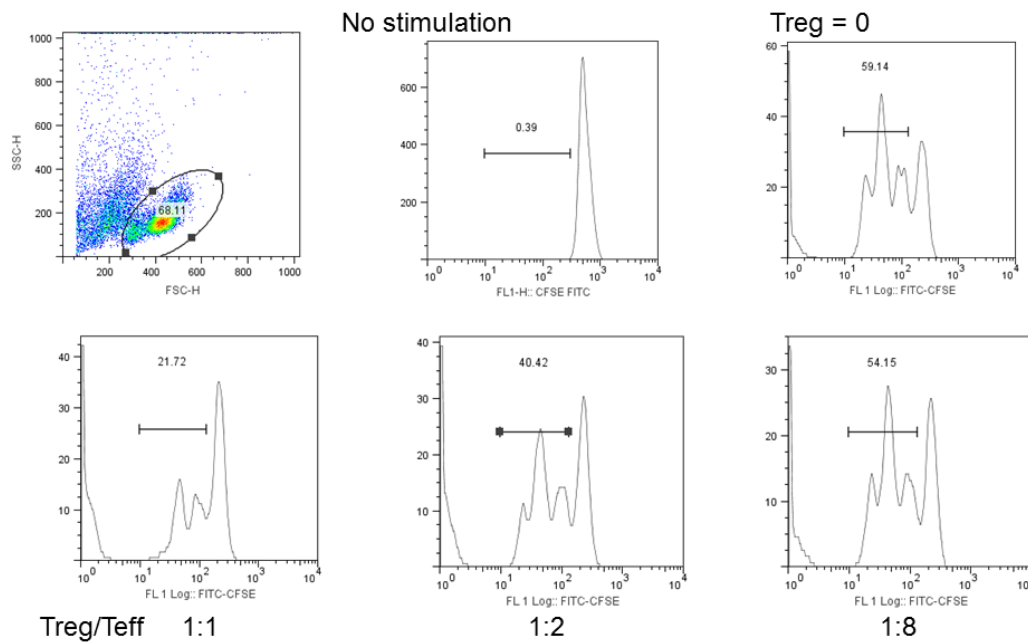


**Figure 8:** Histograms of Treg Cell Suppression Assay. Proliferation of CFSE-labeled Treg cells is shown with each graph representing reduced concentration of Treg cells co-cultured with Treg cells. With serial dilution of the Treg cells in each well there is higher Treg cell proliferation (or less Treg cell suppression) as reflected by increasing numbers of Treg cell generations. Each peak under the horizontal bar represents a generation of proliferating CFSE-labeled Treg cells so the bar reflects the total percentage of proliferating Treg cells, with each generation of Treg cells being represented by a discrete peak.

## **Flow Cytometry for Treg Suppression Assay**

After 4 days incubation, cell suspensions from each row were collected in 1 FACS tube and washed with 2% flow cytometry buffer (FCB) then centrifuged for 5 min at 1300 rpm. The FCB was prepared by adding 20 ml of FBS to 980 ml of DPBS without  $\text{Ca}^{2+}/\text{Mg}^{2+}$  (Mediatech Inc, Cat # 21-040-CV, Manassas, VA, USA). We diluted the anti-human CD4+ PerCP-Cy-5.5 antibody (BD Biosciences, Cat # 341654) in FCB then added 25 $\mu$ l of the stain to each tube, except for 1 tube to serve as negative unstained control. Cell-anti-CD4+ suspension were incubated for 25 min on ice in the dark then washed with 1 ml FCB, centrifuged for 5 min at 1300 rpm and resuspended in 0.4 ml of FCB for flow cytometry analysis. Background fluorescence was assessed using isotype and fluorochrome matched control monoclonal antibody to determine the percent of positive cells. Flow cytometry was done on FACSCalibur using the CellQuest Pro software and data were analyzed using Flowjo software (TreeStar, Inc., Ashland, OR, USA).

## **Isolating and Analyzing the CD4+CD25+CD127-CD49- Treg Cells**

We collected blood in EDTA tubes from more volunteers and processed the blood in a similar aforementioned manner to isolate PBMCs. We then use 2 different kits CD4+CD25+CD127dim/- Reg TC Kit II and CD25+, CD49- T Cell Isolation Kit (Miltenyi, Cat # 130-094-775 and 130-094-551 respectively) to obtain highly purified fraction of FoxP3+ cells (Figure 9).



We proceeded first with magnetic labeling of non-CD4<sup>+</sup> and CD127<sup>high</sup> cells from the isolated PBMCs that were suspended in 40µl of MACS buffer per 10<sup>7</sup> cells and mixed well with 10µl of the CD4<sup>+</sup>CD25<sup>+</sup>CD127<sup>dim/-</sup> T cell Biotin-Antibody cocktail (made of anti-human antibodies against CD8, CD19, CD123, and CD127) and incubated for 5 minutes at 4°C. 30 µl of MACS buffer was added afterward and 20 µl of Anti-Biotin MicroBeads per 10<sup>7</sup> total cells, mixed well and incubated for 15 minutes at 4°C. Cells were washed with 2 ml MACS buffer per 10<sup>7</sup> and centrifuged at 1250 rpm for 10 min then cell pellet resuspended in 500µl of MACS buffer. The LD column was prepared during the last few minutes of centrifugation with 2 ml of MACS buffer. The resuspended cells in 500µl were passed through the LD column in the magnetic field. The column was washed 2x 1ml with MACS buffer while in the magnetic field and the total effluent was collected containing the unlabeled CD4<sup>+</sup>CD127<sup>dim/-</sup> cells. This cell population was resuspended in 80µl of MACS buffer per 10<sup>7</sup> cells and added to 20µl of the CD8<sup>+</sup>CD49d<sup>+</sup> T cell depletion MicroBeads cocktail (made of monoclonal CD8 and CD49d antibodies) per total 10<sup>7</sup> cells. The cell/cocktail suspension was mixed well and incubated for 15 minutes at 4°C. Cells were washed with 2 ml MACS buffer per 10<sup>7</sup> and centrifuged at 1250 rpm for 10 min then cell pellet resuspended in 500µl of MACS buffer. The LD column was prepared during the last few minutes of centrifugation with 2 ml of MACS buffer. The resuspended cells in 500µl were passed through the LD column in the magnetic field. The column was washed 2x 1ml with MACS buffer while in the magnetic field and the total effluent was collected containing the pre-enriched

unlabeled CD4+CD127<sup>dim/-</sup>CD49d<sup>-</sup> cells. The isolated CD4+CD127<sup>dim/-</sup>CD49d<sup>-</sup> cell population were resuspended in 90µl per 10<sup>7</sup> cells, after centrifuging at 1250 rpm at 4°C for 10 min. 10µl per 10<sup>7</sup> of CD25 MicroBeads were added to the cell pellet and incubated for 15 min at 4°C. Cells were then washed with 10ml MACS buffer and centrifuged at 1250 rpm for 10 min at 4°C. During the last 2 minutes of the cell centrifugation, the LS column were rinsed with 2ml of MACS buffer. The cell pellet was resuspended in 500µl per 10<sup>8</sup> in MACS buffer then applied to the LS column that was placed in the magnetic field for positive selection. The CD4+CD127<sup>dim/-</sup>CD49d<sup>-</sup>CD25<sup>-</sup> unlabeled cells that passed through the LS column while in the magnetic field were disregarded after rinsing the column with 3x 1ml MACS buffer. The LS column was then removed from the magnetic field and rinsed with 2x 5ml MACS buffer to collect the labeled CD4+CD127<sup>dim/-</sup>CD49d<sup>-</sup>CD25<sup>+</sup> Treg cells. Of note, we used the CD4+CD25<sup>-</sup> unlabeled Teff cells from the CD4CD25 Reg T Cell Isolation Kit as described above for further analysis of their function and RNA extraction. The final Teff and Treg cell population were then subjected to flow cytometry analysis) and to the suppression assays (Figures 7 and 9) to assess their purity and function before proceeding to lysis for RNA isolation.

The suppression assay was performed in the manner described above using the same culture medium and conditions. As for the purity of the isolated cells we repeated the staining protocol with the surface anti-human CD4+ PerCP-Cy-5.5 antibody as described above but after the 25 min incubation at 4°C in the dark, cells were washed in cold FCB, centrifuged for 8 min at 1250 RPM, then

the cell pellet suspended in 1ml of freshly prepared fixation/permeabilization buffer and reincubated for 45 minutes in the dark at 4°C. We used the eBioscience FoxP3 Staining Buffer Set (eBioscience, Cat # 00-5523, San Diego, CA, USA). Prior to staining the fixation/permeabilization buffer was prepared by diluting the fixation/permeabilization concentrate into its diluent at a ratio of 1/3 (eBioscience, Cat #. 00-5521). The cell suspension was then washed with 2 ml of the permeabilization buffer (made from 10x Permeabilization buffer eBioscience, Cat # 00-8333-56), centrifuged for 8 min at 1250 rpm. Cells were blocked with 2% normal rat serum (eBioscience, Cat # 24-5555-94) in 1x permeabilization buffer for 15 minutes then incubated for 30 minutes with anti-human FoxP3-PE antibody or PE rat IgG2a isotype control (eBioscience, Cat # 12-4776-42). Prior to the current experiments the antibody concentration for both CD4+ and FoxP3 and their respective isotype controls were optimized, using 10µl for anti-CD4+ and its isotype control and 5µl for anti-FoxP3 and its isotype control. Cells were subsequently washed x2 with permeabilization buffer and after the last wash the pellets were resuspended in FCB. Flow cytometry and data analyses were done as described above.

### **RNA Purification**

We used mirVana miRNA Detection kit (Applied Biosystems, Life Technologies, Cat # AM1560, Carlsbad, CA, USA) to extract total and low molecular weight (LMW) RNA from the purified Treg and Teff cells. Isolated T

cells were washed with PBS without  $\text{Ca}^{2+}/\text{Mg}^{2+}$  and centrifuged. The PBS wash was then removed and 600 $\mu\text{l}$  of Lysis/Binding Solution from the kit was added. After lysing the cells, 60 $\mu\text{l}$  of miRNA Homogenate Additive was added and the mixture was left on ice of 10 min. After the 10 min, 600 $\mu\text{l}$  Acid-Phenol:Chloroform was added to the lysate and that was vortex for 60 seconds to mix. The mixed lysate was centrifuged for 5 min at 10,000 rpm at room temperature to separate the aqueous and organic phases. We pipetted carefully the upper (aqueous) phase without disturbing the lower phase. We added 1.25 volumes of 100% ethanol (ambient temperature) to the aqueous phase which was then removed to pass it (i.e. the lysate/ethanol mixture) through a filter cartridge. We centrifuged the cartridges for 15 sec at 10,000 rpm to pass the mixture through the filter and we disregarded the flow-through. We then applied 700 $\mu\text{l}$  miRNA Wash Solution 1 (working solution mixed with ethanol) to the filter cartridge and centrifuged for 10 sec. We disregarded the flow through and repeated the wash twice with 500 $\mu\text{l}$  Wash Solution 2/3. After disregarding the last flow through the filter cartridge was centrifuged again then transferred into a fresh collection tube. We applied 70-100 $\mu\text{l}$  of pre-heated (95°C) nuclease free water (Life Technologies, Cat # AM9937) to the center of the filter, closed the cap, and spun for 30 sec at 10,000 rpm to recover the RNA. We quantified the concentration of total RNA using the Nanodrop Spectrophotometer for all samples and used the Agilent Bioanalyzer to assess for quality of the microarray samples only. All 12 samples were confirmed to have good quality RNA based on their RNA Integrity Number (RIN) and electropherograms (Figure 9). All RNA

work was performed using extra-long barrier tips (SHARP® Precision Barrier Tips, Extra Long, Denville Scientific, Inc. Cat # P1096-FR and P1122, South Plainfield, NJ, USA) and RNase free tubing (Life Technologies, Cat #AM12450).

### **miRNA Microarray Analysis and TaqMan® miRNA Gene Expression**

We labeled 12 samples and hybridized 400ng to 500ng of the extracted RNA on the Human v2 MicroRNA Expression BeadChips (Illumina, San Diego, CA), a platform that contained 743 human miRNAs. The array design can be found on <https://www.ebi.ac.uk/arrayexpress/files/A-GEOD-8179/A-GEOD-8179.adf.txt> (last accessed 2/5/2015). BeadChips were scanned with the Illumina iScan Reader and the experimental data was analyzed using the R, Bioconductor, and GeneSpring software by a consultant bioinformatics expert.

For the miRNA gene expression, we used quantitative real-time RT-PCR to confirm the differential expression of a select number of miRNAs using the Taqman® MicroRNA Assays (Life Technologies, ThermoFisher Scientific, Waltham, MA, USA). The TaqMan® MicroRNA Assays employ a target-specific stem-loop reverse transcription primer that extends the 3' end of the target to produce a template that can be used in standard TaqMan® Assay-based real-time PCR. Also, the stem-loop structure in the tail of the primer confers a key advantage to these assays: specific detection of the mature, biologically active miRNA. The assay consists of a two-step protocol requiring reverse transcription with a miRNA-specific primer, followed by real-time PCR with TaqMan® probes.

We used the TaqMan<sup>®</sup> MicroRNA Reverse Transcription Kit (Life Technologies, Cat # 4366596) to reverse transcribe the RNA into cDNA. We diluted 10ng of the isolated RNA in 5 $\mu$ l nuclease free water (per reaction) and prepared the reverse transcriptase (RT) mix from the kit, adding 0.15 $\mu$ l dNTP, 1.5 $\mu$ l 10x buffer, 0.19 $\mu$ l RNase inhibitor, 1 $\mu$ l RT, and 4.16 $\mu$ l nuclease free water to make a total of 7 $\mu$ l of the mix per reaction. 5 $\mu$ l of the diluted RNA was then added to the mix along with 3 $\mu$ l of the primer of interest to make a total of 15 $\mu$ l per reaction. Samples were run in a thermal cycler (Mastercycler, Eppendorf, Hamburg, Germany) programmed at 16 $^{\circ}$ C for 30 min, 42 $^{\circ}$ C for 30 min, 85 $^{\circ}$ C for 5 min, then maintained at 4 $^{\circ}$ C or on ice. The second step involved setting up and running the real-time PCR amplification reactions. For this step, we first prepared the real-time PCR mix by adding 10 $\mu$ l of the Master Mix (Life Technologies, TaqMan<sup>®</sup> Universal PCR Master Mix, no AmpErase<sup>®</sup> UNG, Cat # 4324018) to 5 $\mu$ l of nuclease free water and 1 $\mu$ l of the 20x Taqman probes. After preparing the real time RT-PCR buffer mix, 5 $\mu$ l of the RT reaction product (cDNA from first step) was added to the mix then we transferred 20 $\mu$ l to a PCR plate (Life Technologies, MicroAmp<sup>®</sup> Optical 96-Well Reaction Plate, Cat # N801-0560). We ran all real-time RT-PCR in triplicate, 20 $\mu$ l/reaction and we used 40 cycles of amplification (10 min at 95 $^{\circ}$ C for enzyme activation followed by 40 cycles of 95 $^{\circ}$ C and 60 $^{\circ}$ C for 15 sec and 60 sec respectively). Data acquisition was carried out with StepOnePlus<sup>™</sup> Real-Time PCR systems (Life Technologies). Table 1 shows the primer sequences for the selected miRNAs and the RNU control obtained from Life Technologies.

**Table 1: Taqman<sup>®</sup> miRNA Primers**

<b>miRNA</b>	<b>Mature miRNA Sequence</b>	<b>Cat #</b>
RNU48	GATGACCCCAGGTA ACTCTGAGTGTGTCGCTGATGCCATCA CCGCAGCGCTCTGACC	001006
miR-19b	UGUGCAA AUCCAUGCAA AACUGA	000396
miR-31*	UGC UAUGCCAACAUAUUGCCA U	002113
miR-95	UUCAACGGGU AUUU AUUGAGCA	00433
miR-99b*	CAAGCUCGUGUCUGUGGGUCCG	002196
miR-193b*	CGGGGUUUUGAGGGCGAGAUGA	002366
miR-199a-5p	CCCAGUGUUCAGACUACCUGUUC	000498
miR-382	GAAGUUGUUCGUGGUGGAUUCG	000572
miR-485-3p	GUCAUACACGGCUCUCCUCUCU	001277
miR-520e	AAAGUGCUUCCUUUUUGAGGG	001119

## ***In Silico* Analysis: Identifying miRNA Targets in the Treg cell Transcriptome and Analyzing their Potential Function**

Three online databases (Targetscan, miRWalk, and miRanda) on miRWalk were used to predict potential miRNAs targets of interest(150). We cross-referenced the list of the predicted miRNA targets to the published gene expression profiles of human Treg cells(151). We then performed pathway and functional analysis of the intersected predicted targets using Ingenuity Pathway Analysis platform (Qiagen, Redwood City, CA, USA) to map the genes into networks, canonical pathways, and molecular function.

### **Validating the Results of the *In Silico* Functional Analysis in Cell Lines**

We employed the human fibroblast CCD-986Sk cells (ATCC, Cat # CRL-1947, Manassas, VA, USA) and the T lymphoblast MOLT-4 cells (ATCC, Cat # CRL-1582) to assess miRNA functional activity. The CCD-986Sk cells express endogenously miR-199a-5p so we used this cell line to perform loss-of-function experiments; whereas the MOLT-4 cells don't express miR-199a-5p so we used them for gain-of-function experiments. The CCD-986Sk cells were transfected with a Locked Nucleic Acid (LNA<sup>TM</sup>) miRNA inhibitor then treated with TGF- $\beta$ 1 and the MOLT-4 cells were transfected with a miRNA mimic. After optimizing culture and transfection conditions, both cell lines showed high transfection efficiency (>80%). We attempted to transfect Jurkat cells but we were not able to obtain adequate transfection efficiency.

## **CCD-986Sk Cell Culture, LNA transfection, and Treatment with TGF- $\beta$ 1**

Human fibroblast CCD-986Sk cells were plated in T-75 flasks and cultured in Iscove's DMEM x1 medium (Fisher Scientific, Cat # 10-016-CV, Waltham, MA, USA) with 10% FBS, incubated at 37°C and 5% CO<sub>2</sub>. Cells were passed every 5-7 days when 80-90% confluent. We confirmed that the CCD-986Sk cells expressed miR-199a-5p by Taqman RT-PCR. For the transfection experiments, cells were passed into 6-well plates (30x10<sup>6</sup>-35x10<sup>6</sup>cell/plate) and after approximately 24 hours incubation at 37°C they were transfected with miR-199a-5p miRCURY LNA™ microRNA inhibitor and LNA negative control 3'-fluorescein labeled (Exiqon, Cat # 410116-00 and Cat # 199004-08, Denmark) using Lipofectamine™ 2000 transfection reagent (Invitrogen, Life Technologies, Cat # 11668-027). The LNA microRNA inhibitors are antisense oligonucleotides with perfect sequence complementary to their target, in this case AACAGGTAGTCTGAACACTGG. When introduced into cells, LNAs sequester their target miRNA in highly stable heteroduplexes preventing the miRNA from hybridizing with its normal target. A second control with only the transfection reagent, Lipofectamine 2000, and without LNA was done as well.

We first prepared the LNA stock solution by adding 250µl of nuclease-free, sterile water, to 5nmole of the miRNA inhibitor to make a 20µM solution (we let the tube stand for few minutes at ambient temperature, gently pipetted 5 times to resuspend, then repeated the prior steps twice before aliquot the LNA to store it

at -20°C having a concentration of 20pmole/μl). We performed dose response experiments to determine the threshold concentrations to minimize toxicity and maximize transfection efficiency. Both LNA and Lipofectamine were diluted in 50μl Opti-MeM Reduced serum Medium (Gibco, Thermo Fisher Scientific, Cat # 31985-062), per 1μl of Lipofectamine and 1μl (20pmole) of LNA, then mixed the 2 solutions to add the final LNA/Lipofectamine mix to each well, 24 hours after seeding of the cells. We assessed transfection efficiency 48 hours after transfection using fluorescent microscopy. The final optimal concentrations for LNA and Lipofectamine that yielded > 90% transfection efficiency were: 100 pmole LNA and 3.5 μl of Lipofectamine. Forty eight hours after transfection (i.e. 3 days from seeding the cells), the medium was changed to Iscove's DMEM x1 medium without the 10% FBS then incubated for another 24 hours in serum-starved conditions to be treated with mammalian derived recombinant human TGF-β1 (Peprotech, Cat # 100-21, Rocky Hill, NJ, USA). On the day of harvest, cells were treated with 10ng/ml of TGF-β1, or medium as control, for 1 hour then lysed for RNA or protein isolation. These experiments were done in triplicates. We isolated the total protein fraction and RNA from these samples in order to test the activation of the TGB-β pathway and changes in gene expression. Of note, RNA from the 3 experiments were pooled then run on the TGF-β pathway TaqMan<sup>®</sup> Array plates Life Technologies, Cat # 4418742).

## **MOLT-4 Cell Culture, miR-Mimic Transfection, and Treatment with EGCG**

We seeded MOLT-4  $2 \times 10^6$  cells in antibiotic-free RPMI with 10% FBS overnight in 6 well-plates at  $37^\circ\text{C}$  and  $5\%\text{CO}_2$ . The cells were transfected with miRIDIAN microRNA Human Hsa-miR-199a-5p and miRIDIAN microRNA transfection control with Dy547, diluted in Dharmacon 5X siRNA Buffer (GE Dharmacon, Cat # C-300533-03-0005, # CP004500-01-05, and # B-002000-ub-100, Lafayette, CO, USA). Similar to the CCD-986Sk cells, we titrated the transfection reagents using the SE cell line 4D-Nucleofactor X Kit L (Lonza, Cat # V4XC-1024, Basel, Switzerland) to minimize toxicity and optimize transfection efficiency. The transfection was carried as such: First, suspend  $1 \times 10^6$  Molt-4 cells (1000rpm, 10mins) in 100 $\mu\text{l}$  SF buffer (82 $\mu\text{l}$  SF buffer +18 $\mu\text{l}$  Sup each)/2 $\mu\text{g}$  GFP or 200nM miRNA mixture for each group (miRNA stock:20 $\mu\text{M}$ , 1:100 dilute). Second, transfect the cells (CA-137 program), add 500 $\mu\text{L}$  antibiotic-free RPMI, and transfer to 6-well plate immediately. Last, add another 1mL antibiotic-free RPMI each well and culture overnight. Transfected cells were then treated with DMSO control, 10 $\mu\text{M}$ , 50 $\mu\text{M}$ , and 100 $\mu\text{M}$  of epigallocatechin gallate (EGCG) (Sigma- Aldrich, Cat # E4143, St. Louis, MO, USA), diluted in DMSO 1:5 (1:1000 dilute), for 48 hours to test for toxicity. Cells were checked for viability and transfection efficiency then collected for total RNA for real time RT-PCR analysis. We noted that with increasing doses of EGCG there was a reduction in cell viability but the 50 $\mu\text{M}$  concentration yielded a greater increase in BMP4 so we performed the analysis on cells that were treated with 50 $\mu\text{M}$  EGCG.

## Western Blot Analysis

MOLT-4 cells from the transfection experiments were first washed with PBS then lysed in 100-150µl RIPA 10x lysis buffer (Cell Signaling, Cat # CST9806S, Danvers, MA, USA), halt protease and phosphatase 100x (Thermo Fisher Scientific, Cat # 78440) for 30 minutes on ice. After centrifugation for 5 minutes at 12000rpm(4°C), the protein content of the samples was determined. 30µg and 45µg protein samples per lane were loaded onto NuPAGE®Novex® 4–12% Bis-Tris Protein Gels, 1.5 mm for electrophoresis (Invitrogen, Thermo Fisher Scientific, Cat # NP0335box) then blotted onto the nitrocellulose membrane by semi-dry method (Novex gel transfer stacks for iBlot®, Life Technology). We used the Ponceau S stain (Sigma-Aldrich, Cat # P7170-1L) to check the membrane, scan, label, and cut them in proper size. We washed nitrocellulose membrane with 5-10ml TBST for 5 min, 3x at room temperature. Non-specific blocking was performed by immersing the membrane in 5% albumin (Sigma-Aldrich, Cat # A1653) in Tris-buffered saline-Tween (TBS/T) for one hour at room temperature then washed it 3x for 5 min each with 5-10 ml of TBS/T. The membrane was incubated with primary antibody in 5-10 ml primary antibody, overnight at 4°C, then washed 3x for 5 min each with 15 ml of TBS/T. The membrane was incubated again with 5-10 ml of secondary antibody for 1 hr, on the rocker, at room temperature then washed 3x for 5 minutes each with 15 ml of TBS/T.

We used Smad2 (L16D3) mouse mAb (Cell Signaling, Cat # 3103) and phospho-Smad2 (ser465/467) antibody (Cell Signaling, Cat # 3101). We used the following working dilution for the primary antibodies: Smad2 1:1000, pSmad2 1:150, and GAPDH 1:500 (Santa Cruz, Cat # sc-47724, Dallas, TX, USA) and we used anti-mouse and anti-rabbit 1:10000 secondary antibody (Santa Cruz, Cat # sc-2031 and # sc-2030), incubated at room temperature for 1 hour or overnight as condition needed. We washed the membrane with TBS/T 3 times (10min/time), and HRP labeled secondary antibody for ECL marker. The membrane was incubated at room temperature for 1 hour and washed with TBS-T 3 times (10 min/time) for removal of excess antibody. The Pierce ECL Western Blotting Substrate (Thermo Fisher Scientific, Cat # 32106) was added to the membrane and incubated for 1 min without agitation. The membrane was wrapped and placed in film cassette with film (Thermo Fisher Scientific, Cat # 34090) in the dark room for optimal exposure condition before final film development. Experiments were done in triplicate but unlike RNA samples, these were not pooled. The resulting western blots were digitized for densitometry analysis. The films were scanned on an Epson V700 scanner, saved at 300 dpi TIFF file. Densitometry of the Western blots was then performed using the Adobe Photoshop CS6 Extended software.

#### *Preparation of Solutions and Reagents*

The lysis Buffer (per ml) was prepared by adding the following: 100x Protease inhibitor: 10 $\mu$ l (Halt protease inhibitor cocktails), 100x EDTA: 10 $\mu$ l (Thermal: Halt protease inhibitor cocktails), 100x phosphatase inhibitor cocktail

set I: 10 $\mu$ l (EMD Millipore, Cat # 524624, Bellrica, MA, USA), 100x phosphatase inhibitor cocktail set II: 10 $\mu$ l (EMD Millipore, Cat # 524625), 10x RIPA buffer: 100ul (Cell Signaling, Cat #9806) and diluted in 860ul DDW. The 10X TBS was prepared with 10 ml of 2 M Tris-HCl pH7.4, 100 ml of 5 MNaCl, 0.5 ml of 100% Tween 20, distilled water 890 ml. The 10X SDS Running Buffer (Invitrogen, Thermo Fisher Scientific, Cat # NP0001) was diluted in 1L DDW, and the 10X Transfer Buffer (Invitrogen, Thermo Fisher Scientific, Cat # NP0006-1) diluted in DDW -with 20% methanol. The wash buffer consisted of 1X TBS, 0.1% Tween-20 (TBS/T). We used Globulin-free Bovine Serum Albumin (BSA) 5% (weight to volume [w/v]), protein marker (Bio-Rad Precision plus protein standards), skim milk 5% (weight to volume [w/v]), and strip buffer (15g glycine/1gSDS/10ml Tween 20/pH2.2 in 1L DDW).

### **Taqman<sup>®</sup> Single Gene RT-PCR and Taqman<sup>®</sup> Array Analysis**

We transcribed the total RNA into cDNA for real-time analysis using the Superscript III kit (Invitrogen, Thermo Fisher Scientific, Cat # 18080-400). We prepared the RNA mix in a 0.2ml RNase-free PCR tubes by adding the following: 1 $\mu$ l annealing buffer, 1 $\mu$ l random hexamers (50ng/ $\mu$ l), 100ng of total RNA with molecular grade RNase-free water (Life Technologies, Cat # AM9937) to bring the total volume to 8 $\mu$ l. The PCR tubes were then placed in the Eppendorf Mastercycler at 65°C for 5 min then immediately placed on ice for at least 1 min. We collected the content of the tube and centrifuged for 1 min to add 10 $\mu$ l of 2x

First-Strand Reaction Mix and 2 $\mu$ l of Superscript<sup>®</sup>III/RNaseOUT<sup>™</sup> Enzyme mix to bring the total volume to 20 $\mu$ l. We vortexed the sample for 10-15 sec and collected the mix by centrifugation then placed the PCR tubes back in the Mastercycler for 10 min at 25°C, 60 min at 50°C, 5 min at 85°C, then placed the tubes on ice or stored at -20°C until analysis by real-time PCR. We obtained the following probes for our Taqman real-time PCR: GAPDH, HIF-1 $\alpha$ , and BMP4 (Life Technologies, Thermo Fisher Scientific, Cat # 4333764F, Hs00153153\_m1, and Hs00370078\_m1). We performed the real-time PCR assays similar to miRNA PCR assays except we mixed 10 $\mu$ l of the Master Mix (Life Technologies, TaqMan<sup>®</sup> Universal PCR Master Mix, no AmpErase<sup>®</sup> UNG, Cat # 4324018), 6 $\mu$ l of nuclease free water, 1 $\mu$ l of the Taqman probes, and 3 $\mu$ l of the cDNA - making a total of 20 $\mu$ l volume per reaction. We also ran all these real-time PCR assays in triplicate and set up the StepOnePlus<sup>™</sup> in a similar way to the miRNA analysis. Data from all real-time RT-PCR experiments were analyzed using the comparative  $\Delta$ Ct method.

To measure the differential TGF- $\beta$  gene expression in our miRNA knock-down (LNA-transfected) CCD-986Sk cells we used the TaqMan<sup>®</sup> Array Human TGF  $\beta$  Pathway, Fast 96-well Plate (Life Technologies, Cat # 4418742). This particular Taqman Array plate contains 92 probes for TGF- $\beta$  associated genes and 4 probes for candidate endogenous control genes; it targets genes encoding members of the TGF- $\beta$  superfamily of ligands including TGF- $\beta$  ( $\beta$ 1,  $\beta$ 2, and  $\beta$ 3), bone morphogenetic proteins (BMPs), growth and differentiation factors (GDFs), Activin A and B, Inhibin A and B, Nodal, and others (Figure 10). We

followed the recommended procedures to perform these experiments: First, we used the High-Capacity cDNA Reverse Transcription Kit with RNase inhibitor (Life Technologies, Cat # 4374966) to generate the cDNA. We prepared the 2x RT Master Mix by adding the following reagents supplied in the kit: 2.0µl 10x RT buffer, 0.8µl 25x dNTP mix (100mM), 2.0µl 10x RT random primers, 1.0µl MultiScribe™ reverse transcriptase, 1.0µl RNase inhibitor and 3.2µl nuclease free water to make a total volume of 10µl/reaction. We placed the 2x RT Master Mix on ice and mixed gently. We then added 1.1µg of RNA, diluted in 10µl of nuclease free water, to the 2x RT Master Mix and gently vortexed and centrifuged the sample for few seconds to run in the Mastercycler as follows: 25°C for 10 min, 37°C for 120 min, 85°C for 5 min, then placed on ice or stored at 4°C. Second, we downloaded the appropriate text file [.txt] from the provided information CD to the StepOnePlus™ system computer in order to set up the plate document and experiment according to the design of the plate. Last, we combined the cDNA with Taqman Fast Universal PCR Master Mix (Life Technologies, Cat # 4444557) then ran the plate in the StepOnePlus™ thermal cycler. For the 96 plate, we mixed our cDNA and DNase free water to make 540µl and that was added to 540µl of the Taqman Fast PCR Master Mix (for a total volume of 1080µl) that was gently vortexed and centrifuged for few seconds. We prepared the plate by centrifuging it at 1000 rpm for 1 min. We then removed the cover and dispensed 10µl of the cDNA/Fast Master Mix solution in each well of the plate. We covered the plate with a MicroAmp® Optical adhesive film (Life Technologies, Cat # 4360954), centrifuged it at 1000 rpm for 1 min and ran it at

50°C for 2 min, 95°C for 20 sec, and 40 cycles of 95°C for 3 sec /60°C for 30 sec. When setting up the StepOnePlus™ cyclers we selected the Fast mode and specified 10µl for the sample volume. Data acquisition and analysis using the relative standard curve quantitation method was carried out with the StepOnePlus™ ExpressionSuite Software (Life Technologies, v 1.0.2).

Assay ID	1	2	3	4	5	6	7	8	9	10	11	12
A	Hs00399001_s1	Hs00399005_m1	Hs00399009_m1	Hs00399008_m1	Hs00153826_m1	Hs00922289_m1	Hs00155668_m1	Hs00609603_m1	Hs00174915_m1	Hs00173716_m1	Hs00357608_m1	Hs00154592_m1
B	Hs00089639_m1	Hs00370076_m1	Hs00234830_m1	Hs00233470_m1	Hs00233476_m1	Hs00176144_m1	Hs00176148_m1	Hs00231733_m1	Hs00754870_s1	Hs00606098_m1	Hs00251092_m1	Hs00230638_m1
C	Hs00157619_m1	Hs00357739_m1	Hs00211913_m1	Hs00193363_m1	Hs00193364_m1	Hs00192033_m1	Hs00174443_m1	Hs00174431_m1	Hs00171410_m1	Hs00170103_m1	Hs00173582_m1	Hs00173745_m1
D	Hs000386449_m1	Hs00166367_m1	Hs00221445_m1	Hs00195432_m1	Hs00183425_m1	Hs00232222_m1	Hs00232068_m1	Hs00195437_m1	Hs00178696_m1	Hs00178696_m1	Hs00195441_m1	Hs00415443_m1
E	Hs00427259_m1	Hs00602137_m1	Hs00177066_m1	Hs00385075_m1	Hs00765707_m1	Hs00180562_m1	Hs00178463_m1	Hs00403062_m1	Hs00234686_m1	Hs00174932_s1	Hs00263889_s1	Hs00177373_m1
F	Hs00955491_gh	Hs00608187_m1	Hs00999918_m1	Hs00233424_m1	Hs00234245_m1	Hs00745761_s1	Hs00610319_m1	Hs00659661_m1	Hs00224267_m1	Hs00174428_m1	Hs00165760_m1	Hs00158605_m1
G	Hs0117001_m1	Hs00415315_m1	Hs00193764_m1	Hs00271552_s1	Hs00245109_m1	Hs00193614_m1	Hs00178154_m1	Hs00171132_m1	Hs00220998_m1	Hs00300274_m1	Hs00195156_m1	Hs00195300_m1
H	Hs00248256_m1	Hs00764428_s1	Hs00205566_m1	Hs00479759_m1	Hs00410929_m1	Hs00224203_m1	Hs00368884_gt	Hs00369406_m1	Hs00377065_m1	Hs00766203_m1	Hs00198143_m1	Hs00177023_m1
Gene Symbol	1	2	3	4	5	6	7	8	9	10	11	12
A	18S	GAPDH	HRT1	GUSB	ACVR1	ACVR1B	ACVR2A	ACVR2B	AMH	AMHR2	RHOA	BMP2
B	BMP3	BMP4	BMP5	BMP6	BMP7	BMPR1B	BMPR2	CREBBP	DCN	E2F4	E2F5	EP300
C	FNOD	FNIT4	GDF2	MST1	GDF3	GDF10	IFIG	IL6	INHBA	INHBB	INHBB	INHBC
D	LTBP1	LTBP2	LTBP3	SMAD1	SMAD2	SMAD3	SMAD4	SMAD5	SMAD6	SMAD7	SMAD9	NOGAL
E	PP2CA	PP2CB	MAPK3	MAPK3	RBL1	RBL2	ROCK1	BMPER	TSC2D1	SKP1	SP1	MAP3K7
F	TRIP1	TGFA	TGFB1	TGFB2	TGFB3	LEFTY2	TGFBR1	TGFBR2	TGFBR3	TIE	GDF5	LTBP4
G	CULT1	CHRD	BMP15	NOG	ZFYVE9	TGFBRAPI	ROCK2	GDF15	GDF3	RBX1	GDF11	STUB1
H	FST	LEFTY1	BMP10	HIPK2	SHURF1	SHURF2	INHBE	IL17F	ACVR1C	GDF7	MAP3K1P1	CDH1

**Figure 10.**The TaqMan® TGF-β pathway Array Plate. The arrangement of the 96 genes and controls in the plate as provided by Life Technologies (Cat # 4418742).

## Bioinformatics and Statistical Analysis

For quantitative data, including demographics, cellular density, real time RT-PCR data, and Western blot analysis we performed one-way ANOVA followed by Student-Newman-Keuls method for pairwise multiple comparisons on SigmaPlot® (Systat Software Inc. v 12.5, San Jose, Ca, USA). As for the Treg cell functional assays, the data were normalized (min-max) then transformed into suppression curves to calculate and compare the area under the curve (AUC) using ANOVA for repeated measures. Data are expressed as mean  $\pm$  SD unless otherwise specified. The miRNA microarray data were analyzed using the R, Bioconductor, and GeneSpring software. After cleaning and checking for data quality by standard methods for microarrays and Principal Component Analysis (PCA) we used a cutoff of  $\geq 1.5$ -fold differential expression as a threshold. Statistical t-test was then run on biological replicate samples to identify those miRNAs meeting a statistical threshold of  $p < 0.05$ . A Benjamini-Hochberg correction was used for minimizing type 1 errors associated with multiple testing. We performed on the first 12 microarray samples (representing 4 subjects/group) two sets of comparisons. First, to define the specific Treg miRNA signature for each cohort of subjects, we identified differentially expressed miRNA between Treg and Teff cells for that cohort (e.g. healthy Treg vs. healthy Teff cells, and COPD Treg cells vs. COPD Teff cells,...). Second, we did group comparisons of the miRNA expression within the same cell populations (healthy Treg vs. smokers Treg vs. COPD Treg cells) to identify miRNAs associated with each cohort of subjects but for that particular T cell phenotype.

## CHAPTER 3

### RESULTS

#### **FoxP3+ T Cells are Increased in the Lungs of Patients with COPD and Correlate with Disease Severity**

We have previously demonstrated, like other investigators(34;61;90), the presence of increased T cell infiltration into small airways in COPD, with a predominance of CD8+ cells(90;152). In order to examine the association between COPD and Treg cells we performed immunohistochemical staining and quantitated the presence of FoxP3+CD4+ in lung tissue of COPD patients and controls. We examined 49 lung specimens to include 8 non-smokers, 14 smokers, 3 patients with mild COPD (GOLD stage 1), 8 patients with moderate COPD (stage 2), 5 patients with severe COPD (stage 3), and 11 with very severe COPD (stage 4) (Table 2). Healthy smokers (n=14) showed no evidence of airflow obstruction. Lung tissue was obtained from lung reduction surgery, transplantations, and resection surgeries (of COPD patients and smokers), and unused donor lung (smokers and non-smokers). Despite screening first the lung tissue section with H&E staining, there were lower numbers of identifiable BALTs per case in non-smoker subjects compared to smokers and COPD patients. There was no difference in age and gender between the three groups. CD4+ cells were significantly lower in small airways of non-smokers and tended to be lower in BALTs as well. Our results show that FoxP3+ cells exist both in small

airways and BALTs (Figure 11) and that these cells are increased in COPD (expressed as /mm<sup>2</sup> and as % of CD4+ cells) compared to smokers in both BALTs and small airways (Table 2). Interestingly, the Foxp3/CD4+ percent within each group was no different between BALT and small airways suggesting that the same process is driving BALT and small airways Treg cell homing and recruitment.

**Table 2:** Characteristics of Subjects Having Immunohistochemical Analysis of FoxP3+ Cells

	COPD (n = 27)	Smokers (n = 14)	Non-smokers (n = 8)	p
Age, years	61 ± 7	55 ± 17	48 ± 17	ns
Gender, males	52%	50%	50%	ns
FEV <sub>1</sub> , % predicted	46 ± 24 <sup>‡</sup>	93 ± 12		<0.001
FEV <sub>1</sub> /FVC %	46 ± 17 <sup>‡</sup>	82 ± 12		<0.001
Number of patients with				
BALT	26	10	5	
Small airways	24	12	8	
Number of BALT analyzed	133 <sup>†</sup>	40	9	<0.05
Number of airway analyzed	100	45	28	ns
CD4+, cells/mm <sup>2</sup>				
BALT	1051 ± 536	1261 ± 1123	757 ± 532	ns
Small airways	98 ± 97	104 ± 105	29 ± 36 <sup>*</sup>	<0.05
Foxp3, cells/mm <sup>2</sup>				
BALT	319 ± 273 <sup>†‡</sup>	100 ± 128	143 ± 150	<0.05
Small airways	21 ± 28 <sup>†‡</sup>	9 ± 14	4 ± 6	<0.05
Foxp3/CD4+, %				
BALT	37 ± 39 <sup>‡</sup>	11 ± 18	29 ± 48	<0.05
Small airways	39 ± 108 <sup>‡</sup>	12 ± 19	27 ± 60	<0.05

\* Non-smokers versus smokers and COPD

† COPD versus smokers and non-smokers

‡ COPD versus smokers

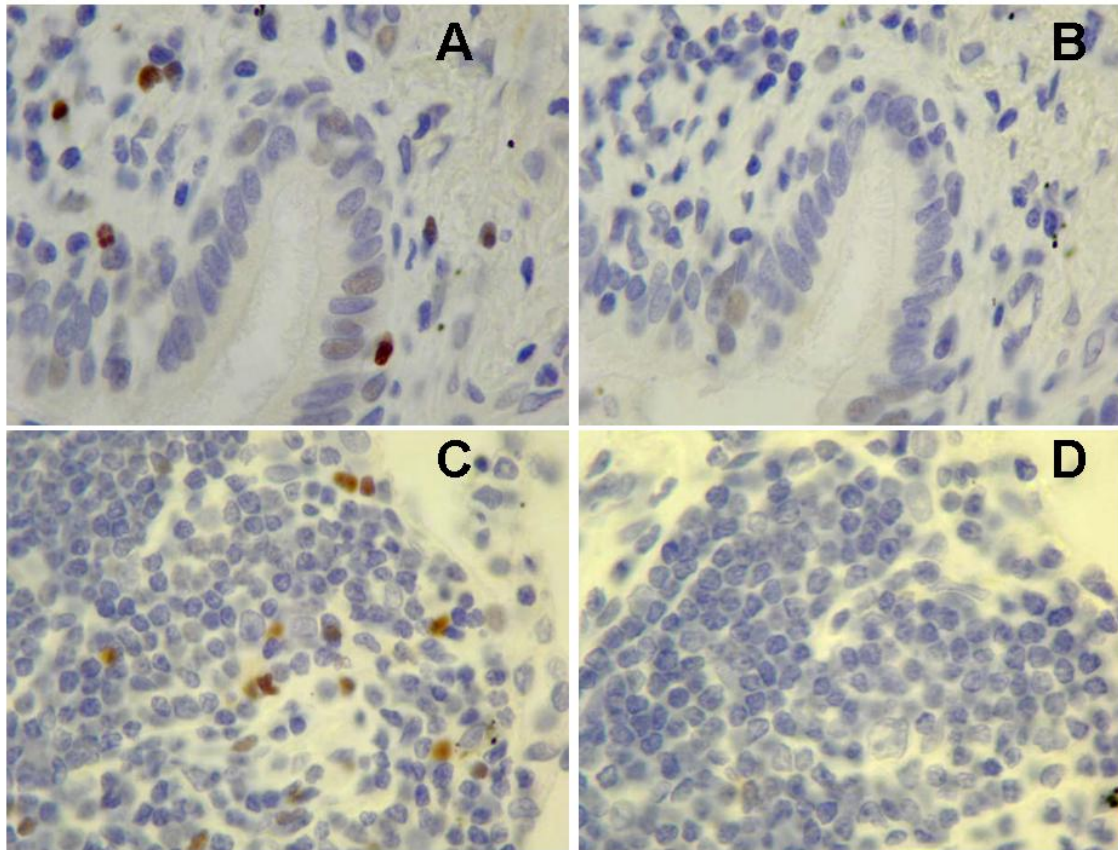


**Figure 11:** FoxP3 Immunohistochemical Staining of Lung Tissue. Panels A and B show a small airway and panels C and D show a BALT from a patient with COPD. Brown cells are positive for the intracellular staining of Foxp3+. Panels B and D are negative controls.

We then performed further statistical analyses on the same patients (Table 2) correlating FoxP3+ cells with both spirometry data and GOLD stages, classifying them into a control group (non-smokers and smokers), GOLD stages 1-2, and GOLD stages 3-4. Non-smokers were grouped with smokers because of their small numbers, lack of differences between them (except CD4+ in small airways), and presence of ex-smokers in the smokers group. Our results showed more FoxP3+ cells in small airways of patients GOLD stages 3-4 compared to control group, with similar trend that did not reach statistical significance in BALTs (Figure 12). The same association was observed when we analyzed the correlations between FoxP3+ cells (in both small airways and BALTs) with severity of disease based on degree of airflow obstruction and GOLD stages (Table 3).

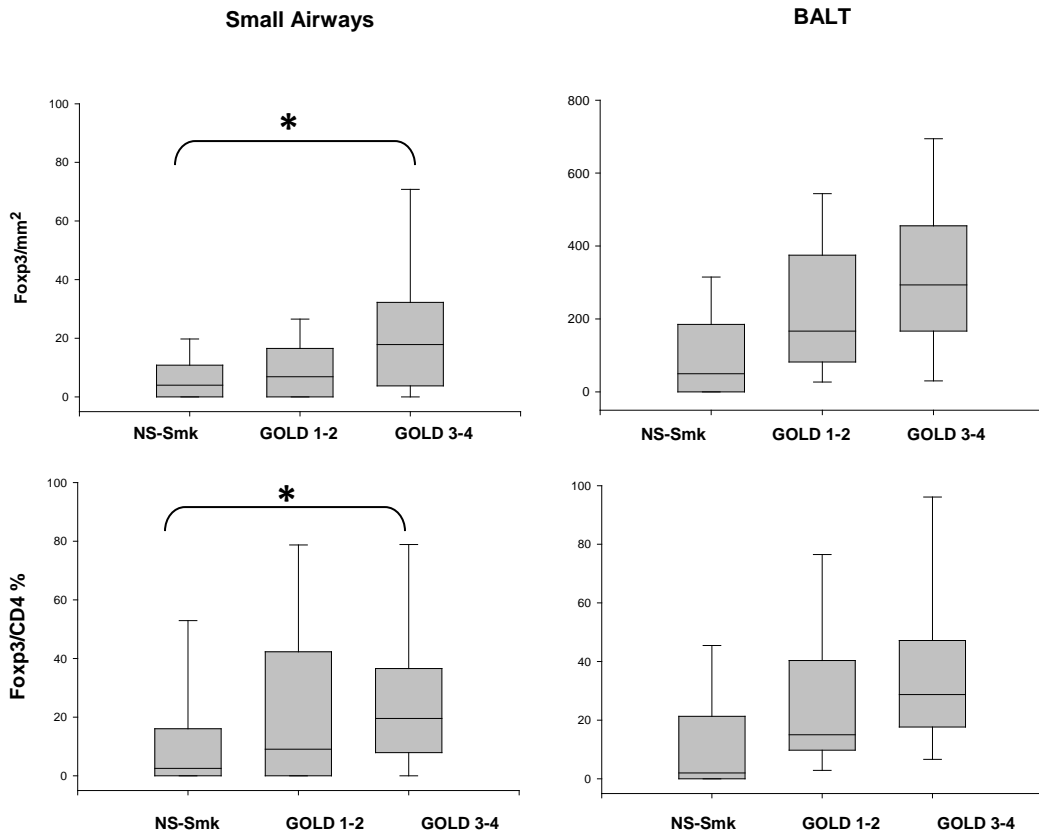


**Figure 12:** FoxP3+ Cells Density in Small Airways and BALTs. Data are expressed /mm<sup>2</sup> and as % of CD4+ cells in our COPD patients and controls.

\* p < 0.05. (NS= nonsmokers, Smk = smokers)

**Table 3:** Correlations of Foxp3+ and CD4+ Cells with Disease Severity

	Small Airways			BALT		
	CD4/mm <sup>2</sup>	FoxP3/mm <sup>2</sup>	FoxP3/CD4	CD4/mm <sup>2</sup>	FoxP3/mm <sup>2</sup>	FoxP3/CD4
Age	-	-	-	-	-	-0.18 (p = 0.05)
FEV <sub>1</sub> , % predicted	-	-0.26 (p = 0.01)	-	0.19 (p = 0.04)	-0.30 (p = 0.0004)	-0.20 (p = 0.04)
FEV <sub>1</sub> /FVC, % predicted	-	-0.30 (p = 0.005)	-	-	-0.34 (p <0.0001)	-0.25 (p = 0.01)
GOLD stage	0.22 (p = 0.001)	0.34 (p <0.0001)	-	-	0.38 (p <0.0001)	-
BALT area, mm <sup>2</sup>	-	-	-	-	-	-
CD4/mm <sup>2</sup>		0.55 (p < 0.0001)	-0.15 (p = 0.04)		-	-0.42 (p < 0.0001)

## **Non-Specific Suppressive Function of Peripheral CD4+CD25+ Treg Cells is not Impaired in COPD**

We tested the Treg cell suppressive activity by culturing these cells along with autologous Teff cells while serially diluting the Treg cell population in round-bottom 96-well plates, as described in Material and Methods (Figures 6 and 7). Effector T cells and Treg cells were isolated from peripheral blood mononuclear cells (PBMC) using the CD4+CD25+ Treg kit (Miltenyi Biotech). We confirmed the phenotype of the cells by flow cytometry (CD4-PerCP5.5, Foxp3-PE, eBioscience) demonstrating that our isolated CD4+CD25+ cells were 62-80% FoxP3+. Each well was stimulated with Treg Suppression Inspector beads (Miltenyi, Cat # 130-092-909) at a Teff cell to bead ratio of 1:1. After 4 days of incubation, we determined Teff cell divisions by CFSE dilution (Figure 8).

The Treg cell suppression assays were done in peripheral blood T cells obtained from healthy nonsmokers, smokers without COPD, and COPD patients (Table 4). We found significant variability of Teff cell proliferation curves within each group of subjects which may be attributed to either the purity of the isolated Treg cells or to the variability of Treg cell suppression and Teff cell responses, or to both factors. Consequently we observed no difference in Teff cell proliferation, hence no difference in Treg suppression, between COPD and both control groups (Figure 13).

**Table 4:** Demographics of Subjects Having Functional Treg Cell Assays

<b>Group</b>	<b>Healthy Non-smokers (n = 6)</b>	<b>Smokers without COPD (n = 10)</b>	<b>COPD (n = 7)</b>
<b>Age, years</b>	53 ± 10	54 ± 9	58 ± 8
<b>Gender (M)</b>	33%	62%	45%
<b>Race (AA)</b>	33%	75%	78%
<b>FEV<sub>1</sub>, % predicted</b>		95 ± 22	68 ± 12*
<b>FEV<sub>1</sub>/FVC, %</b>		74 ± 3	54 ± 13*

\* p < 0.01

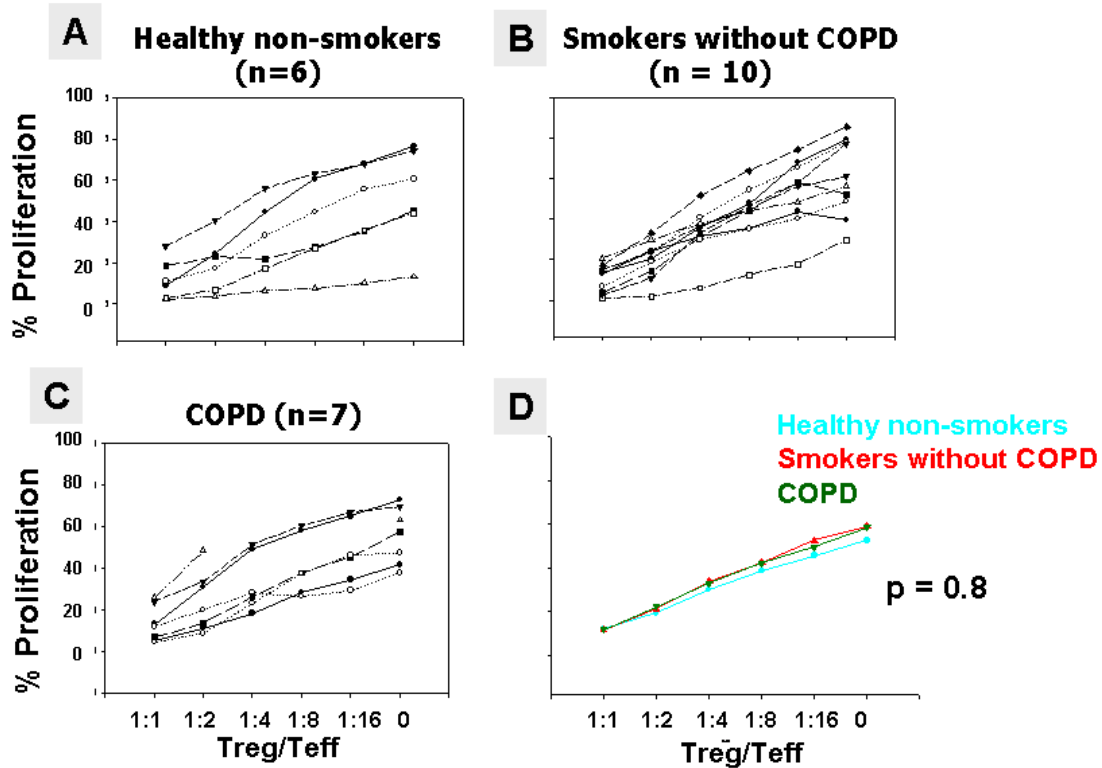


**Figure 13:** Teff Cell Proliferation Graphs in Our Three Groups of Subjects. Each line in every panel represents one individual in that group. Panel D shows no differences in the Teff proliferation (or Treg suppressive function) in the 3 groups (each line in panel D represents the mean Teff proliferation curve for each group of subjects).

## **Cigarette Smoke Alters the Treg Cell Function in COPD but not in Healthy Controls**

Before we determined the effects of cigarette smoke extract (CSE) on Treg cells function we performed toxicity assays in these cells. After identifying the optimal CSE concentration we repeated the Treg cell suppression experiments after exposing Treg cells to CSE. These experiments were done in a subset of subjects that were included in the previous functional Treg cell assays (Table 4). Our results show that after CSE exposure COPD isolated Treg cells increased suppression by 16% whereas there was no change in suppression in healthy Treg cells (Figure 14).

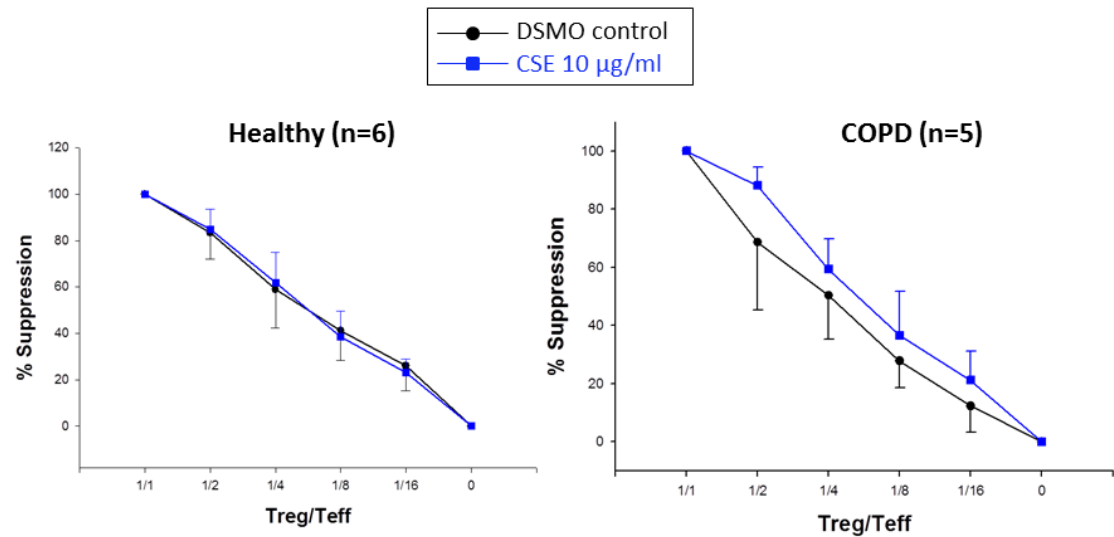


**Figure 14:** Treg Cell Suppression with Exposure to CSE. There is increased Treg suppression in CSE-treated Treg cells in COPD patients but not in healthy subjects ( $p = 0.9$  for healthy,  $p = 0.01$  for COPD)

## Improving Treg Cell Purity

To study gene expression and miRNA profile of Treg cells we changed the protocol for Treg cell separation. This was done because there were significant Foxp3<sup>-</sup> cells (20-38%) in the CD4<sup>+</sup>CD25<sup>+</sup> cell population. In addition, activated non-Treg CD4<sup>+</sup> cells may transiently express FoxP3 so we had to improve on the purity Treg cell population before performing the miRNA profiling to avoid a substantial miRNome overlap between Treg and Teff cells. We collected blood in EDTA tubes, obtained the PBMCs by Ficoll-Paque gradient centrifugation, isolated CD4<sup>+</sup> CD127<sup>-</sup> cells using magnetic cell separation (Miltenyi, Cat # 130-094-775), then used these purified cells in another Treg kit (CD25<sup>+</sup>CD49<sup>-</sup> T Cell Isolation Kit, Miltenyi, Cat # 130-094-551) to isolate our final CD4<sup>+</sup>CD25<sup>+</sup>CD127<sup>-</sup>CD49<sup>-</sup> Treg cells. T effector (Teff) cells were purified from a different CD4<sup>+</sup>CD25<sup>+</sup> Treg kit (Miltenyi, Cat # 130-091-30) isolating the CD4<sup>+</sup>CD25<sup>-</sup> cells as our Teff cells of interest. We confirmed the phenotype of the cells by flow cytometry (CD4-PerCP5.5, Foxp3-PE, eBioscience) and tested their suppressive activity as done in previous section by suspending  $50 \times 10^3$  cells along with  $50 \times 10^3$  Teff cells in culture medium in 96-well plates, while serially diluting the Treg cell population. The resulting Treg cell population was > 90% FoxP3<sup>+</sup> (Figure 9) and showed the typical suppression activity as demonstrated in prior assays.

## **Extracting RNA for miRNA Analysis**

We used mirVana miRNA Detection kit (Applied Biosystems, Life Technologies, Carlsbad CA) to extract total and low molecular weight (LMW) RNA from the purified Treg and Teff cells. We quantified the concentration of total RNA using the Nanodrop Spectrophotometer then used the Agilent Bioanalyzer to assess for quality of the microarray samples (Figure 9). We were able to obtain adequate samples from 4 COPD active smokers ( $FEV_1$   $52\pm 20\%$ ,  $FEV_1/FVC$   $47\pm 11\%$ ), 4 active smokers without COPD ( $FEV_1$   $84\pm 22$ ,  $FEV_1/FVC$   $82\pm 2\%$ ), and healthy never smokers. Subjects and patients were matched by age and gender for these experiments ( $p > 0.05$ ). All 12 samples were confirmed to have good quality RNA based on their RNA Integrity Number (RIN) and electropherograms. We labeled and hybridized 400ng to 500ng of the extracted RNA on the Human v2MicroRNA Expression BeadChips (Illumina, San Diego, CA).

### **COPD Affects Expression of miRNA in Peripheral**

#### **Treg Cells but not Teff Cells**

After baseline transformation and quantile normalization of the array scans, data were then exported in tab-delimited format and checked for quality. The miRNA profile in COPD Treg cells was more heterogeneous compared to healthy subjects. All of healthy samples in each of the two cell categories

exhibited strong correlation in principal component analysis (PCA) (Figure 15). For COPD we observed some degree of clustering in Teff cells but not in Treg cells suggesting that COPD, rather than smoking, may be in part responsible for miRNA differences. In total, 38 miRNAs could be considered Treg-specific since they were differentially expressed between Treg and Teff cells, 7 were found in COPD current smokers. Figure 16 shows the 38 miRNAs that were differentially expressed between Treg and Teff cells in the three subject groups with few miRNA overlapping between them. Of note miR-31, the one common to all samples, has been reported to be downregulated in Treg cells and has been validated to target FoxP3(112). This finding further confirms that we were successful in isolating the FoxP3+ Treg cell population. We also approached the miRNA analysis from a different perspective by performing group comparisons of their respective Treg cells independently of Teff cells, i.e. we compared the miRNA expression of COPD Treg cells versus smokers Treg cells versus nonsmokers Treg cells, in an attempt to identify disease-specific miRNAs. There were 6 and 96 miRNAs that were specific to COPD versus healthy nonsmokers and smokers respectively (Table 5). Remarkably, of the 743 miRNAs tested on the Illumina platform, we found no difference in miRNA expression between the Treg cells of healthy nonsmokers and healthy smokers. Moreover, the data show that the steady-state levels of miRNAs in Teff are not different in smokers, healthy and COPD, whereas the miRNAs changes were mostly observed in their Treg cells suggesting that miRNA alteration in Treg cells may play a role in the immune dysfunction in COPD.

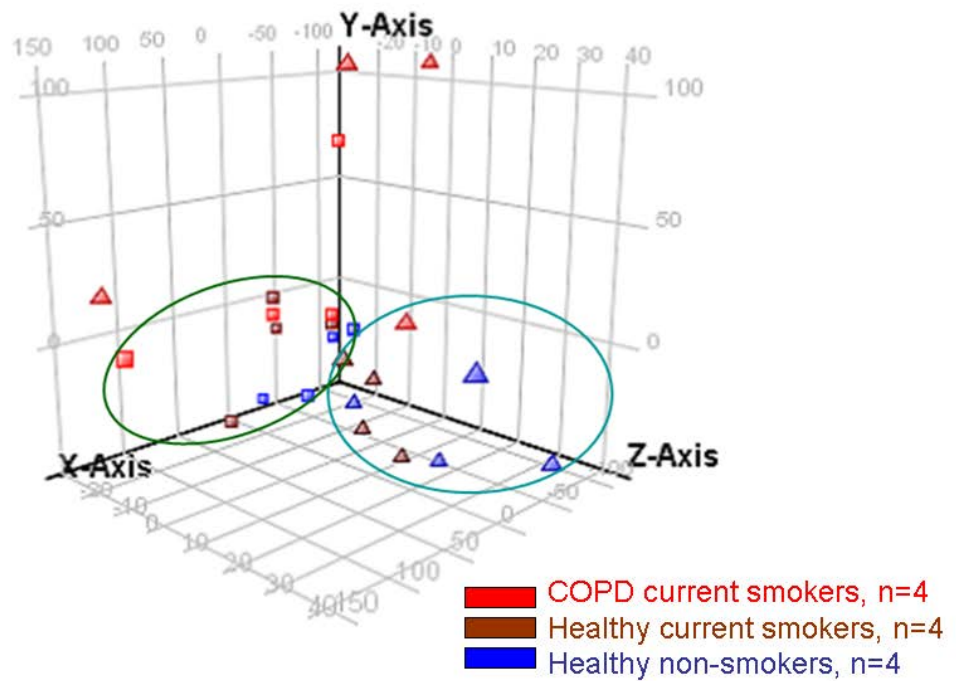


**Figure 15:** Clustering Based on Principal Component Analysis of the miRNome. 3-D graph demonstrating strong clustering of both cell phenotypes in healthy individuals (non-smokers and current smokers) but not in COPD patients. ▲ Treg cells; ■ Teff cells.

## Treg vs. Teff cells

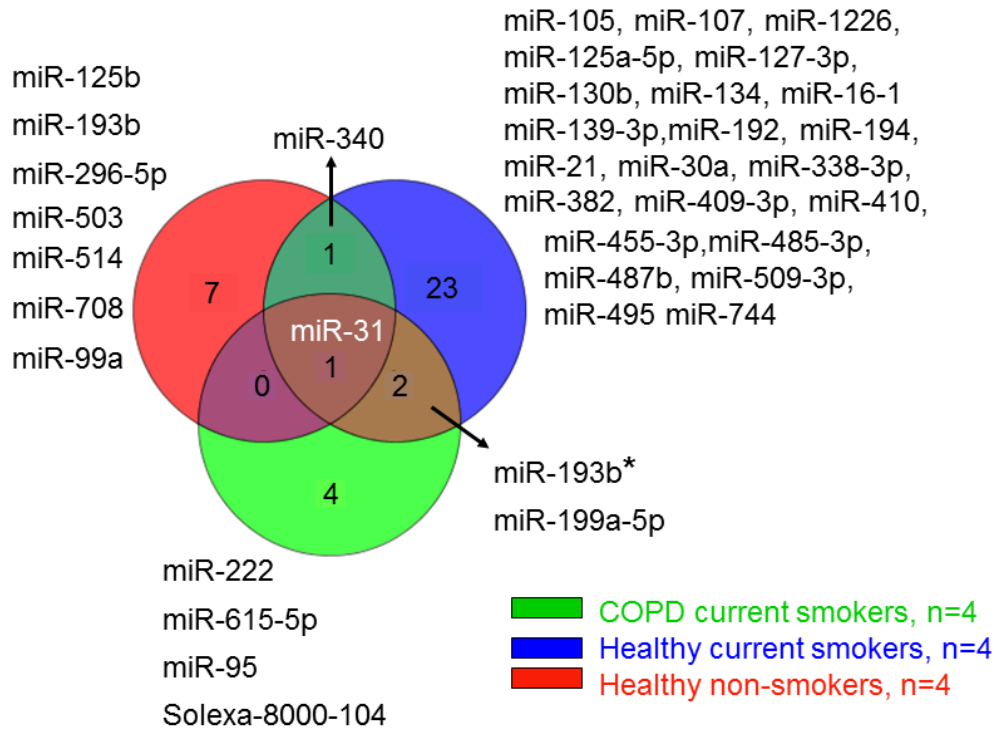


**Figure 16:** Differential Expression of Treg-Teff Cell miRNAs. Venn diagram showing the Treg-Teff cell miRNA differential expression in the three groups (n = 12 subjects, 4/group) based on our miRNA microarray analysis.

**Table 5:** Differential Expression of miRNAs in Treg Cells in the 3 Subject Groups*Healthy Smokers vs. COPD (n=4/group)*

<b>miRNA</b>	<b>Regulation</b>	<b>Fold Change</b>	<b>Corrected p-value</b>
HS_89	up	27.38317	0.01125464
HS_45.1	up	23.08529	0.01125464
hsa-miR-455-5p	up	16.383944	0.01125464
hsa-miR-588	up	13.59832	0.01125464
HS_239	up	6.163242	0.01125464
hsa-miR-485-3p	down	5.93402	0.01125464
hsa-miR-1226	down	5.129203	0.01125464
HS_279_a	down	3.141802	0.01125464
hsa-miR-24-2*	up	2.887127	0.01125464
hsa-miR-766	down	2.8561344	0.01125464
hsa-miR-1255a	down	2.3575296	0.01125464
HS_265.1	up	9.219544	0.013895049
HS_54	down	6.1080256	0.013895049
hsa-miR-129-5p	up	3.9794931	0.013895049
HS_261.1	up	23.864618	0.01403595
hsa-miR-1254	up	4.4488416	0.015032484
hsa-miR-518b	up	15.467727	0.015255101
HS_7	up	13.783942	0.015255101
HS_231	up	20.770237	0.016770795
hsa-miR-488*	up	19.46952	0.016770795
HS_9	up	8.412415	0.016770795
hsa-miR-382	down	5.043064	0.016770795
hsa-miR-1288	up	3.1544547	0.016770795
HS_140	up	32.486202	0.01796271
hsa-miR-130a*	up	16.472689	0.01796271
hsa-miR-512-5p	up	13.189547	0.01796271
hsa-miR-517a,hsa-miR-517b	up	12.700941	0.01796271
hsa-miR-1293	up	10.3773775	0.01796271
HS_69	up	10.135265	0.01796271
hsa-miR-557	up	9.471078	0.01796271
hsa-miR-220b	up	9.369737	0.01796271
hsa-miR-589	up	9.189124	0.01796271
hsa-miR-7-2*	up	8.774289	0.01796271

**Table 5, continued**

HS_86	up	8.203338	0.01796271
hsa-miR-585	up	5.713425	0.01796271
hsa-miR-219-1-3p	up	5.547852	0.01796271
hsa-miR-642	down	4.8320518	0.01796271
hsa-miR-1289	up	3.9599297	0.01796271
HS_3	up	3.6332407	0.01796271
HS_97	up	3.4529877	0.01796271
hsa-miR-495	down	3.0257738	0.01796271
hsa-miR-744	down	2.8843436	0.01796271
hsa-miR-92a-1*	down	4.3537264	0.018288007
hsa-miR-646	up	7.6273828	0.020417802
HS_131	down	3.0816085	0.020624436
hsa-miR-1282	up	14.016881	0.020950753
HS_280_b	up	4.933263	0.020950753
hsa-miR-133b	up	3.2376683	0.020950753
hsa-miR-493	up	20.183887	0.021170437
hsa-miR-9*	up	6.0745497	0.021170437
hsa-miR-148b	down	3.7227008	0.021170437
hsa-miR-520e	up	3.7197418	0.021170437
HS_104	up	2.3564506	0.021170437
HS_188	down	3.0010757	0.024830526
hsa-miR-671-3p	down	5.5437617	0.027729966
hsa-miR-645	up	2.9136062	0.027729966
hsa-miR-1247	up	2.315489	0.027729966
hsa-miR-15a*	up	24.498096	0.027765214
hsa-miR-595	up	18.01384	0.027765214
hsa-miR-1231	up	8.167572	0.027765214
hsa-miR-34a*	up	6.3349833	0.027765214
hsa-miR-940	up	3.138609	0.027765214
hsa-miR-664*	down	2.9273129	0.027765214
hsa-miR-532-5p	up	2.8860922	0.027765214
hsa-miR-193a-3p	up	2.2486937	0.027765214
hsa-miR-25*	down	2.0282176	0.027765214
hsa-miR-614	up	5.6294622	0.032409694
hsa-miR-1228*	down	2.4538271	0.03297551
hsa-miR-99b	down	7.825595	0.033210814
hsa-miR-1181	up	11.279975	0.034011308

**Table 5, continued**

hsa-miR-302b*	up	6.207734	0.034011874
hsa-miR-622	up	8.545404	0.03428022
hsa-miR-512-3p	up	8.479208	0.03428022
hsa-miR-654-3p	up	5.275083	0.03428022
hsa-miR-196a	down	3.790756	0.03428022
hsa-miR-1468	up	11.807145	0.036633596
hsa-miR-1301	up	2.6259694	0.036633596
hsa-miR-521	up	2.5828485	0.036633596
HS_33	up	9.56027	0.039744373
hsa-miR-130b*	down	3.1034508	0.039744373
HS_87	up	8.089956	0.04282038
solexa-3793-229	down	4.7279954	0.04282038
hsa-miR-302d	up	4.82556	0.043252748
HS_176	up	12.213609	0.04353352
hsa-miR-644	up	11.627363	0.04363611
solexa-7297-115	up	7.621438	0.04363611
hsa-miR-509-3p	up	4.8446107	0.04363611
hsa-miR-216a	up	4.044855	0.04363611
hsa-miR-1295	up	2.062371	0.04363611
HS_202.1	up	13.652235	0.045086987
hsa-miR-185	down	2.336318	0.045086987
HS_189.1	down	2.29202	0.045086987
hsa-miR-98	down	2.444851	0.047097936
hsa-miR-152	down	5.3975444	0.048580367
HS_52	up	3.2116907	0.048580367
hsa-miR-1200	up	2.770809	0.048580367

***Healthy non-smokers vs. COPD (n=4/group)***

<b>miRNA</b>	<b>Regulation</b>	<b>Fold Change</b>	<b>Corrected p-value</b>
HS_104	up	2.5134962	0.04564798
HS_131	down	3.1777682	0.02006529
HS_231	up	36.687412	0.036239892
HS_89	up	22.116358	0.036239892
hsa-miR-28-3p	down	2.4953096	0.005443225
hsa-miR-520e	up	4.571128	0.036239892

## **miR-199a-5p and HIF-1 $\alpha$ Are Downregulated in COPD Treg Cells**

We used quantitative real-time RT-PCR to confirm the differential expression of a select number of miRNAs. We analyzed the differential expression of miR-19b, miR-31, miR-95, miR-99a, miR-193\*, miR-199a-5p, miR-382, miR-485, and miR-520e, normalized to expression of endogenous control RNU48. All PCR were run in triplicate. Data from all qRT-PCR experiments were analyzed using the comparative  $\Delta\Delta C_t$  method. We chose a select subset of miRNAs based on their level of significance and potential function and we included miR-19b as control, which is known to have similar expression between Treg and Teff cells(151). We performed our validation on miR-31, miR-95, miR-99b, miR-193b\*, miR-199a-5p, miR-382, miR-485, and miR-520e in the same microarray samples, except for one sample because we ran out of his RNA, and enrolled additional subjects in each group (n=18) (Figure 17). As expected from our control, there was no difference in miR-19b expression between the Treg and Teff cells within and between the groups. We were unable to detect miR-99a and miR-520e in Treg cells based on the RNA concentrations we used. The expression of miR-31 and miR-193b\* was too low or undetectable in many of Treg cell samples to perform meaningful comparisons between the groups. As for miR-95, miR-199a-5p, miR-382, and miR-485-3p we only found significant differences in expression in two miRNAs between COPD and smokers' Treg cells, miR-95 and miR-199a-5p (Figure 17A). We decided to pursue and report on miR-199a-5p after we expanded our sample size (Table 6) because we were

able to maintain a statistical significant difference in the previous analysis and because this miRNA, in comparison to the rest of our selected miRNAs, had the most hits when we performed the *In Silico* analysis. We found miR-199a-5p to be significantly overexpressed in Treg cells compared to Teff cells ( $p < 0.001$ ) and that it was consistently upregulated by almost 4-fold in healthy smokers Treg cells than COPD and healthy nonsmokers Treg cells ( $p = 0.04$ ) (Figure 17B). We found a weak but significant correlation between miR-199a-5p expression and age ( $r^2 = 0.13$ ,  $p = 0.03$ ) but no significant associations/differences with % predicted FEV<sub>1</sub>, FEV<sub>1</sub>/FVC, race, gender, or being on inhaled corticosteroids.

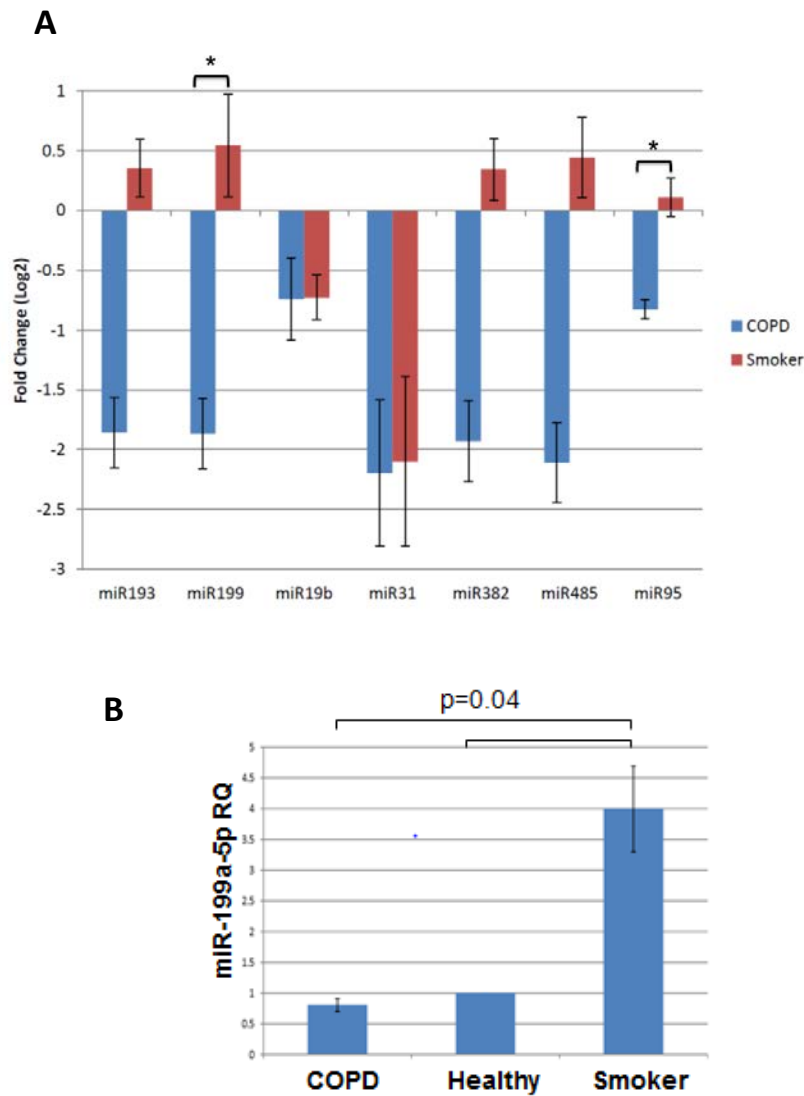


**Figure 17:** Differential miRNA Expression in Treg Cells by Real Time RT-PCR. **A.** Log2 RQ plots showing fold change for some of the RT-PCR validated miRNAs referenced to healthy nonsmokers in Treg cells. COPD patients and healthy smokers are referenced to healthy nonsmokers ( $n = 6, 7,$  and  $5$  respectively). \*  $p < 0.05$  between COPD and both healthy subjects, mean  $\pm$  SEM). **B.** Plot comparing miR-199a-5p expression between COPD and controls. This panel shows RQ plot, based on  $\Delta\Delta CT$  obtained from real time RT-PCR, fold change in expression of miR-199a-5p Treg cells in the 3 groups referenced to healthy non-smokers ( $n=35$ ; 12 healthy non-smokers, 12 healthy smokers, and 11 COPD patients). miR-199a-5p were normalized to expression of endogenous control RNU48. The COPD group had 1 less subject because his RNA sample ran out after running the microarray (mean  $\pm$  SEM).

**Table 6:** Demographics of Subjects Having miRNA Validation (n=12/group)

	Healthy Non-smokers	Current Smokers without COPD	Current Smokers with COPD
Age, years	53 ± 5	49 ± 6*	56 ± 5
Gender (male)	6	5	10
Race <sup>‡</sup>			
Caucasian	8	4	11
African American	2	8	1
Other	2	0	0
FEV <sub>1</sub> , % predicted		88 ± 15*	59 ± 19
FEV <sub>1</sub> /FVC, %		80 ± 5*	53 ± 12

\* p < 0.05, COPD vs. smokers without COPD. (postbronchodilator values)

‡ The proportion of racial composition in groups is different, p = 0.048

Data presented as mean ± SD.

HIF-1 $\alpha$  is a validated target of miR-199a-5p and modulates the Th17/Treg response(153) so we measured its expression in Treg and Teff cells. We found HIF-1 $\alpha$  to be downregulated by 41 $\pm$ 27% in Treg cells compared to Teff cells ( $p < 0.001$ ) and that its expression although lower in COPD versus healthy smoker Treg cells but it didn't reach statistical significance in this sample size (Figure 18). Surprisingly, HIF-1 $\alpha$  expression in Treg cells was weakly but positively correlated with miR-199a-5p expression ( $r^2 = 0.27$ ,  $p < 0.002$ ). There was no correlation between HIF-1 $\alpha$  and severity of disease, race, gender, and age.

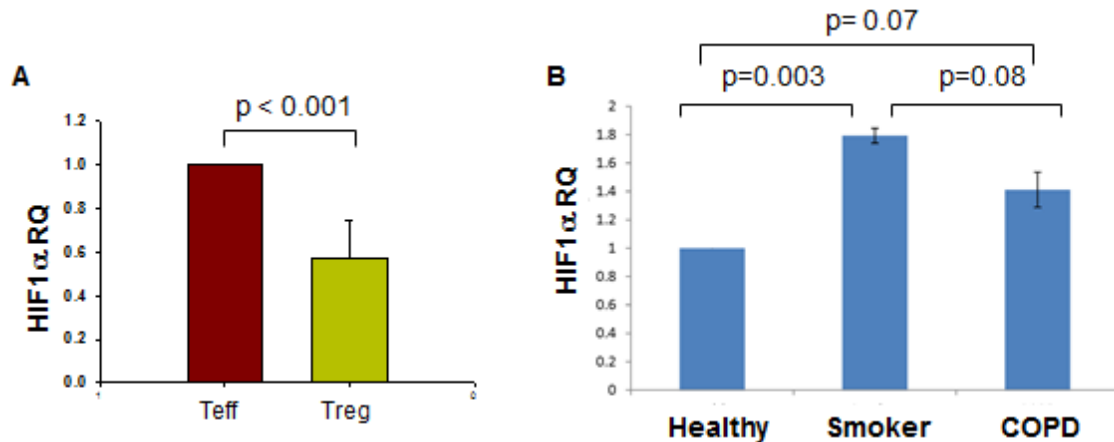


**Figure 18:** HIF-1 $\alpha$  Expression. RQ plot, based on  $\Delta\Delta CT$  obtained from real time RT-PCR, showing fold change in expression of HIF-1 $\alpha$  in all Treg and Teff cells (A) and in Treg cells in the 3 groups (B). HIF-1 $\alpha$  was normalized to expression of endogenous GAPDH. (A) There is a significant downregulation of HIF-1 $\alpha$  in Treg cells compared to Teff cells. (B) HIF-1 $\alpha$  expression in Treg cells in smokers was higher than in non-smokers Treg cells. (n=35; 12 healthy non-smokers, 12 healthy smokers, and 11 COPD patients, mean  $\pm$  SEM).

## ***In Silico* Analysis Identifies the TGF- $\beta$ Pathway and Putative Target Genes of miR-199a-5p**

Predicted mRNA targets under the regulatory control of the identified miRNAs were obtained from three databases (Targetscan, miRWalk, and miRanda) on miRWalk(150) and cross-referenced with published gene expression profiles of Treg cells(151). We then performed analysis of the intersected potential targets using the Ingenuity Pathway Analysis (IPA) platform to map them into networks, canonical pathways, and molecular function. We found a significant number of putative downregulated targets of miR-199a-5p in the mRNA 3' UTR region (Table 7)(151). These predicted genes were overrepresented in the cell movement, amino acid metabolism, and post-translational modification networks (scores = 2-13, Table 8). Ingenuity Pathway Analysis assigns network scores and p values for pathways that reflect the probability that each network or pathway can be achieved by chance alone. A score of 3 is considered to be significant (1 in 1000 chance that genes are integrated in that network by pure chance). The classification of these genes according to top pathways showed the strongest association with the TGF- $\beta$  signaling pathway (Table 9, Figures 19-20). We were also able to grow the TGF- $\beta$  signaling network by 7 additional molecules at 14 relationships when we included any gene that is associated with the interaction network and was identified as relevant within the miR-199a target list (Figure 21).

**Table 7:** Treg cell Genes that Are Predicted miR-199a-5p Targets

Gene Name	Treg v. Thelp (Stimulated)	Treg v. Thelp (Resting)	Treg v. Thelp (Stimulated)	Treg v. Thelp (Resting)
ANK3	-2.232	-1.773	0.001	0.012
ARHGEF12	-1.950	-1.534	0.010	0.096
ACVR2A	-1.538	-1.456	0.005	0.007
GLIPR1	-0.754	-1.093	0.053	0.078
ZNF215	-1.094	-0.766	0.017	0.069
SRGAP3	-0.626	-0.764	0.049	0.067
KLF12	-0.669	-0.724	0.021	0.079
C1GALT1	-1.036	-0.683	0.013	0.096
SOS2	-0.568	-0.546	0.015	0.034
ZNF117	-0.804	-0.506	0.062	0.094
GALC*	-0.682	-0.443	0.010	0.070

Differentially expressed Treg cell genes that are downregulated and are predicted targets of miR-199a-5p. The first 2 columns are log2 fold change, and the last 2 columns represent the respective FDR adjusted p value. \*GALC was predicted by miRanda only; all other genes were found in the three databases (Targetscan , MiRanda, and MirWalk).

**Table 8:** Top Networks of miR-199a-5p Targets

Associated Network Functions	Score*
Cellular Movement, Amino Acid Metabolism, Post-Translational Modification	13
Cardiovascular System Development and Function, Cell-To-Cell Signaling and Interaction, Connective Tissue Development and Function	3
Carbohydrate Metabolism, Cell-To-Cell Signaling and Interaction, Hematological System Development and Function	3
Gene Expression, Cell Cycle, Cell Morphology	3
Cell Death, Cell Cycle, Cancer	2

\* In Ingenuity Pathway Analysis a score of 3 is considered to be significant (1 in 1000 chance that genes are integrated in that network by pure chance)

**Table 9:** Top Canonical Pathways Associated with Predicted Targets of miR-199a-5p

Name	p-value
TGF- $\beta$ Signaling	1.4E-03
Axonal Guidance Signaling	2.3E-03
PPAR $\alpha$ /RXR $\alpha$ Activation	6.6E-03
Breast Cancer Regulation by Stathmin1	8.4E-03
Actin Cytoskeleton Signaling	1.1E-02



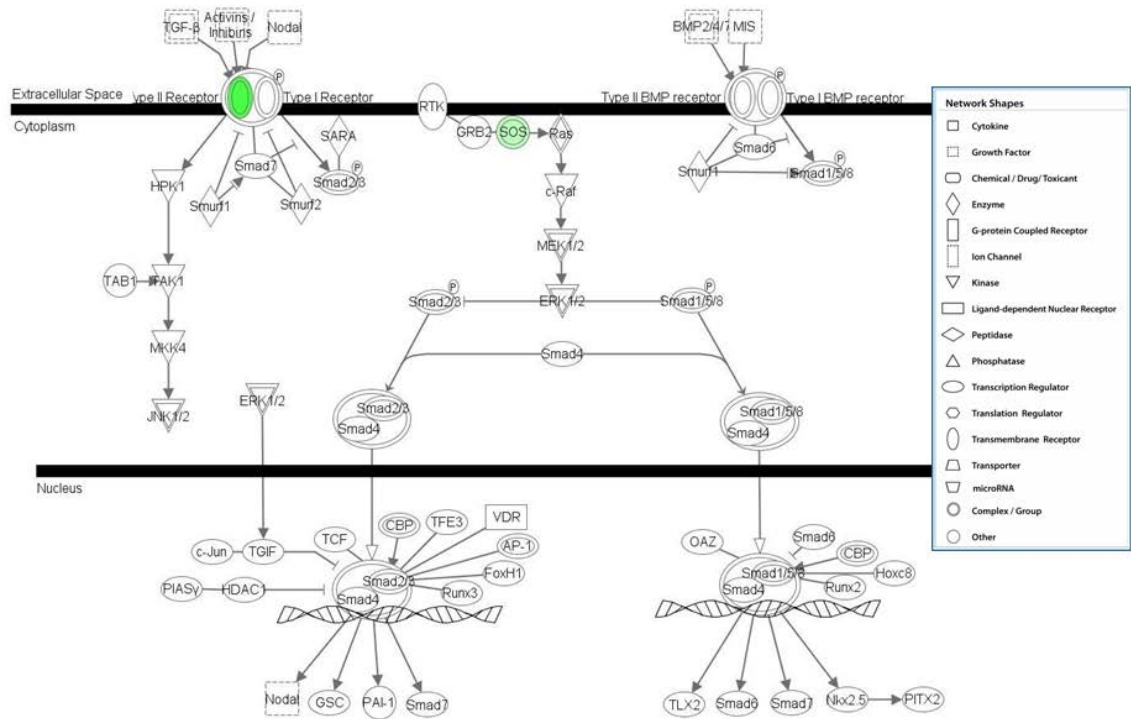


**Figure 20: TGF- $\beta$  and PPAR $\alpha$  Signaling Pathways.** Ingenuity Pathway Analysis of the TGF- $\beta$  and PPAR $\alpha$  signaling pathways overlapping with same components. (PPAR $\alpha$  activation pathway,  $p = 0.006$ ).

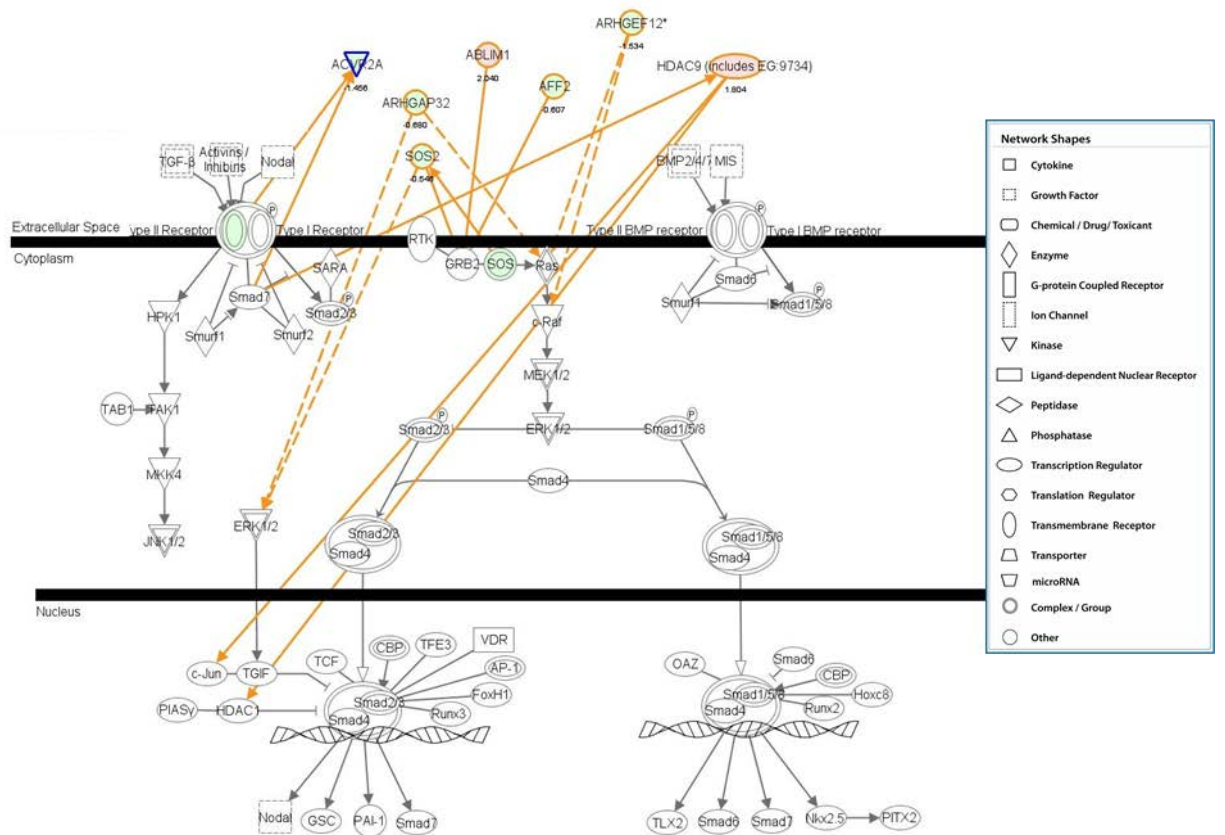


**Figure 21:** Growing the Signaling Network. We included any gene that appear from the miR-199a target list adds 7 additional molecules at 14 relationships to the TGF- $\beta$  signaling pathway.

## **Knockdown of miR-199a-5p Upregulates the Expression Of Some of Its Predicted Target Genes**

To analyze the TGF- $\beta$  pathway we used TGF- $\beta$  treated CCD-986Sk human fibroblast cells (ATCC) and ran their mRNA on TaqMan<sup>®</sup> Array Human TGF- $\beta$  Pathway 96-well plates (Life Technologies, Cat # 4418742) (Figure 10). We used these particular cells because they are known to endogenously express miR-199a-5p(131).

To assess the potential functional activity of miR-199a-5p miRNA we transfected the CCD-986Sk cells with LNA<sup>™</sup> microRNA inhibitor and negative control then treated them with TGF- $\beta$ . The final optimal concentrations for LNA and Lipofectamine that yielded > 90% transfection efficiency were: 100 pmole LNA and 3.5  $\mu$ l of Lipofectamine. We assessed the transfection efficiency under direct visualization using fluorescently labeled miRCURY LNA<sup>™</sup>. Our transfection efficiency was achieved without causing significant cell death or changing the phenotype of the cells (Figure 22). We also performed Western Blot analysis of phosphoSmad2 (pSmad2) to confirm activation of the TGF- $\beta$  pathway (Figure 23A). Our results show that miR-199a-5p may serve to repress expression of some of the gene in the panel in vitro, most pronounced being genes within the bone morphogenic protein (BMP) pathway (Figure 23B).

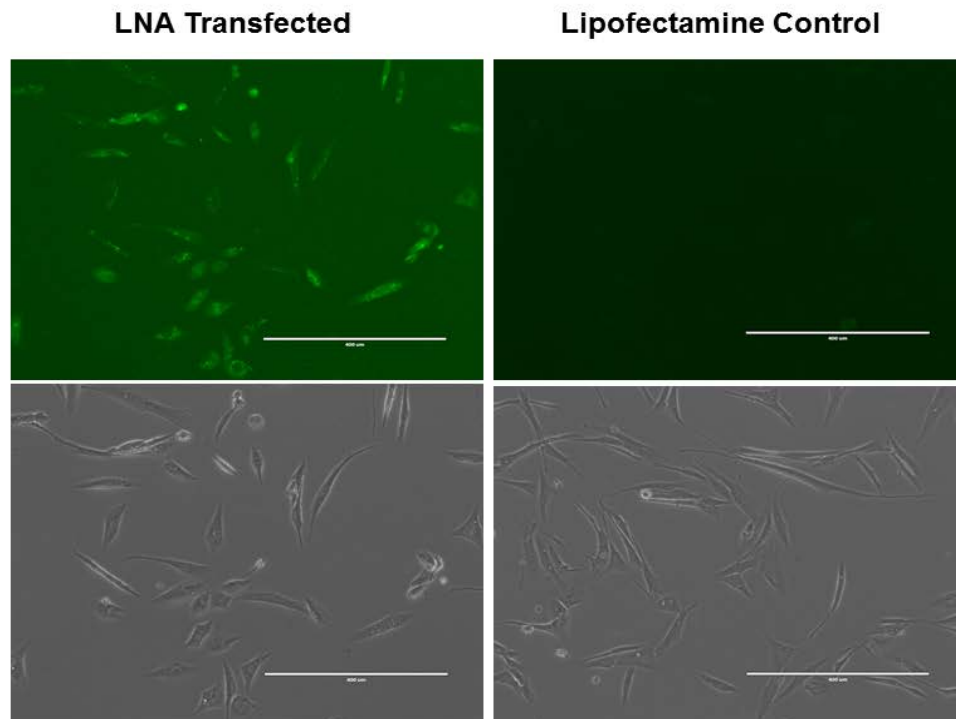


**Figure 22:** Transfection of CCD-986Sk Cells With LNA. Photomicrographs of CCD-986Sk cells obtained 48 hours after the transfection reaction with 3'-fluorescein labeled miR-199a-5p miRCURY LNA™ microRNA inhibitor versus Lipofectamine™ 2000. The negative control miRCURY LNA™ showed the same transfection efficiency (>90%) as the miR-199a-5p miRCURY LNA™ inhibitor.

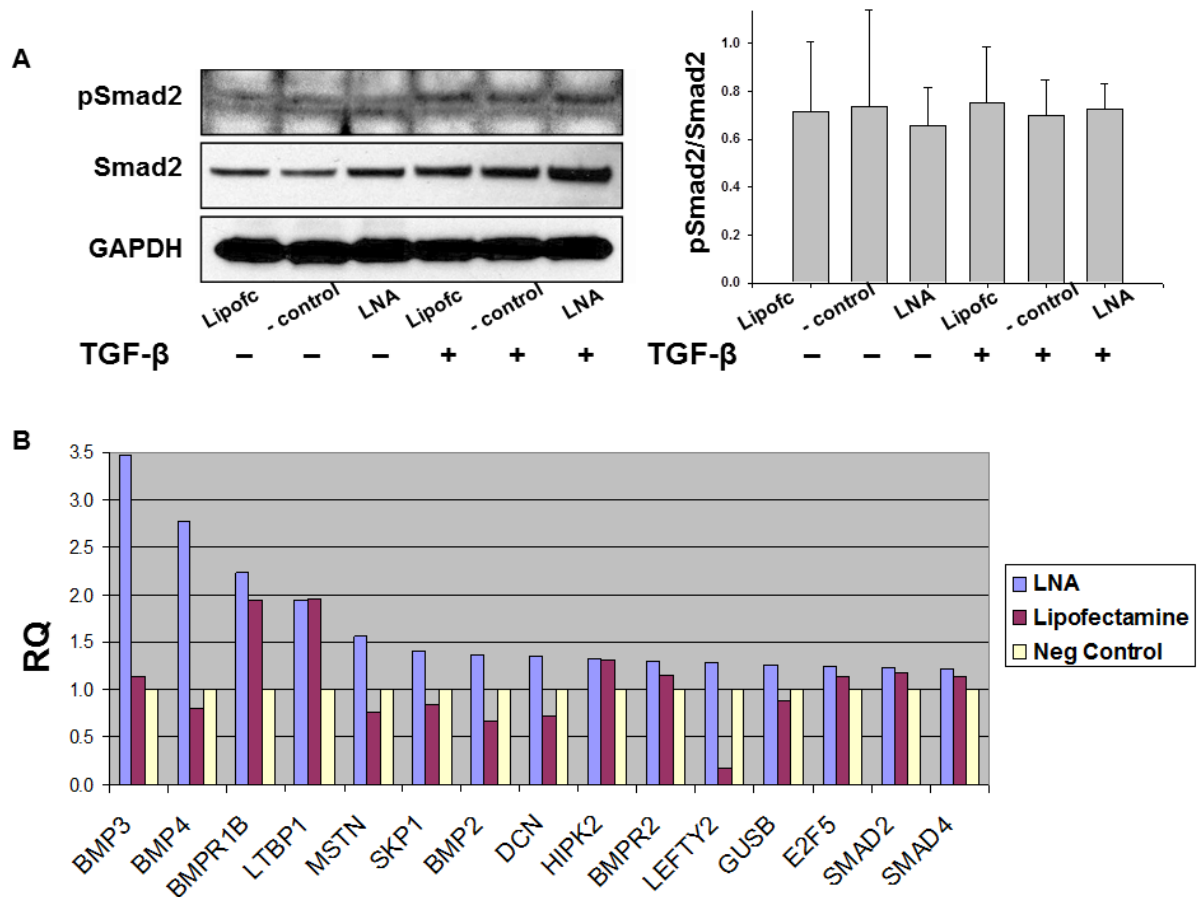


**FIGURE 23:** Effects of miR-199a-5p Inhibition on TGF-β Pathway in CCD-986Sk Cells. A- Western blot analysis of miR-199a-5p LNA transfected CCD-986Sk cells treated with TGF-β compared to Lipofectamine control and negative control shows no difference in pSmad2 expression when normalized to Smad2 ( $p = 0.92$ ). The same was noted when pSmad2 was normalized to GAPDH. Data are presented as mean  $\pm$  SD,  $n = 3$ . B- RQ plot obtained from the Taqman TGF-β array plate analysis of the pooled RNA of LNA transfected CCD-986Sk cells showing fold change of genes that were overexpressed by  $> 20\%$  versus negative control ( $n = 3$ ).

The disinhibition of BMP3 and BMP4 was most pronounced in the CCD-986Sk cells without any increase in Smad expression which suggests that miR-199a-5p may be playing its role by regulating the Smad-independent pathways. We were also interested in analyzing the expression of HIF-1 $\alpha$  in our knockdown model because HIF-1 $\alpha$  is a validated target of miR-199a-5p and a modulator of the T cell response(150;153). As expected, we observed an increase HIF-1 $\alpha$  expression with miR-199a-5p inhibition and TGF- $\beta$  treatment but it didn't reach statistical significance possibly because of small sample size (relative expression of HIF-1 $\alpha$  in negative control and LNA  $1.39 \pm 0.27$  and  $1.52 \pm 0.26$  compared to Lipofectamine control, n=3, p = 0.2).

### **Overexpressing miR-199a-5p Downregulates BMP4 Gene**

#### **Expression in MOLT-4 cells**

We used MOLT-4 cells, a lymphoblastic leukemia cell line, to study the effects of overexpressing miR-199a-5p on BMP4 regulation. We found that this cell line does not express miR-199a-5p, had better survival and transfection efficiency, and had higher expression of BMP4 with EGCG stimulation by real-time RT-PCR. EGCG is a polyphenol and is the most abundant catechin in tea; it is found mainly in white tea, green tea and, in smaller quantities, black tea. EGCG is a strong topoisomerase inhibitor similar to certain chemotherapeutic antineoplastic agents but may reduce the bioavailability of other drugs(154). MOLT-4 cells were transfected with a miRNA mimic and labeled control,

(miRIDIAN microRNA Human Hsa-miR-199a-5p and miRIDIAN microRNA transfection control with Dy547) diluted in Dharmacon 5X siRNA Buffer. We treated transfected MOLT-4 cells with 10 and 50nM of EGCG diluted in 1:1000 DMSO for 48 hours but the 50nM gave a more pronounced increase in BMP4. The same aforementioned kit was used to extract RNA followed by Taqman<sup>®</sup> real time RT-PCR to quantitate BMP4 gene expression. We noted that overexpression of miR-199a-5p in MOLT-4 cells resulted in significant downregulation of BMP4 expression which also supports the observation that some BMP members may be directly or indirectly regulated by miR-199a-5p (Figure 24).

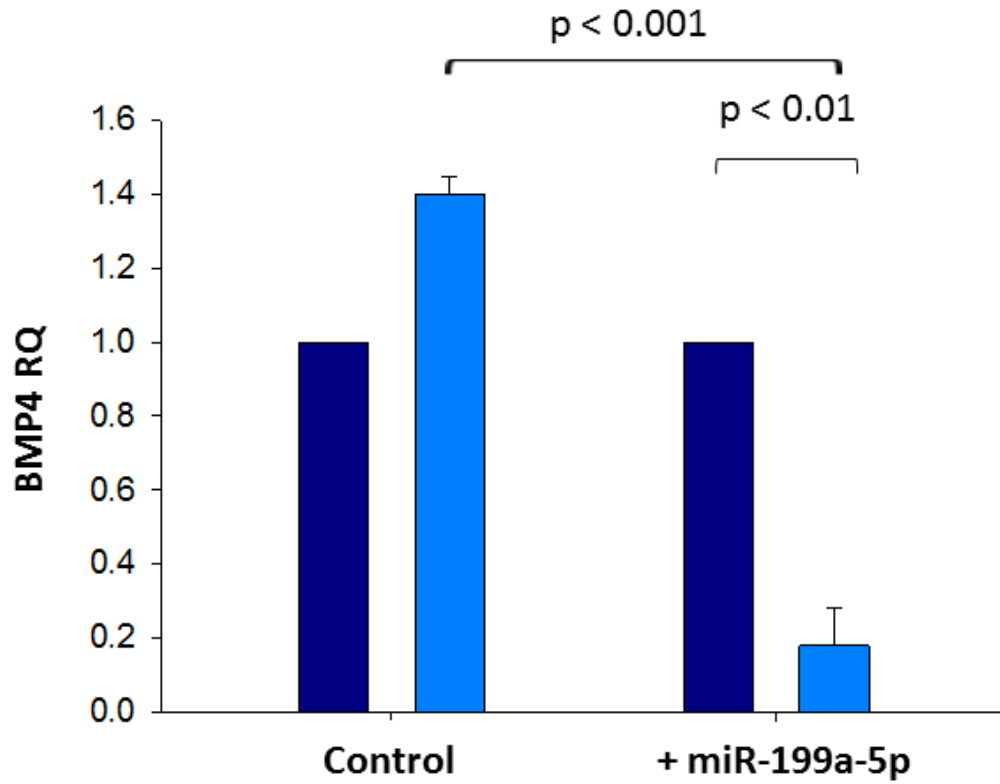


**Figure 24:** Effect of miR-199a-5p Overexpression on BMP4 in MOLT-4 Cells. miR-199a-5p resulted in > 80% suppression of BMP4 expression after treatment with epigallocatechin gallate (EGCG) (n = 3, mean  $\pm$  SEM, light blue color columns + EGCG treatment diluted in DMSO vs. dark blue columns DMSO only).

## CHAPTER 4

### DISCUSSION

There is an exaggerated T cell inflammatory response in COPD with evidence of a disturbed balance between the various CD4+ populations including Th1, Th17, and Treg cells(68;69;71) but current knowledge about mechanisms contributing to such observations remains fairly limited. In addition, earlier and even more recent investigations regarding Treg cells in COPD have demonstrated conflicting results(49;82;83). The main goal of this project was to characterize the Treg cell response in COPD with the initial focus revolving around the Treg cell function. We then moved on to investigate the Treg cell miRNA expression in order to identify particular pathways that are involved in modulating their function and/or regulation. First, we found a correlation between lung FoxP3+ cells and disease severity but we didn't observe any difference in the function of blood-isolated Treg cells between COPD and control subjects. Second, we observed a significant change in the Treg cells suppressive activity with exposure to cigarette smoke extract in COPD but there was a great variability in response. With the limitations of the *ex vivo* functional assays in mind, we proceeded to isolate a highly purified peripheral Treg cell population so to compare their miRnome to that of Teff cells. We found that COPD, rather than smoking, has a significant impact on miRNA expression profile in Treg cells based on the miRNA microarray analysis. We confirmed specific miRNAs that

were identified in the microarray miRNA signature of smokers with and without COPD and found that the miR-199a-5p response is significantly blunted in COPD Treg cells compared to Treg cells in healthy unaffected smokers. We also showed that miR-199a-5p was specific to Treg cells, versus Teff cells, and that a significant overrepresentation of its target genes was found in the Treg cell transcriptome. Importantly, many of the identified miR-199a-5p target genes were associated with the TGF- $\beta$  signaling pathway. Interrogating the TGF- $\beta$  pathway in select cell lines also suggested that BMP signaling may be regulated by miR-199a-5p and implicating a non-Smad2 component within the TGF- $\beta$  signaling pathway.

Studies that addressed the active immune suppressive mechanisms involving Treg cells in COPD are inconclusive(49;77;80;152;155). However, more recent data suggest that a Treg cell pro-inflammatory response prevails in COPD, rather than having an exaggerated suppressive activity(12;68;69;71). We observed a correlation between the lung Treg cell density and severity of airflow obstruction which may suggest that the Treg cell response is disturbed and contributes to development of COPD. However, as with most descriptive data, it is not possible to conclude whether the Treg cell increase in lung tissue is pathogenic or not. Unfortunately the design of the initial experiments was of major limitation in trying to reach a conclusion regarding the Treg cells suppressive activity in our patient population. In retrospect, it was not surprising to see no difference in Treg cell function with just anti-CD3/CD28 mAb Teff cell stimulation as there are probably many other factors that are involved in shaping

the Treg cell differentiation and function (e.g. oxidative stress and presence of other activators of the adaptive and innate immunity); in addition, identical results were obtained when almost the same protocol was used by other investigators (using soluble anti-CD3 and CD28 mAb along with irradiated T cell-depleted PBMC cells as antigen presenting cells [APCs])(49). Likewise, in cigarette smoke exposed mouse model, and performing a slight variation of our Treg suppression assay to stimulate the responder T cells (using Dynabeads M-450 Epoxy coated with anti-mouse CD3e Ab) there was no evidence of any change in Treg cell suppression(156). On the other hand, the two studies that had a different approach to study Treg cell function reported conflicting results with one study showing impaired Treg cell suppression(83) while the other study showing excessive suppression in COPD compared to controls(82). In the first study, the investigators co-cultured Treg-depleted and non-depleted PBMCs stimulated with staphylococcal enterotoxin-B (SEB) then analyzed T-cell activation by HLA-DR expression; they reported that 15/15 healthy controls and 9/14 COPD patients demonstrated adequate Treg-mediated suppression. The remaining 5 COPD patients had evidence of a failure of Treg-mediated suppression. Of note, patients with impaired Treg suppression had a higher body mass index (BMI) (33–38 kg/m<sup>2</sup>)(83). In the second study, Teff cells (CD4+CD25–CD127+) were stimulated with endotoxin-free P6 lipoprotein in the presence or absence of autologous Treg cells (CD4+CD25+CD127–) at a 2:1 ratio of Teff to Treg cells. Importantly and relevant to this study, the same investigators had shown that lymphocytes from patients with COPD who had frequent nontypeable

*Haemophilus influenzae* (NTHI) exacerbations responded poorly to P6 lipoprotein, which is an outer membrane protein of NTHI(82). Therefore, the sum of all these functional studies do not appear to be sufficient to conclude, or to generalize, that Treg cell function in COPD is overly or inadequately suppressive causing recurrent infection versus uncontrolled lung inflammation; hence, this experimental approach does not seem to be ideal to answer this question. In view of the limited results with the functional Treg suppression assays, I proceeded to study the miRNA profiles of the Treg cells in order to identify potential pathways that can explain the shift in the Treg/Th1 and Th17 cell balance.

More convincing data showing a predominance of a pro-inflammatory Treg, as well as a Th1 and Th17, cell responses were obtained from studies that analyzed T cell phenotypic changes under various conditions. Shan et al. examined chemokine receptors expression induced by lung APCs and found that only lung APCs isolated from subjects with emphysema induced expression of Th1 and Th17 cell-specific chemokine receptors in PBMC-derived CD4+ cells (CXCR3 and CCR5 for Th1 and CCR4 and CCR6 for Th17)(68). They showed that the expression of FoxP3 was upregulated in CD4+ cells cultured with lung myeloid dendritic cells from controls but not emphysema under similar conditions. Furthermore, and to support of their findings, the investigators found significantly larger numbers of CD4+ cells that express CCR4/CCR6 and CXCR3/CCR5 in the lungs of individuals with emphysema when compared to controls. They also

demonstrated that with increasing concentrations of IL-17A and IFN- $\gamma$  lung macrophages expressed CCL20 thus sustaining recruitment of the pro-inflammatory DCs to the lung and inducing MMP12 expression. Chen et al. studied the effects of cigarette smoking on CD4 cell differentiation in mouse model and reported that smoking is a selective adjuvant that augments mucosal Th17 but not Th1 cell differentiation(71). They substantiated the role of Th17 cells in the development of emphysema by observing that IL-17RA $^{-/-}$  mice had reduced macrophage recruitment with lower CCL2 and CXCL10 in BAL and failure to develop emphysema after 6 months of cigarette smoking compared to wild type (WT) mice. In another mouse model of COPD induced by chronic cigarette smoking, Wang et al. found a significant increase in lung Th17 cells, along with their corresponding cytokines (IL-17A, IL-6 and IL-23), in smoking mice(85). They reported that lung tissue Treg cells were decreased with cigarette smoke exposure and noted a similar tendency for the Th17/Treg ratio in peripheral blood. These findings were duplicated by Eppert et al in their cigarette smoke mouse model(156) and are likely to be of relevance in humans because Di Stefano et al also found increased expression of some of the Th17-related cytokines (IL-17A, IL-22 and IL-23) in bronchial airways of COPD patients(69). Hou et al, on the other hand, separated the FoxP3 $^{+}$  Treg cell population in peripheral blood into a suppressive versus pro-inflammatory phenotypes (resting Treg cells [CD25 $^{++}$ CD45RA $^{+}$ ], activated Treg cells [CD25 $^{+++}$ CD45RA $^{-}$ ], and IL-17 and IFN- $\gamma$  secreting Treg subset [CD25 $^{++}$ CD45RA $^{-}$ ])(78). They found a decrease in both resting and activated blood Treg cells (the suppressive

phenotypes) and an increase in the cytokine-secreting Treg cells (the pro-inflammatory phenotype). They showed also that the imbalance in Treg cell populations was found in local Treg cells (from BAL) and that it was significantly associated with severity of airflow obstruction along with enhanced CD8 cell activation(78). Taken together, these studies support the concept of a modulated CD4+ cell reaction in COPD characterized by a dominant Th1 and Th17 responses and a weakened Treg cell suppressive response.

While mechanisms for the observed Th17/Treg cell imbalance and Treg cell dysfunction have not been explored in most of the aforementioned studies a number of transcription factors(153;157) and miRNAs(158) have been reported to modulate the Treg cell response, some of which could be involved in COPD and explain such shift. Smoking components could activate aryl hydrocarbon receptors (AHR) which are ligand-activated transcription factors involved in reactivation of xenotoxic metabolism(14). In animal models activation of the AHR on both CD4+ and CD8+ cells leads to suppression of the cytotoxic T cell response(15). Lin et al compared wild type Treg cells to ones with mutant FoxP3 expression and showed that the AHR is expressed at 5 folds higher levels in the normal Treg cells (in supplement)(159). The investigators have done also comparisons between the normal Treg cells and normal conventional cells, and found a 3 fold enrichment of these receptors in the normal Treg cells as compared to normal conventional T cells. Importantly, Quintana et al demonstrated that AHR activation by its ligand 2,3,7,8-tetrachlorodibenzo-p-

dioxin (TCDD) induced functional Treg cells that suppressed experimental autoimmune encephalomyelitis. They also found that AHR activation by 6-formylindolo[3,2-b]carbazole (FICZ) interfered with Treg cell development, boosted Th17 cell differentiation and increased the severity of experimental autoimmune encephalomyelitis in mice(157). Thus, AHR regulates both Treg and Th17 cell differentiation in a ligand-specific fashion in a way that resembles TGF- $\beta$ 1, which is also known to be critical differentiation factor for both. Similarly, Chen et al showed that CSE augmented IL-17 and IL-22 expression in Th17 cells postulating that one mechanism by which cigarette smoke acts as a Th17 adjuvant is via AHR. In support of their conclusion, they found that T cells from Ahr<sup>-/-</sup> mice did not show increased Th17 differentiation with CSE or with FICZ(71). Other metabolic factors such as retinoic acid and hypoxia have been reported to be involved in reciprocal regulation of Treg and Th17 cell differentiation(153;160). Mucida et al reported that retinoic acid is capable of inhibiting the IL-6–driven induction of the Th17 cells and promoting Treg cell differentiation(160) whereas Dang et al found that HIF-1 $\alpha$  promotes Th17 differentiation (by directly inducing ROR $\gamma$ t transcription) and inhibits Treg differentiation(153). Dang et al also found that the highest HIF-1 $\alpha$  expression in CD4 cells was found in Th17 cells(153). When we compared the expression of HIF-1 $\alpha$  between Treg and T responder cells we found that Treg cells have a significantly lower expression than Teff cells (Figure 18). This finding is to a certain extent expected based on the fact that HIF-1 $\alpha$  binds to FoxP3 and as a result recruits the von Hippel-Lindau (VHL) protein ubiquitination machinery to

mark FoxP3 for degradation(153). It is unclear how HIF-1 $\alpha$  is regulated in Treg cells and whether there is an ongoing HIF-1 $\alpha$  repression in these cells under hypoxic conditions. Having found overexpression of miR-199a-5p in Treg cells, we postulate that miR-199a-5p may be involved in regulation of HIF-1 $\alpha$  in this context. Of note, however, we found no correlation between HIF-1 $\alpha$  and miR-199a-5p but this is possibly due to the fact that cells were studied under normoxic basal/unstimulated state and without measuring protein expression.

miRNAs play an important role in down regulating protein expression from a gene at either the transcriptional or translational level. Computational analysis estimates that miRNAs regulate >60% of the protein-coding genes in the human genome(161). One miRNA may regulate a vast number of mRNAs forming regulatory networks; conversely, a single mRNA may be affected by numerous miRNAs based on their seed regions. Of interest, miRNAs are stable molecules that have been assayed in whole lung tissue, sputum, serum, BAL fluid, in specific lung cells including fibroblasts, airway epithelium, endothelial cells, and in peripheral blood cells. Importantly, cigarette smoke is an important factor that correlates with dysregulation of several miRNAs. The expression of miRNAs is generally downregulated in smokers compared to non-smokers in airway epithelium(134), alveolar macrophages(162), and lung tissue(133). This downregulation of miRNA expression in smokers was found to be in part related to dysregulation of enzymes that are involved in miRNA generation (Figure 2). Gross et al demonstrated that smoker alveolar macrophages have a defect in

miRNA maturation and that was related to sumoylation of Dicer thus reducing its activity(163). Several studies reported similar downregulation of miRNAs in COPD including Let-7c in sputum and miR-146a in lung fibroblasts(132). However, other investigators who also profiled differentially expressed miRNAs in COPD tissue or cell samples reported an upregulation in certain miRNAs (Table10). miR-223, miR-1274a, miR-15b, miR-146a were all found to be upregulated in COPD lung tissue. Likewise, miR-638 was amongst the most upregulated miRNAs in regional emphysema(140) and was inversely correlated with extracellular matrix maintenance, oxidative stress response, and lung aging pathways.

**Table 10:** Select miRNAs That Are Involved in COPD

miRNA	Source	Change	Reference
Let-7, miR-125b	Sputum (vs. HNS)	↓	Van Pottelberge(132) 2011
miR-20a/100/34c-5p/283	Serum (vs. HS)	↓	Akbas(197) 2012
miR-7		↑	
miR-1	Skeletal muscle (U)	↓	Lewis(198) 2012
miR-1/499/206/133	Plasma (U)	↑	Donaldson(199) 2013
miR-15b/1274a/223	Lung tissue (vs. HS)	↑	Ezzie(133) 2012
miR-26b/29b/101/106b/133b	Plasma (vs. HS)	↓	Soeda(200) 2013
miR-483-5p/152/629/532-5p		↓	
miR-132-212 clusters	BAL (vs. HS)	↑	Molina-Pinelo(201) 2014
miR-520e/302/92a/638/211/150	Regional lung tissue (vs. donor lungs)	↑	Christenson(140) 2014
miR-Let7- 181-30 clusters		↓	
miR-34/199a-5p	Lung tissue (U)	↑	Mizuno(137) 2012
miR-199a-5p	Monocytes (U)	↓	Hassan(144) 2014
miR-95/199a-5p	Treg and Teff (vs. HS)	↓	Chatila(130) 2014

Comparisons were made between COPD and different control subjects (HNS = healthy non-smoker, HS= healthy smokers, U=unspecified).

Our interest was to identify miRNAs that polarize the adaptive immune response because they have the potential to contribute to the development of COPD and may explain, to a certain extent, its inflammatory cellular and humoral component. We analyzed the miRNA expression in Treg and Teff cells and observed a strong clustering of samples in healthy subjects (nonsmokers and smokers) for both CD4 cell phenotypes, but the difference between COPD patients and healthy subjects was most striking in Treg cells (Figure 15, Table 5). The miRNA profiles of the two T cell phenotypes were almost identical in healthy subjects but not when compared with COPD Treg cells. In contrast, there was no difference in the miRnome of Teff cells of COPD and healthy smokers. Since we matched our subjects for smoking, these findings provide somewhat compelling evidence that the miRNA expression is mostly altered in COPD Treg cells and suggest that these changes are likely to be more relevant to COPD immunopathogenesis than in Teff cells. In order to identify potential pathways that are affected by the miRNA changes we overlapped the predicted targets of miRNAs found in the COPD profile with published mRNA data of Treg cells. We found that most hits were for miR-199a-5p (11 genes for miR-199a-5p versus  $\leq 5$  genes for the other miRNAs) and these hits were significantly associated with the TGF- $\beta$  pathway (Figures 19-21, Table 9).

miR-199a-5p is expressed in synovial and skin fibroblasts(131) and has been shown to have a divergent functions in different models of carcinogenesis, embryonic development, and cell differentiation(164). Its expression is finely

regulated by promoter methylation and direct binding of transcription factors (TWIST1 and EGR1)(131). There are two mature forms of miR-199a that are derived from the same miR-199 precursor that was cloned from human osteoblast sarcoma cells and mouse skin (from the 5' half and the 3' half)(165). Both mature forms were eventually named miR-199a-5p and miR-199a-3p and were shown to be expressed in humans. There are two loci that encode the precursor of both mature forms in the human genome, one is on chromosome 1 (miR-199a-2) and the second on chromosome 19 (miR-199a-1). Studies showed that both promoter regions on Chr 1 and Chr 19 are hypermethylated (>90%) in cancer cells (testicular, breast, non-small lung, and colorectal cancers) but hypomethylated in normal fibroblasts(131). In peripheral monocytes and leukocytic cell lines miR-199a-5a is downregulated and its locus is hypermethylated(131) except under normal ER stress response(144). miR-199a, however, can be upregulated in many other cancers thus having important roles in tumorigenesis (biliary, esophageal, ovarian, melanoma, cervical, bronchial squamous cell cancers and acute myeloid leukemia)(164). It has been shown to promote tumor progression in a few cancers(166) whereas in others it suppresses growth and invasiveness(167). In non-malignant conditions, studies revealed that miR-199a-5p is related to cardiomyocyte function and stress response including hypoxia whereas miR-199a-3p is more involved in hepatitis(164).

We found that miR-199a-5p is specifically upregulated in Treg cells but its expression is repressed in COPD. These are novel findings and have not been

reported before. Our findings raise questions about the function of miR-199a-5p in these cells and the mechanism of its deregulation in COPD. Bioinformatics analysis in the context of T cells was significantly positive in identifying the TGF- $\beta$ 1 pathway as a main target of miR-199a-5p. Consistent with its putative function in TGF- $\beta$  signaling, Zhang et al demonstrated that miR-199a-5p is upregulated by TGF- $\beta$  in pulmonary artery smooth muscle cells and suggested that they may form a negative feedback loop to ensure a contained TGF- $\beta$  response(168). In addition, they reported that miR-199a-5p regulates the TGF- $\beta$  signaling by targeting Smad4 in a cancer cell line(168). We interrogated the TGF- $\beta$  pathway in fibroblasts to explore other potential targets of miR-199a-5p to TGF- $\beta$ . Interestingly we found that the BMP pathway could be involved as well and we were able to demonstrate the association between miR-199a and BMP4 in transfected MOLT-4 cells (Figures 23-24). Although we did not provide functional data of miR-199a-5p on BMP pathway in primary T cells, two groups reported strong and convincing evidence on the role of BMP signaling in T cell biology. In the first study, Lu et al neutralized the BMP pathway using Noggin and showed that BMP2/4 have a synergistic effect with TGF- $\beta$  on the induction of Treg cells (169). Noggin is a BMP antagonist that inhibits the binding of BMP to their cognate receptor. Interestingly, both BMP2/4 were upregulated with miR-199a-5p inhibition in our cell model. In the second study, Yoshioka et al analyzed the functional consequences of inhibiting BMP in Jurkat cells and mouse CD4+ cells(170). They found that BMPR inhibition didn't affect phosphorylation of Smad2 but rather decreased the phosphorylation of

Smad1/5/8 and inhibited the differentiation of Th17 and iTreg cells with marked suppression of *Tbx21* and *Rorc*(170).

BMPs are the largest members of the TGF- $\beta$  superfamily of secreted polypeptide growth factors. The TGF- $\beta$  superfamily is comprised of three subgroups: the TGF- $\beta$ s, the activins, and the BMPs. This protein superfamily shares a similar signal transduction cascade. For signaling, each ligand requires a set of type I and type II serine/threonine kinase receptors. Originally, 3 type II receptors (BMPR2, ActR2A and ActR2B) and 3 type I receptors (ALK2, ALK3 and ALK6) were described for the BMPs. However, ligand-receptor promiscuity can occur in the TGF- $\beta$  superfamily indicating that ligands can bind to several receptors of either subtype and vice versa(171). The activated receptor complex propagates the signal into the canonical pathway through phosphorylation of the receptor-regulated Smads (R-Smads), passing the signal on through R-Smad1, R-Smad5 and R-Smad8, translocating to the nucleus and forming a complex with co-Smad4 to regulate gene expression. Other pathways can also be activated by the TGF- $\beta$  family, such as mitogen-activated protein kinase (MAPK) and phosphoinositide 3-kinase (PI3K), and are referred to as 'non-canonical' signaling(172). BMPs can be classified into at least 4 subgroups based on their amino acid sequence similarity: BMP-2/4, BMP-5/6/7/8, BMP-9/10, BMP-12/13/14(173). Most BMP ligands and their receptors are present in the lung, more specifically in pulmonary artery smooth muscle cells, airway epithelium, lung fibroblasts, and pulmonary endothelium(174).

BMPs mediate a diverse range of biological processes involved in regulating growth, differentiation, and apoptosis through complex regulation of the signal transduction and cross-talk between other critical signaling pathways. Among them, BMP4 is critical for lung development, homeostasis, and repair. Early in life, BMP4 coordinates with other growth factors in the lung to correctly mediate branching morphogenesis. In adult airway-injury repair models, the canonical BMP4 pathway gets re-activated in bronchial and alveolar epithelial cells in a manner reminiscent to early lung development and in tissue areas where reparatory progenitor cells reside(175;176). In a similar model, increased BMP4 signaling coincided with inflammation and induced changes consistent with epithelial-mesenchymal transition (EMT)(177;178). In the immune system, BMP6 inhibits the proliferation of human B cell progenitors as well as mature B cells through the Smad-dependent pathway(179). Likewise, different members of BMP family were reported to have anti-proliferative and pro-apoptotic effects in multiple myeloma cells(180). Other investigators reported that BMP2, BMP4 and BMP7 are the main ligands expressed in the human and murine thymus(181;182) and that BMP4 enhances the survival of thymocyte precursors and inhibits their proliferation(182). Also, BMP4 arrests early T cell development(181;183) and may function as a maintenance factor for intrathymic precursor cells(184). Peripheral T cells also express BMP receptors and BMP stimulation activates the canonical and non-canonical BMP pathways(185). BMP signaling was found to regulate CD4+ T cell proliferation by regulating IL-2 transcription(170). BMP4 and BMP6 have been reported to increase T cell

proliferation, while BMP2 decreased their proliferation(185). Other investigators showed the BMP signaling enhances the antigen-induced IFN- $\gamma$  production by effector/memory CD8+ T cells and synergizes with TGF- $\beta$  to induce FoxP3+ Treg cells(169;186). Crosstalk exists also between BMP and Toll-like receptor signaling suggesting that BMP signaling may be involved in the production of pro-inflammatory stimuli. Treatment of macrophages with BMP stimulates the production of pro-inflammatory factors, such as TNF- $\alpha$  and inducible nitric oxide synthase(187;188). Different BMPs stimulate chemotactic responses and induce TGF- $\beta$  expression in monocytes(189;190). The expression of BMP receptors are found as well in murine bone marrow dendritic cells(191). In humans, however, BMP signaling activation was found to promote the phenotypic maturation of dendritic cells by increasing the expression of co-stimulatory molecules, thus enhancing their allostimulatory capacity, and stimulating IL-8 and TNF- $\alpha$  secretion(192).

Whether miR-199a-5p is directly involved in regulating the BMP signaling pathway in T cell will need to be confirmed but both Lu et al. and Yoshioka et al. studies(169;170), put together with our results, suggest that miR-199a-5p is potentially an important regulator of the adaptive T cell response. In this context, the observed overexpression of miR-199a-5p in the Treg cells of unaffected smokers versus their blunted response in COPD (Figure 17) could be explained by 2 different mechanisms. Recently He et al demonstrated that reactive oxygen species (ROS) inhibit miR-199a expression through increasing its promoter methylation(193) and it is now well recognized that the antioxidant capacity in

COPD is substantially reduced even after smoking cessation due to the continued production of ROS(28). Therefore, it is possible that in susceptible individuals the excessive ROS from smoking contributes to dampening the miR-199a-5p response in COPD which would hypothetically explain the shift in the Treg/Th1-Th17 balance (Figure 25). On the other hand, in unaffected smokers one can hypothesize that miR-199a-5p is upregulated by Egr-1. Egr-1 is a transcription factor that can occupy the miR-199a gene promoter inducing its expression in certain cancer cells(194). Of interest, however, the Egr-1 protein expression is increased in multiple lung cells after exposure to cigarette smoke in a dose and time-dependent manner(195) thus potentially explaining the miR-199a-5p de-repression in our T cell population.

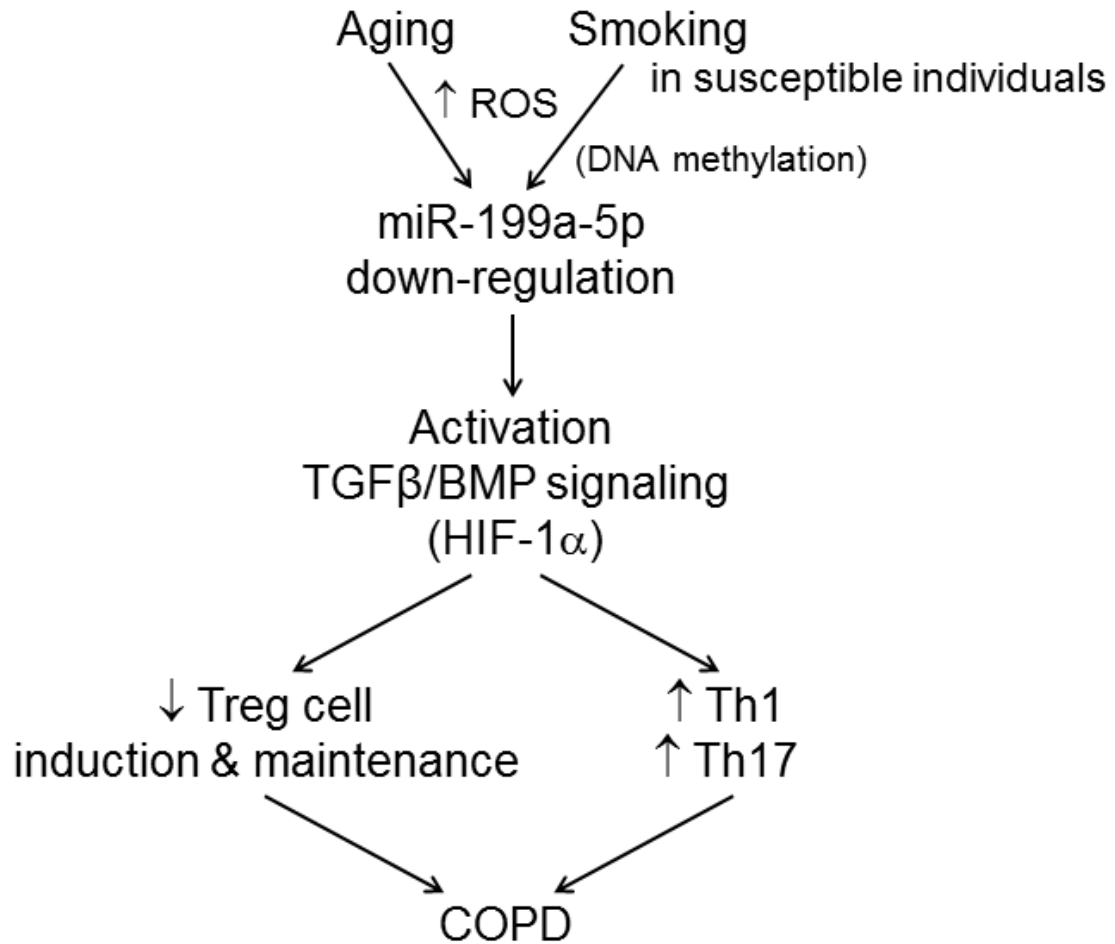


**FIGURE 25:** A Schematic of the Proposed Function of miR-199a-5p in Treg Cells. Deregulation of miR-199a-5p possibly due to the increased production of reactive oxygen species (ROS) eventually leads to an overexpression of the TGF- $\beta$ /BMP signaling pathway thus skewing the T cell response to Th1 and Th17 cells. Since we found a positive correlation between miR-199a-5p expression and age it is also possible that any of the aberrant aging mechanisms in COPD may be involved in the deregulation of miR-199a-5p.

Our miRNAs analysis has the limitations of a small number of subjects, with some patients being on inhaled corticosteroids, not being perfectly matched for age, and may not fully reflect Treg cell changes in the lungs. With that in mind, the isolation of highly purified Treg and Teff cells helped in reproducing the same trends for the observed differences with validation in the final cohort of patients. Second, although the groups were not perfectly matched I observed only a correlation between age and miR-199a-5p expression and that association was very weak and is unlikely to have such a dramatic impact on miRNA expression. Third, the fact that I found significant differences in the peripheral blood Treg cells suggest that the response of the peripheral Treg cell pool has been altered either directly, by antigenic stimulation, or indirectly due to the systemic effects of COPD. This conclusion is in-line with a recent study by Rahman et al who reported significant changes in the peripheral blood Treg cell kinetics among patients with inactive Crohn's disease when compared to non-Treg cells and Treg cells from healthy control subjects(196), again suggesting that the effect of persistent tissue antigenic stimulation in chronic inflammatory conditions may spill into the periphery. Moreover, Hou et al demonstrated in patients with COPD changes of peripheral blood Treg cells that mirrored tissue Treg cell changes and correlated the changes with loss of lung function and immune activation(78). Last, inhaled corticosteroids are unlikely to have a major effect miR-199a-5p expression since we didn't see any correlation between this miRNA and their use and they obviously do not explain the upregulation of miR-199a-5p in unaffected smokers.

In conclusion, we have found no changes in Treg cell function in COPD but found substantial differences in their miRNome, and not that of Teff cells. We also demonstrated that miR-199a-5p is upregulated in Treg cells compared to Teff cells. Both findings are novel and support future functional studies to determine if miR-199a-5p repression, as observed in our COPD patients, has a significant impact on modulating the adaptive immune balance in favor of Th1 and Th17 cell responses in COPD and other inflammatory conditions.

## REFERENCE CITED

1. Global strategy for the diagnosis, management, and prevention of chronic obstructive pulmonary disease: NHLBI/WHO workshop report; updated 2003. Bethesda, MD: National Institute of Health.
2. Hogg, J.C. (2004). Pathophysiology of airflow limitation in chronic obstructive pulmonary disease. *Lancet* 364, 709-721.
3. van der Strate, B.W., D.S. Postma, C.A. Brandsma, B.N. Melgert, M.A. Luinge, M. Geerlings, M.N. Hylkema, et al. (2006). Cigarette smoke-induced emphysema: A role for the B cell? *American Journal of Respiratory and Critical Care Medicine* 173, 751-758.
4. Bracke, K.R., F.M. Verhamme, L.J. Seys, C. Bantsimba-Malanda, D.M. Cunoosamy, R. Herbst, H. Hammad, et al. (2013). Role of CXCL13 in cigarette smoke-induced lymphoid follicle formation and chronic obstructive pulmonary disease. *American Journal of Respiratory and Critical Care Medicine* 188, 343-355.
5. Agusti, A., P. Sobradillo & B. Celli. (2011). Addressing the complexity of chronic obstructive pulmonary disease: from phenotypes and biomarkers to scale-free networks, systems biology, and P4 medicine. *American Journal of Respiratory and Critical Care Medicine* 183, 1129-1137.

6. MacNee, W. (2011). Aging, inflammation, and emphysema. *American Journal of Respiratory and Critical Care Medicine* 184, 1327-1329.
7. Hogg, J.C. (2012). A pathologist's view of airway obstruction in chronic obstructive pulmonary disease. *American Journal of Respiratory and Critical Care Medicine* 186, v-vii.
8. Suki, B., K.R. Lutchen & E.P. Ingenito. (2003). On the progressive nature of emphysema: roles of proteases, inflammation, and mechanical forces. *American Journal of Respiratory and Critical Care Medicine* 168, 516-521.
9. van Eeden, S.F., W.C. Tan, T. Suwa, H. Mukae, T. Terashima, T. Fujii, D. Qui, et al. (2001). Cytokines involved in the systemic inflammatory response induced by exposure to particulate matter air pollutants (PM(10)). *American Journal of Respiratory and Critical Care Medicine* 164, 826-830.
10. Laan, M., S. Bozinovski & G.P. Anderson. (2004). Cigarette smoke inhibits lipopolysaccharide-induced production of inflammatory cytokines by suppressing the activation of activator protein-1 in bronchial epithelial cells. *Journal of Immunology (Baltimore, Md.: 1950)* 173, 4164-4170.
11. Woodruff, P.G., L.L. Koth, Y.H. Yang, M.W. Rodriguez, S. Favoreto, G.M. Dolganov, A.C. Paquet, et al. (2005). A distinctive alveolar macrophage activation state induced by cigarette smoking. *American Journal of Respiratory and Critical Care Medicine* 172, 1383-1392.

12. Kalra, R., S.P. Singh, S.M. Savage, G.L. Finch & M.L. Sopori. (2000). Effects of cigarette smoke on immune response: chronic exposure to cigarette smoke impairs antigen-mediated signaling in T cells and depletes IP3-sensitive Ca(2+) stores. *The Journal of Pharmacology and Experimental Therapeutics* 293, 166-171.
13. Finklea, J.F., V. Hasselblad, W.B. Riggan, W.C. Nelson, D.I. Hammer & V.A. Newill. (1971). Cigarette smoking and hemagglutination inhibition response to influenza after natural disease and immunization. *The American Review of Respiratory Disease* 104, 368-376.
14. Kim, J.H., H. Kim, K.Y. Lee, J.W. Kang, K.H. Lee, S.Y. Park, H.I. Yoon, et al. (2006). Aryl hydrocarbon receptor gene polymorphisms affect lung cancer risk. *Lung Cancer (Amsterdam, Netherlands)*.
15. Kerkvliet, N.I., D.M. Shepherd & L. Baecher-Steppan. (2002). T lymphocytes are direct, aryl hydrocarbon receptor (AhR)-dependent targets of 2,3,7,8-tetrachlorodibenzo-p-dioxin (TCDD): AhR expression in both CD4+ and CD8+ T cells is necessary for full suppression of a cytotoxic T lymphocyte response by TCDD. *Toxicology and Applied Pharmacology* 185, 146-152.
16. Geng, Y., S.M. Savage, L.J. Johnson, J. Seagrave & M.L. Sopori. (1995). Effects of nicotine on the immune response. I. Chronic exposure to nicotine impairs antigen receptor-mediated signal transduction in lymphocytes. *Toxicology and Applied Pharmacology* 135, 268-278.

17. Geiselhart, L.A., T. Christian, F. Minnear & B.M. Freed. (1997). The cigarette tar component p-benzoquinone blocks T-lymphocyte activation by inhibiting interleukin-2 production, but not CD25, ICAM-1, or LFA-1 expression. *Toxicology and Applied Pharmacology* 143, 30-36.
18. Glader, P., S. Moller, J. Lilja, E. Wieslander, C.G. Lofdahl & K. von Wachenfeldt. (2006). Cigarette smoke extract modulates respiratory defence mechanisms through effects on T-cells and airway epithelial cells. *Respiratory Medicine* 100, 818-827.
19. Lambert, C., J. McCue, M. Portas, Y. Ouyang, J. Li, T.G. Rosano, A. Lazis, et al. (2005). Acrolein in cigarette smoke inhibits T-cell responses. *The Journal of Allergy and Clinical Immunology* 116, 916-922.
20. Ouyang, Y., N. Virasch, P. Hao, M.T. Aubrey, N. Mukerjee, B.E. Bierer & B.M. Freed. (2000). Suppression of human IL-1beta, IL-2, IFN-gamma, and TNF-alpha production by cigarette smoke extracts. *The Journal of Allergy and Clinical Immunology* 106, 280-287.
21. Hagiwara, E., K.I. Takahashi, T. Okubo, S. Ohno, A. Ueda, A. Aoki, S. Odagiri, et al. (2001). Cigarette smoking depletes cells spontaneously secreting Th(1) cytokines in the human airway. *Cytokine* 14, 121-126.
22. Miravittles, M., C. de la Roza, J. Morera, T. Montemayor, E. Gobartt, A. Martin & J.L. Alvarez-Sala. (2006). Chronic respiratory symptoms, spirometry

- and knowledge of COPD among general population. *Respiratory Medicine* 100, 1973-1980.
23. Pelkonen, M., I.L. Notkola, A. Nissinen, H. Tukiainen & H. Koskela. (2006). Thirty-year cumulative incidence of chronic bronchitis and COPD in relation to 30-year pulmonary function and 40-year mortality: a follow-up in middle-aged rural men. *Chest* 130, 1129-1137.
24. Gan, W.Q., J.M. FitzGerald, C. Carlsten, M. Sadatsafavi & M. Brauer. (2013). Associations of ambient air pollution with chronic obstructive pulmonary disease hospitalization and mortality. *American Journal of Respiratory and Critical Care Medicine* 187, 721-727.
25. Rice, M.B., P.L. Ljungman, E.H. Wilker, D.R. Gold, J.D. Schwartz, P. Koutrakis, G.R. Washko, et al. (2013). Short-term exposure to air pollution and lung function in the Framingham Heart Study. *American Journal of Respiratory and Critical Care Medicine* 188, 1351-1357.
26. Lepeule, J., A.A. Litonjua, B. Coull, P. Koutrakis, D. Sparrow, P.S. Vokonas & J. Schwartz. (2014). Long-term effects of traffic particles on lung function decline in the elderly. *American Journal of Respiratory and Critical Care Medicine* 190, 542-548.
27. Hnizdo, E., P.A. Sullivan, K.M. Bang & G. Wagner. (2002). Association between chronic obstructive pulmonary disease and employment by industry and occupation in the US population: a study of data from the Third National

- Health and Nutrition Examination Survey. *American Journal of Epidemiology* 156, 738-746.
28. Kirkham, P.A. & P.J. Barnes. (2013). Oxidative Stress in COPD. *Chest* 144, 266-273.
29. Dekhuijzen, P.N., K.K. Aben, I. Dekker, L.P. Aarts, P.L. Wielders, C.L. van Herwaarden & A. Bast. (1996). Increased exhalation of hydrogen peroxide in patients with stable and unstable chronic obstructive pulmonary disease. *American Journal of Respiratory and Critical Care Medicine* 154, 813-816.
30. Montuschi, P., J.V. Collins, G. Ciabattini, N. Lazzeri, M. Corradi, S.A. Kharitonov & P.J. Barnes. (2000). Exhaled 8-isoprostane as an in vivo biomarker of lung oxidative stress in patients with COPD and healthy smokers. *American Journal of Respiratory and Critical Care Medicine* 162, 1175-1177.
31. Paredi, P., S.A. Kharitonov, D. Leak, S. Ward, D. Cramer & P.J. Barnes. (2000). Exhaled ethane, a marker of lipid peroxidation, is elevated in chronic obstructive pulmonary disease. *American Journal of Respiratory and Critical Care Medicine* 162, 369-373.
32. Rahman, I., A.A. van Schadewijk, A.J. Crowther, P.S. Hiemstra, J. Stolk, W. MacNee & W.I. De Boer. (2002). 4-Hydroxy-2-nonenal, a specific lipid peroxidation product, is elevated in lungs of patients with chronic obstructive

- pulmonary disease. *American Journal of Respiratory and Critical Care Medicine* 166, 490-495.
33. Hodge, S., G. Hodge, M. Holmes & P.N. Reynolds. (2005). Increased airway epithelial and T-cell apoptosis in COPD remains despite smoking cessation. *The European Respiratory Journal* 25, 447-454.
34. Cosio, M.G., M. Saetta & A. Agusti. (2009). Immunologic aspects of chronic obstructive pulmonary disease. *The New England Journal of Medicine* 360, 2445-2454.
35. Faner, R., M. Rojas, W. Macnee & A. Agusti. (2012). Abnormal lung aging in chronic obstructive pulmonary disease and idiopathic pulmonary fibrosis. *American Journal of Respiratory and Critical Care Medicine* 186, 306-313.
36. Rando, T.A. & H.Y. Chang. (2012). Aging, rejuvenation, and epigenetic reprogramming: resetting the aging clock. *Cell* 148, 46-57.
37. MacNee, W. & R.M. Tuder. (2009). New paradigms in the pathogenesis of chronic obstructive pulmonary disease I. *Proceedings of the American Thoracic Society* 6, 527-531.
38. Hogg, J.C., J.E. McDonough & M. Suzuki. (2013). Small airway obstruction in COPD: new insights based on micro-CT imaging and MRI imaging. *Chest* 143, 1436-1443.

39. Yokohori, N., K. Aoshiba, A. Nagai & Respiratory Failure Research Group in Japan. (2004). Increased levels of cell death and proliferation in alveolar wall cells in patients with pulmonary emphysema. *Chest* 125, 626-632.
40. Kasahara, Y., R.M. Tuder, C.D. Cool, D.A. Lynch, S.C. Flores & N.F. Voelkel. (2001). Endothelial cell death and decreased expression of vascular endothelial growth factor and vascular endothelial growth factor receptor 2 in emphysema. *American Journal of Respiratory and Critical Care Medicine* 163, 737-744.
41. Muller, K.C., L. Welker, K. Paasch, B. Feindt, V.J. Erpenbeck, J.M. Hohlfeld, N. Krug, et al. (2006). Lung fibroblasts from patients with emphysema show markers of senescence in vitro. *Respiratory Research* 7, 32.
42. Tsuji, T., K. Aoshiba & A. Nagai. (2006). Alveolar cell senescence in patients with pulmonary emphysema. *American Journal of Respiratory and Critical Care Medicine* 174, 886-893.
43. Serra, V., T. von Zglinicki, M. Lorenz & G. Saretzki. (2003). Extracellular superoxide dismutase is a major antioxidant in human fibroblasts and slows telomere shortening. *The Journal of Biological Chemistry* 278, 6824-6830.
44. Shelton, D.N., E. Chang, P.S. Whittier, D. Choi & W.D. Funk. (1999). Microarray analysis of replicative senescence. *Current Biology : CB* 9, 939-945.

45. Franceschi, C. & J. Campisi. (2014). Chronic inflammation (inflammaging) and its potential contribution to age-associated diseases. *The Journals of Gerontology. Series A, Biological Sciences and Medical Sciences* 69 Suppl 1, S4-9.
46. Feghali-Bostwick, C.A., A.S. Gadgil, L.E. Otterbein, J.M. Pilewski, M.W. Stoner, E. Csizmadia, Y. Zhang, et al. (2008). Autoantibodies in patients with chronic obstructive pulmonary disease. *American Journal of Respiratory and Critical Care Medicine* 177, 156-163.
47. Nunez, B., J. Sauleda, J.M. Anto, M.R. Julia, M. Orozco, E. Monso, A. Noguera, et al. (2011). Anti-tissue antibodies are related to lung function in chronic obstructive pulmonary disease. *American Journal of Respiratory and Critical Care Medicine* 183, 1025-1031.
48. Taraseviciene-Stewart, L., R. Scerbavicius, K.H. Choe, M. Moore, A. Sullivan, M.R. Nicolls, A.P. Fontenot, et al. (2005). An animal model of autoimmune emphysema. *American Journal of Respiratory and Critical Care Medicine : An Official Journal of the American Thoracic Society, Medical Section of the American Lung Association* 171, 734-742.
49. Lee, S.H., S. Goswami, A. Grudo, L.Z. Song, V. Bandi, S. Goodnight-White, L. Green, et al. (2007). Antielastin autoimmunity in tobacco smoking-induced emphysema. *Nature Medicine* 13, 567-569.

50. Karayama, M., N. Inui, T. Suda, Y. Nakamura, H. Nakamura & K. Chida. (2010). Antiendothelial Cell Antibodies in Patients With COPD. *Chest* 138, 1303-1308.
51. Kirkham, P.A., G. Caramori, P. Casolari, A.A. Papi, M. Edwards, B. Shamji, K. Triantaphyllopoulos, et al. (2011). Oxidative stress-induced antibodies to carbonyl-modified protein correlate with severity of chronic obstructive pulmonary disease. *American Journal of Respiratory and Critical Care Medicine* 184, 796-802.
52. Polverino, F., S. Baraldo, E. Bazzan, S. Agostini, G. Turato, F. Lunardi, E. Balestro, et al. (2010). A novel insight into adaptive immunity in chronic obstructive pulmonary disease: B cell activating factor belonging to the tumor necrosis factor family. *American Journal of Respiratory and Critical Care Medicine* 182, 1011-1019.
53. Finkelstein, R., R.S. Fraser, H. Ghezzi & M.G. Cosio. (1995). Alveolar inflammation and its relation to emphysema in smokers. *American Journal of Respiratory and Critical Care Medicine* 152, 1666-1672.
54. Hogg, J.C., F. Chu, S. Utokaparch, R. Woods, W.M. Elliott, L. Buzatu, R.M. Cherniack, et al. (2004). The nature of small-airway obstruction in chronic obstructive pulmonary disease. *The New England Journal of Medicine* 350, 2645-2653.

55. Zheng, T., Z. Zhu, Z. Wang, R.J. Homer, B. Ma, R.J. Riese Jr, H.A. Chapman Jr, et al. (2000). Inducible targeting of IL-13 to the adult lung causes matrix metalloproteinase- and cathepsin-dependent emphysema. *The Journal of Clinical Investigation* 106, 1081-1093.
56. Boutten, A., M. Bonay, S. Laribe, G. Leseche, Y. Castier, V. Lecon-Malas, M. Fournier, et al. (2004). Decreased expression of interleukin 13 in human lung emphysema. *Thorax* 59, 850-854.
57. Di Stefano, A., G. Caramori, A. Capelli, I. Gnemmi, F.L. Ricciardolo, T. Oates, C.F. Donner, et al. (2004). STAT4 activation in smokers and patients with chronic obstructive pulmonary disease. *The European Respiratory Journal : Official Journal of the European Society for Clinical Respiratory Physiology* 24, 78-85.
58. Gosman, M.M., B.W. Willemse, D.F. Jansen, T.S. Lapperre, A. van Schadewijk, P.S. Hiemstra, D.S. Postma, et al. (2006). Increased number of B-cells in bronchial biopsies in COPD. *The European Respiratory Journal* 27, 60-64.
59. Ansel, K.M., V.N. Ngo, P.L. Hyman, S.A. Luther, R. Forster, J.D. Sedgwick, J.L. Browning, et al. (2000). A chemokine-driven positive feedback loop organizes lymphoid follicles. *Nature* 406, 309-314.
60. Litsiou, E., M. Semitekolou, I.E. Galani, I. Morianos, A. Tsoutsas, P. Kara, D. Rontogianni, et al. (2013). CXCL13 production in B cells via Toll-like

receptor/lymphotoxin receptor signaling is involved in lymphoid neogenesis in chronic obstructive pulmonary disease. *American Journal of Respiratory and Critical Care Medicine* 187, 1194-1202.

61. Saetta, M., A. Di Stefano, G. Turato, F.M. Facchini, L. Corbino, C.E. Mapp, P. Maestrelli, et al. (1998). CD8+ T-lymphocytes in peripheral airways of smokers with chronic obstructive pulmonary disease. *American Journal of Respiratory and Critical Care Medicine : An Official Journal of the American Thoracic Society, Medical Section of the American Lung Association* 157, 822-826.
62. Proklou, A., N. Soultzis, E. Neofytou, N. Rovina, E. Zervas, M. Gaga, N.M. Siafakas, et al. (2013). Granule cytotoxic activity and oxidative DNA damage in smoking and nonsmoking patients with asthma. *Chest* 144, 1230-1237.
63. Sullivan, A.K., P.L. Simonian, M.T. Falta, J.D. Mitchell, G.P. Cosgrove, K.K. Brown, B.L. Kotzin, et al. (2005). Oligoclonal CD4+ T cells in the lungs of patients with severe emphysema. *American Journal of Respiratory and Critical Care Medicine* 172, 590-596.
64. Barcelo, B., J. Pons, A. Fuster, J. Sauleda, A. Noguera, J.M. Ferrer & A.G. Agusti. (2006). Intracellular cytokine profile of T lymphocytes in patients with chronic obstructive pulmonary disease. *Clinical and Experimental Immunology* 145, 474-479.

65. Barczyk, A., W. Pierzchala, O.M. Kon, B. Cosio, I.M. Adcock & P.J. Barnes. (2006). Cytokine production by bronchoalveolar lavage T lymphocytes in chronic obstructive pulmonary disease. *The Journal of Allergy and Clinical Immunology* 117, 1484-1492.
66. Kikly, K., L. Liu, S. Na & J.D. Sedgwick. (2006). The IL-23/Th(17) axis: therapeutic targets for autoimmune inflammation. *Current Opinion in Immunology* 18, 670-675.
67. Ouyang, W., J.K. Kolls & Y. Zheng. (2008). The biological functions of T helper 17 cell effector cytokines in inflammation. *Immunity* 28, 454-467.
68. Shan, M., H.F. Cheng, L.Z. Song, L. Roberts, L. Green, J. Hacken-Bitar, J. Huh, et al. (2009). Lung myeloid dendritic cells coordinately induce TH1 and TH17 responses in human emphysema. *Science Translational Medicine* 1, 4ra10.
69. Di Stefano, A., G. Caramori, I. Gnemmi, M. Contoli, C. Vicari, A. Capelli, F. Magno, et al. (2009). T helper type 17-related cytokine expression is increased in the bronchial mucosa of stable chronic obstructive pulmonary disease patients. *Clinical and Experimental Immunology* 157, 316-324.
70. Molet, S., Q. Hamid, F. Davoine, E. Nutku, R. Taha, N. Page, R. Olivenstein, et al. (2001). IL-17 is increased in asthmatic airways and induces human bronchial fibroblasts to produce cytokines. *The Journal of Allergy and Clinical Immunology* 108, 430-438.

71. Chen, K., D.A. Pociask, J.P. McAleer, Y.R. Chan, J.F. Alcorn, J.L. Kreindler, M.R. Keyser, et al. (2011). IL-17RA is required for CCL2 expression, macrophage recruitment, and emphysema in response to cigarette smoke. *PloS One* 6, e20333.
72. Kelsen, S.G., M.O. Aksoy, Y. Yang, S. Shahabuddin, J. Litvin, F. Safadi & T.J. Rogers. (2004). The chemokine receptor CXCR3 and its splice variant are expressed in human airway epithelial cells. *American Journal of Physiology. Lung Cellular and Molecular Physiology* 287, L584-91.
73. Grumelli, S., D.B. Corry, L.Z. Song, L. Song, L. Green, J. Huh, J. Hacken, et al. (2004). An immune basis for lung parenchymal destruction in chronic obstructive pulmonary disease and emphysema. *PLoS Medicine* 1, e8.
74. van Oosterhout, A.J. & N. Bloksma. (2005). Regulatory T-lymphocytes in asthma. *The European Respiratory Journal : Official Journal of the European Society for Clinical Respiratory Physiology* 26, 918-932.
75. Bluestone, J.A., A.W. Thomson, E.M. Shevach & H.L. Weiner. (2007). What does the future hold for cell-based tolerogenic therapy? *Nature Reviews.Immunology* 7, 650-654.
76. Barcelo B, Pons J, Sauleda J, Fuster A, Ferrer JM, Agusti AGN. (2006). Decreased percentage of CD4+CD25+ regulatory T cells in bronchoalveolar lavage fluid of patients with COPD. *Proc Am Thor Soc* 3, A635.

77. Smyth, L.J., C. Starkey, J. Vestbo & D. Singh. (2007). CD4-regulatory cells in COPD patients. *Chest* 132, 156-163.
78. Hou, J., Y. Sun, Y. Hao, J. Zhuo, X. Liu, P. Bai, J. Han, et al. (2013). Imbalance between subpopulations of regulatory T cells in COPD. *Thorax*.
79. Barcelo, B., J. Pons, J.M. Ferrer, J. Sauleda, A. Fuster & A.G. Agusti. (2008). Phenotypic characterisation of T-lymphocytes in COPD: abnormal CD4+CD25+ regulatory T-lymphocyte response to tobacco smoking. *The European Respiratory Journal : Official Journal of the European Society for Clinical Respiratory Physiology* 31, 555-562.
80. Plumb, J., L.J. Smyth, H.R. Adams, J. Vestbo, A. Bentley & S.D. Singh. (2009). Increased T-regulatory cells within lymphocyte follicles in moderate COPD. *The European Respiratory Journal : Official Journal of the European Society for Clinical Respiratory Physiology* 34, 89-94.
81. Isajevs, S., I. Taivans, G. Strazda, U. Kopeika, M. Bukovskis, V. Gordjusina & A. Kratovska. (2009). Decreased FOXP3 expression in small airways of smokers with COPD. *The European Respiratory Journal : Official Journal of the European Society for Clinical Respiratory Physiology* 33, 61-67.
82. Kalathil, S.G., A.A. Lugade, V. Pradhan, A. Miller, G.I. Parameswaran, S. Sethi & Y. Thanavala. (2014). T-regulatory cells and programmed death 1+ T cells contribute to effector T-cell dysfunction in patients with chronic

- obstructive pulmonary disease. *American Journal of Respiratory and Critical Care Medicine* 190, 40-50.
83. Tan, D.B., S. Fernandez, P. Price, M.A. French, P.J. Thompson & Y.P. Moodley. (2014). Impaired function of regulatory T-cells in patients with chronic obstructive pulmonary disease (COPD). *Immunobiology*.
84. Kocks, J.R., A.C. Davalos-Misslitz, G. Hintzen, L. Ohl & R. Forster. (2007). Regulatory T cells interfere with the development of bronchus-associated lymphoid tissue. *The Journal of Experimental Medicine* 204, 723-734.
85. Wang, H., W. Peng, Y. Weng, H. Ying, H. Li, D. Xia & W. Yu. (2012). Imbalance of Th17/Treg cells in mice with chronic cigarette smoke exposure. *International Immunopharmacology* 14, 504-512.
86. Liu, M.F., C.R. Wang, L.L. Fung & C.R. Wu. (2004). Decreased CD4+CD25+ T cells in peripheral blood of patients with systemic lupus erythematosus. *Scandinavian Journal of Immunology* 59, 198-202.
87. Kriegel, M.A., T. Lohmann, C. Gabler, N. Blank, J.R. Kalden & H.M. Lorenz. (2004). Defective suppressor function of human CD4+ CD25+ regulatory T cells in autoimmune polyglandular syndrome type II. *The Journal of Experimental Medicine* 199, 1285-1291.

88. Viglietta, V., C. Baecher-Allan, H.L. Weiner & D.A. Hafler. (2004). Loss of functional suppression by CD4+CD25+ regulatory T cells in patients with multiple sclerosis. *The Journal of Experimental Medicine* 199, 971-979.
89. Bacchetta, R., E. Gambineri & M.G. Roncarolo. (2007). Role of regulatory T cells and FOXP3 in human diseases. *The Journal of Allergy and Clinical Immunology* 120, 227-35; quiz 236-7.
90. Hogg, J.C., F. Chu, S. Utokaparch, R. Woods, W.M. Elliott, L. Buzatu, R.M. Cherniack, et al. (2004). The nature of small-airway obstruction in chronic obstructive pulmonary disease. *The New England Journal of Medicine* 350, 2645-2653.
91. Sakaguchi, S., T. Yamaguchi, T. Nomura & M. Ono. (2008). Regulatory T cells and immune tolerance. *Cell* 133, 775-787.
92. Curotto de Lafaille, M.A. & J.J. Lafaille. (2009). Natural and adaptive foxp3+ regulatory T cells: more of the same or a division of labor? *Immunity* 30, 626-635.
93. Liston, A. & D.H. Gray. (2014). Homeostatic control of regulatory T cell diversity. *Nature Reviews.Immunology* 14, 154-165.
94. Pierson, W., B. Cauwe, A. Policheni, S.M. Schlenner, D. Franckaert, J. Berges, S. Humblet-Baron, et al. (2013). Antiapoptotic Mcl-1 is critical for the

- survival and niche-filling capacity of Foxp3(+) regulatory T cells. *Nature Immunology* 14, 959-965.
95. Vukmanovic-Stejic, M., Y. Zhang, J.E. Cook, J.M. Fletcher, A. McQuaid, J.E. Masters, M.H. Rustin, et al. (2006). Human CD4+ CD25hi Foxp3+ regulatory T cells are derived by rapid turnover of memory populations in vivo. *The Journal of Clinical Investigation* 116, 2423-2433.
96. Tai, X., B. Erman, A. Alag, J. Mu, M. Kimura, G. Katz, T. Ginter, et al. (2013). Foxp3 transcription factor is proapoptotic and lethal to developing regulatory T cells unless counterbalanced by cytokine survival signals. *Immunity* 38, 1116-1128.
97. Cretney, E., A. Xin, W. Shi, M. Minnich, F. Masson, M. Miasari, G.T. Belz, et al. (2011). The transcription factors Blimp-1 and IRF4 jointly control the differentiation and function of effector regulatory T cells. *Nature Immunology* 12, 304-311.
98. Linterman, M.A., W. Pierson, S.K. Lee, A. Kallies, S. Kawamoto, T.F. Rayner, M. Srivastava, et al. (2011). Foxp3+ follicular regulatory T cells control the germinal center response. *Nature Medicine* 17, 975-982.
99. Burzyn, D., W. Kuswanto, D. Kolodin, J.L. Shadrach, M. Cerletti, Y. Jang, E. Sefik, et al. (2013). A special population of regulatory T cells potentiates muscle repair. *Cell* 155, 1282-1295.

100. Fu, W., A. Ergun, T. Lu, J.A. Hill, S. Haxhinasto, M.S. Fassett, R. Gazit, et al. (2012). A multiply redundant genetic switch 'locks in' the transcriptional signature of regulatory T cells. *Nature Immunology* 13, 972-980.
101. Rudra, D., P. deRoos, A. Chaudhry, R.E. Niec, A. Arvey, R.M. Samstein, C. Leslie, et al. (2012). Transcription factor Foxp3 and its protein partners form a complex regulatory network. *Nature Immunology* 13, 1010-1019.
102. Rubtsov, Y.P., R.E. Niec, S. Josefowicz, L. Li, J. Darce, D. Mathis, C. Benoist, et al. (2010). Stability of the regulatory T cell lineage in vivo. *Science (New York, N.Y.)* 329, 1667-1671.
103. Liang, T.J. & C.Y. Qin. (2009). The emerging role of microRNAs in immune cell development and differentiation. *APMIS : Acta Pathologica, Microbiologica, Et Immunologica Scandinavica* 117, 635-643.
104. Li, Q.J., J. Chau, P.J. Ebert, G. Sylvester, H. Min, G. Liu, R. Braich, et al. (2007). miR-181a is an intrinsic modulator of T cell sensitivity and selection. *Cell* 129, 147-161.
105. Kohlhaas, S., O.A. Garden, C. Scudamore, M. Turner, K. Okkenhaug & E. Vigorito. (2009). Cutting edge: the Foxp3 target miR-155 contributes to the development of regulatory T cells. *Journal of Immunology (Baltimore, Md.: 1950)* 182, 2578-2582.

106. Rodriguez, A., E. Vigorito, S. Clare, M.V. Warren, P. Couttet, D.R. Soond, S. van Dongen, et al. (2007). Requirement of bic/microRNA-155 for normal immune function. *Science (New York, N.Y.)* 316, 608-611.
107. Horwitz, D.A., S.G. Zheng, J. Wang & J.D. Gray. (2008). Critical role of IL-2 and TGF-beta in generation, function and stabilization of Foxp3+CD4+ Treg. *European Journal of Immunology* 38, 912-915.
108. Liston, A., L.F. Lu, D. O'Carroll, A. Tarakhovsky & A.Y. Rudensky. (2008). Dicer-dependent microRNA pathway safeguards regulatory T cell function. *The Journal of Experimental Medicine* 205, 1993-2004.
109. Zhou, X., L.T. Jeker, B.T. Fife, S. Zhu, M.S. Anderson, M.T. McManus & J.A. Bluestone. (2008). Selective miRNA disruption in T reg cells leads to uncontrolled autoimmunity. *The Journal of Experimental Medicine* 205, 1983-1991.
110. Cobb, B.S., A. Hertweck, J. Smith, E. O'Connor, D. Graf, T. Cook, S.T. Smale, et al. (2006). A role for Dicer in immune regulation. *The Journal of Experimental Medicine* 203, 2519-2527.
111. Chong, M.M., J.P. Rasmussen, A.Y. Rudensky & D.R. Littman. (2008). The RNaseIII enzyme Droscha is critical in T cells for preventing lethal inflammatory disease. *The Journal of Experimental Medicine* 205, 2005-2017.

112. Rouas, R., H. Fayyad-Kazan, N. El Zein, P. Lewalle, F. Rothe, A. Simion, H. Akl, et al. (2009). Human natural Treg microRNA signature: role of microRNA-31 and microRNA-21 in FOXP3 expression. *European Journal of Immunology* 39, 1608-1618.
113. Fayyad-Kazan, H., R. Rouas, M. Fayyad-Kazan, R. Badran, N. El Zein, P. Lewalle, M. Najjar, et al. (2012). MicroRNA profile of circulating CD4-positive regulatory T cells in human adults and impact of differentially expressed microRNAs on expression of two genes essential to their function. *The Journal of Biological Chemistry* 287, 9910-9922.
114. Sonkoly, E., M. Stahle & A. Pivarcsi. (2008). MicroRNAs and immunity: novel players in the regulation of normal immune function and inflammation. *Seminars in Cancer Biology* 18, 131-140.
115. Lu, L.F., T.H. Thai, D.P. Calado, A. Chaudhry, M. Kubo, K. Tanaka, G.B. Loeb, et al. (2009). Foxp3-dependent microRNA155 confers competitive fitness to regulatory T cells by targeting SOCS1 protein. *Immunity* 30, 80-91.
116. Zhan, Y., G.M. Davey, K.L. Graham, H. Kiu, N.L. Dudek, T. Kay & A.M. Lew. (2009). SOCS1 negatively regulates the production of Foxp3+ CD4+ T cells in the thymus. *Immunology and Cell Biology* 87, 473-480.
117. Lu, L.F., M.P. Boldin, A. Chaudhry, L.L. Lin, K.D. Taganov, T. Hanada, A. Yoshimura, et al. (2010). Function of miR-146a in controlling Treg cell-mediated regulation of Th1 responses. *Cell* 142, 914-929.

119. Jiang, S., C. Li, V. Olive, E. Lykken, F. Feng, J. Sevilla, Y. Wan, et al. (2011). Molecular dissection of the miR-17-92 cluster's critical dual roles in promoting Th1 responses and preventing inducible Treg differentiation. *Blood* 118, 5487-5497.
120. de Kouchkovsky, D., J.H. Esensten, W.L. Rosenthal, M.M. Morar, J.A. Bluestone & L.T. Jeker. (2013). microRNA-17-92 regulates IL-10 production by regulatory T cells and control of experimental autoimmune encephalomyelitis. *Journal of Immunology (Baltimore, Md.: 1950)* 191, 1594-1605.
121. Skinner, J.P., A.A. Keown & M.M. Chong. (2014). The miR-17 approximately 92a cluster of microRNAs is required for the fitness of Foxp3+ regulatory T cells. *PloS One* 9, e88997.
122. Huang, B., J. Zhao, Z. Lei, S. Shen, D. Li, G.X. Shen, G.M. Zhang, et al. (2009). miR-142-3p restricts cAMP production in CD4+CD25- T cells and CD4+CD25+ TREG cells by targeting AC9 mRNA. *EMBO Reports* 10, 180-185.
123. Bopp, T., C. Becker, M. Klein, S. Klein-Hessling, A. Palmetshofer, E. Serfling, V. Heib, et al. (2007). Cyclic adenosine monophosphate is a key component of regulatory T cell-mediated suppression. *The Journal of Experimental Medicine* 204, 1303-1310.

124. Jeker, L.T., X. Zhou, K. Gershberg, D. de Kouchkovsky, M.M. Morar, G. Stadthagen, A.H. Lund, et al. (2012). MicroRNA 10a marks regulatory T cells. *PloS One* 7, e36684.
125. Guo, C., J.F. Sah, L. Beard, J.K. Willson, S.D. Markowitz & K. Guda. (2008). The noncoding RNA, miR-126, suppresses the growth of neoplastic cells by targeting phosphatidylinositol 3-kinase signaling and is frequently lost in colon cancers. *Genes, Chromosomes & Cancer* 47, 939-946.
126. Qin, A., Z. Wen, Y. Zhou, Y. Li, Y. Li, J. Luo, T. Ren, et al. (2013). MicroRNA-126 regulates the induction and function of CD4(+) Foxp3(+) regulatory T cells through PI3K/AKT pathway. *Journal of Cellular and Molecular Medicine* 17, 252-264.
127. Josefowicz, S.Z., C.B. Wilson & A.Y. Rudensky. (2009). Cutting edge: TCR stimulation is sufficient for induction of Foxp3 expression in the absence of DNA methyltransferase 1. *Journal of Immunology (Baltimore, Md.: 1950)* 182, 6648-6652.
128. Zheng, Y., S.Z. Josefowicz, A. Kas, T.T. Chu, M.A. Gavin & A.Y. Rudensky. (2007). Genome-wide analysis of Foxp3 target genes in developing and mature regulatory T cells. *Nature* 445, 936-940.
129. Takahashi, H., T. Kanno, S. Nakayamada, K. Hirahara, G. Sciume, S.A. Muljo, S. Kuchen, et al. (2012). TGF-beta and retinoic acid induce the

microRNA miR-10a, which targets Bcl-6 and constrains the plasticity of helper T cells. *Nature Immunology* 13, 587-595.

130. Chatila, W.M., G.J. Criner, W.W. Hancock, T. Akimova, B. Moldover, J.K. Chang, W. Cornwell, et al. (2014). Blunted expression of miR-199a-5p in regulatory T cells of patients with chronic obstructive pulmonary disease compared to unaffected smokers. *Clinical and Experimental Immunology* 177, 341-352.
131. Kim, S., U.J. Lee, M.N. Kim, E.J. Lee, J.Y. Kim, M.Y. Lee, S. Choung, et al. (2008). MicroRNA miR-199a\* regulates the MET proto-oncogene and the downstream extracellular signal-regulated kinase 2 (ERK2). *The Journal of Biological Chemistry* 283, 18158-18166.
132. Van Pottelberge, G.R., P. Mestdagh, K.R. Bracke, O. Thas, Y.M. van Durme, G.F. Joos, J. Vandesompele, et al. (2011). MicroRNA expression in induced sputum of smokers and patients with chronic obstructive pulmonary disease. *American Journal of Respiratory and Critical Care Medicine* 183, 898-906.
133. Ezzie, M.E., M. Crawford, J.H. Cho, R. Orellana, S. Zhang, R. Gelinas, K. Batte, et al. (2012). Gene expression networks in COPD: microRNA and mRNA regulation. *Thorax* 67, 122-131.
134. Schembri, F., S. Sridhar, C. Perdomo, A.M. Gustafson, X. Zhang, A. Ergun, J. Lu, et al. (2009). MicroRNAs as modulators of smoking-induced gene

expression changes in human airway epithelium. *Proceedings of the National Academy of Sciences of the United States of America* 106, 2319-2324.

135. Sato, T., X. Liu, A. Nelson, M. Nakanishi, N. Kanaji, X. Wang, M. Kim, et al. (2010). Reduced miR-146a increases prostaglandin E(2) in chronic obstructive pulmonary disease fibroblasts. *American Journal of Respiratory and Critical Care Medicine* 182, 1020-1029.
136. Togo, S., O. Holz, X. Liu, H. Sugiura, K. Kamio, X. Wang, S. Kawasaki, et al. (2008). Lung fibroblast repair functions in patients with chronic obstructive pulmonary disease are altered by multiple mechanisms. *American Journal of Respiratory and Critical Care Medicine* 178, 248-260.
137. Mizuno, S., H.J. Bogaard, J. Gomez-Arroyo, A. Alhussaini, D. Kraskauskas, C.D. Cool & N.F. Voelkel. (2012). MicroRNA-199a-5p is associated with hypoxia-inducible factor-1alpha expression in lungs from patients with COPD. *Chest* 142, 663-672.
138. Gonsalves, C.S. & V.K. Kalra. (2010). Hypoxia-mediated expression of 5-lipoxygenase-activating protein involves HIF-1alpha and NF-kappaB and microRNAs 135a and 199a-5p. *Journal of Immunology (Baltimore, Md.: 1950)* 184, 3878-3888.
139. Chang, T.C., E.A. Wentzel, O.A. Kent, K. Ramachandran, M. Mullendore, K.H. Lee, G. Feldmann, et al. (2007). Transactivation of miR-34a by p53

broadly influences gene expression and promotes apoptosis. *Molecular Cell* 26, 745-752.

140. Christenson, S.A., C.A. Brandsma, J.D. Campbell, D.A. Knight, D.V. Pechkovsky, J.C. Hogg, W. Timens, et al. (2013). miR-638 regulates gene expression networks associated with emphysematous lung destruction. *Genome Medicine* 5, 114.
141. Maes, O.C., H. Sarojini & E. Wang. (2009). Stepwise up-regulation of microRNA expression levels from replicating to reversible and irreversible growth arrest states in WI-38 human fibroblasts. *Journal of Cellular Physiology* 221, 109-119.
142. Savarimuthu Francis, S.M., M.R. Davidson, M.E. Tan, C.M. Wright, B.E. Clarke, E.E. Duhig, R.V. Bowman, et al. (2014). MicroRNA-34c is associated with emphysema severity and modulates SERPINE1 expression. *BMC Genomics* 15, 88-2164-15-88.
143. Kelsen, S.G., X. Duan, R. Ji, O. Perez, C. Liu & S. Merali. (2008). Cigarette smoke induces an unfolded protein response in the human lung: a proteomic approach. *American Journal of Respiratory Cell and Molecular Biology* 38, 541-550.
144. Hassan, T., T.P. Carroll, P.G. Buckley, R. Cummins, S.J. O'Neill, N.G. McElvaney & C.M. Greene. (2014). miR-199a-5p silencing regulates the unfolded protein response in chronic obstructive pulmonary disease and

- alpha1-antitrypsin deficiency. *American Journal of Respiratory and Critical Care Medicine* 189, 263-273.
145. Mercado, N., R. Thimmulappa, C.M. Thomas, P.S. Fenwick, K.K. Chana, L.E. Donnelly, S. Biswal, et al. (2011). Decreased histone deacetylase 2 impairs Nrf2 activation by oxidative stress. *Biochemical and Biophysical Research Communications* 406, 292-298.
146. Adenuga, D., H. Yao, T.H. March, J. Seagrave & I. Rahman. (2009). Histone deacetylase 2 is phosphorylated, ubiquitinated, and degraded by cigarette smoke. *American Journal of Respiratory Cell and Molecular Biology* 40, 464-473.
147. Christenson, S.A., C.A. Brandsma, J.D. Campbell, D.A. Knight, D.V. Pechkovsky, J.C. Hogg, W. Timens, et al. (2013). miR-638 regulates gene expression networks associated with emphysematous lung destruction. *Genome Medicine* 5, 114.
148. Stahl, H.F., T. Fauti, N. Ullrich, T. Bopp, J. Kubach, W. Rust, P. Labhart, et al. (2009). miR-155 inhibition sensitizes CD4+ Th cells for TREG mediated suppression. *PloS One* 4, e7158.
149. Executive Summary: Global Strategy for the Diagnosis, Management, and Prevention of COPD. *NHLBI/WHO Workshop Reports (Updated 2005)*. Available at [Www.Goldcopd.Org](http://www.goldcopd.org).

150. miRWalk. The database on predicted and validated microRNA targets.  
<http://www.umm.uni-heidelberg.de/apps/zmf/mirwalk/micronapredictedtarget.html>. 2013, .
151. Sadlon, T.J., B.G. Wilkinson, S. Pederson, C.Y. Brown, S. Bresatz, T. Gargett, E.L. Melville, et al. (2010). Genome-wide identification of human FOXP3 target genes in natural regulatory T cells. *Journal of Immunology* 185, 1071-1081.
152. Chatila, W., M. Aksoy, V. Arguello, R. Ji & S. Kelsen. COPD is not Caused by a Defect in T-regulatory Cell Infiltration into the Lung. *Am J Respir Crit Care Med*(2008). 177, A874.
153. Dang, E.V., J. Barbi, H.Y. Yang, D. Jinasena, H. Yu, Y. Zheng, Z. Bordman, et al. (2011). Control of T(H)17/T(reg) balance by hypoxia-inducible factor 1. *Cell* 146, 772-784.
154. Bandele, O.J. & N. Osheroff. (2008). Epigallocatechin gallate, a major constituent of green tea, poisons human type II topoisomerases. *Chemical Research in Toxicology* 21, 936-943.
155. Barcelo, B., J. Pons, J.M. Ferrer, J. Sauleda, A. Fuster & A.G. Agusti. (2008). Phenotypic characterisation of T-lymphocytes in COPD: abnormal CD4+CD25+ regulatory T-lymphocyte response to tobacco smoking. *The European Respiratory Journal : Official Journal of the European Society for Clinical Respiratory Physiology* 31, 555-562.

156. Eppert, B.L., B.W. Wortham, J.L. Flury & M.T. Borchers. (2013). Functional characterization of T cell populations in a mouse model of chronic obstructive pulmonary disease. *Journal of Immunology (Baltimore, Md.: 1950)* 190, 1331-1340.
157. Quintana, F.J., A.S. Basso, A.H. Iglesias, T. Korn, M.F. Farez, E. Bettelli, M. Caccamo, et al. (2008). Control of T(reg) and T(H)17 cell differentiation by the aryl hydrocarbon receptor. *Nature* 453, 65-71.
158. Sethi, A., N. Kulkarni, S. Sonar & G. Lal. (2013). Role of miRNAs in CD4 T cell plasticity during inflammation and tolerance. *Frontiers in Genetics* 4, 8.
159. Lin, W., D. Haribhai, L. Relland, N. Truong, M. Carlson, C. Williams & T. Chatila. (2007). Regulatory T cell development in the absence of functional Foxp3. *Nature Immunology*.
160. Mucida, D., Y. Park, G. Kim, O. Turovskaya, I. Scott, M. Kronenberg & H. Cheroutre. (2007). Reciprocal TH17 and regulatory T cell differentiation mediated by retinoic acid. *Science (New York, N.Y.)* 317, 256-260.
161. Friedman, R.C., K.K. Farh, C.B. Burge & D.P. Bartel. (2009). Most mammalian mRNAs are conserved targets of microRNAs. *Genome Research* 19, 92-105.

162. Graff, J.W., L.S. Powers, A.M. Dickson, J. Kim, A.C. Reisetter, I.H. Hassan, K. Kremens, et al. (2012). Cigarette smoking decreases global microRNA expression in human alveolar macrophages. *PLoS One* 7, e44066.
163. Gross, T.J., L.S. Powers, R.L. Boudreau, B. Brink, A. Reisetter, K. Goel, A.K. Gerke, et al. (2014). A microRNA processing defect in smokers' macrophages is linked to SUMOylation of the endonuclease DICER. *The Journal of Biological Chemistry* 289, 12823-12834.
164. Gu, S. & W.Y. Chan. (2012). Flexible and Versatile as a Chameleon-Sophisticated Functions of microRNA-199a. *International Journal of Molecular Sciences* 13, 8449-8466.
165. Lagos-Quintana, M., R. Rauhut, J. Meyer, A. Borkhardt & T. Tuschl. (2003). New microRNAs from mouse and human. *RNA (New York, N.Y.)* 9, 175-179.
166. Magrelli, A., G. Azzalin, M. Salvatore, M. Viganotti, F. Tosto, T. Colombo, R. Devito, et al. (2009). Altered microRNA Expression Patterns in Hepatoblastoma Patients. *Translational Oncology* 2, 157-163.
167. Dai, L., L. Gu & W. Di. (2012). MiR-199a attenuates endometrial stromal cell invasiveness through suppression of the IKKbeta/NF-kappaB pathway and reduced interleukin-8 expression. *Molecular Human Reproduction* 18, 136-145.

168. Zhang, Y., K.J. Fan, Q. Sun, A.Z. Chen, W.L. Shen, Z.H. Zhao, X.F. Zheng, et al. (2012). Functional screening for miRNAs targeting Smad4 identified miR-199a as a negative regulator of TGF-beta signalling pathway. *Nucleic Acids Research* 40, 9286-9297.
169. Lu, L., J. Ma, X. Wang, J. Wang, F. Zhang, J. Yu, G. He, et al. (2010). Synergistic effect of TGF-beta superfamily members on the induction of Foxp3+ Treg. *European Journal of Immunology* 40, 142-152.
170. Yoshioka, Y., M. Ono, M. Osaki, I. Konishi & S. Sakaguchi. (2012). Differential effects of inhibition of bone morphogenic protein (BMP) signalling on T-cell activation and differentiation. *European Journal of Immunology* 42, 749-759.
171. Mueller, T.D. & J. Nickel. (2012). Promiscuity and specificity in BMP receptor activation. *FEBS Letters* 586, 1846-1859.
172. Massague, J. (2012). TGFbeta signalling in context. *Nature Reviews.Molecular Cell Biology* 13, 616-630.
173. Kawabata, M., T. Imamura & K. Miyazono. (1998). Signal transduction by bone morphogenetic proteins. *Cytokine & Growth Factor Reviews* 9, 49-61.
174. Verhamme, F.M., K.R. Bracke, G.F. Joos & G.G. Brusselle. (2014). TGF-beta Superfamily in Obstructive Lung Diseases: More Suspects than TGF-beta Alone. *American Journal of Respiratory Cell and Molecular Biology*.

175. Sountoulidis, A., A. Stavropoulos, S. Giaglis, E. Apostolou, R. Monteiro, S.M. Chuva de Sousa Lopes, H. Chen, et al. (2012). Activation of the canonical bone morphogenetic protein (BMP) pathway during lung morphogenesis and adult lung tissue repair. *PloS One* 7, e41460.
176. Monteiro, R.M., S.M. de Sousa Lopes, M. Bialecka, S. de Boer, A. Zwijsen & C.L. Mummery. (2008). Real time monitoring of BMP Smads transcriptional activity during mouse development. *Genesis (New York, N.Y.: 2000)* 46, 335-346.
177. Masterson, J.C., E.L. Molloy, J.L. Gilbert, N. McCormack, A. Adams & S. O'Dea. (2011). Bone morphogenetic protein signalling in airway epithelial cells during regeneration. *Cellular Signalling* 23, 398-406.
178. McCormack, N., E.L. Molloy & S. O'Dea. (2013). Bone morphogenetic proteins enhance an epithelial-mesenchymal transition in normal airway epithelial cells during restitution of a disrupted epithelium. *Respiratory Research* 14, 36-9921-14-36.
179. Kersten, C., G. Dosen, J.H. Myklebust, E.A. Sivertsen, M.E. Hystad, E.B. Smeland & E. Rian. (2006). BMP-6 inhibits human bone marrow B lymphopoiesis--upregulation of Id1 and Id3. *Experimental Hematology* 34, 72-81.
180. Ro, T.B., R.U. Holt, A.T. Brenne, H. Hjorth-Hansen, A. Waage, O. Hjertner, A. Sundan, et al. (2004). Bone morphogenetic protein-5, -6 and -7 inhibit

- growth and induce apoptosis in human myeloma cells. *Oncogene* 23, 3024-3032.
181. Cejalvo, T., R. Sacedon, C. Hernandez-Lopez, B. Diez, C. Gutierrez-Frias, J. Valencia, A.G. Zapata, et al. (2007). Bone morphogenetic protein-2/4 signalling pathway components are expressed in the human thymus and inhibit early T-cell development. *Immunology* 121, 94-104.
182. Hager-Theodorides, A.L., S.V. Outram, D.K. Shah, R. Sacedon, R.E. Shrimpton, A. Vicente, A. Varas, et al. (2002). Bone morphogenetic protein 2/4 signaling regulates early thymocyte differentiation. *Journal of Immunology (Baltimore, Md.: 1950)* 169, 5496-5504.
183. Graf, D., S. Nethisinghe, D.B. Palmer, A.G. Fisher & M. Merckenschlager. (2002). The developmentally regulated expression of Twisted gastrulation reveals a role for bone morphogenetic proteins in the control of T cell development. *The Journal of Experimental Medicine* 196, 163-171.
184. Varas, A., R. Sacedon, L. Hidalgo, V.G. Martinez, J. Valencia, T. Cejalvo, A. Zapata, et al. (2009). Interplay between BMP4 and IL-7 in human intrathymic precursor cells. *Cell Cycle (Georgetown, Tex.)* 8, 4119-4126.
185. Sivertsen, E.A., K. Huse, M.E. Hystad, C. Kersten, E.B. Smeland & J.H. Myklebust. (2007). Inhibitory effects and target genes of bone morphogenetic protein 6 in Jurkat TAg cells. *European Journal of Immunology* 37, 2937-2948.

186. Takai, S., H. Tokuda, R. Matsushima-Nishiwaki, M. Saio, T. Takami & O. Kozawa. (2010). TGF-beta superfamily enhances the antigen-induced IFN-gamma production by effector/memory CD8+ T cells. *International Journal of Molecular Medicine* 25, 105-111.
187. Hong, J.H., G.T. Lee, J.H. Lee, S.J. Kwon, S.H. Park, S.J. Kim & I.Y. Kim. (2009). Effect of bone morphogenetic protein-6 on macrophages. *Immunology* 128, e442-50.
188. Kwon, S.J., G.T. Lee, J.H. Lee, W.J. Kim & I.Y. Kim. (2009). Bone morphogenetic protein-6 induces the expression of inducible nitric oxide synthase in macrophages. *Immunology* 128, e758-65.
189. Cunningham, N.S., V. Paralkar & A.H. Reddi. (1992). Osteogenin and recombinant bone morphogenetic protein 2B are chemotactic for human monocytes and stimulate transforming growth factor beta 1 mRNA expression. *Proceedings of the National Academy of Sciences of the United States of America* 89, 11740-11744.
190. Perron, J.C. & J. Dodd. (2009). ActRIIA and BMPRII Type II BMP receptor subunits selectively required for Smad4-independent BMP7-evoked chemotaxis. *PloS One* 4, e8198.
191. Pluchino, S., L. Zanotti, E. Brambilla, P. Rovere-Querini, A. Capobianco, C. Alfaro-Cervello, G. Salani, et al. (2009). Immune regulatory neural

- stem/precursor cells protect from central nervous system autoimmunity by restraining dendritic cell function. *PloS One* 4, e5959.
192. Martinez, V.G., C. Hernandez-Lopez, J. Valencia, L. Hidalgo, A. Entrena, A.G. Zapata, A. Vicente, et al. (2011). The canonical BMP signaling pathway is involved in human monocyte-derived dendritic cell maturation. *Immunology and Cell Biology* 89, 610-618.
193. He, J., Q. Xu, Y. Jing, F. Agani, X. Qian, R. Carpenter, Q. Li, et al. (2012). Reactive oxygen species regulate ERBB2 and ERBB3 expression via miR-199a/125b and DNA methylation. *EMBO Reports* 13, 1116-1122.
194. Sakurai, K., C. Furukawa, T. Haraguchi, K. Inada, K. Shioyama, T. Tagawa, S. Fujita, et al. (2011). MicroRNAs miR-199a-5p and -3p target the Brm subunit of SWI/SNF to generate a double-negative feedback loop in a variety of human cancers. *Cancer Research* 71, 1680-1689.
195. Chen, Z.H., H.P. Kim, F.C. Sciruba, S.J. Lee, C. Feghali-Bostwick, D.B. Stolz, R. Dhir, et al. (2008). Egr-1 regulates autophagy in cigarette smoke-induced chronic obstructive pulmonary disease. *PloS One* 3, e3316.
196. Rahman, M.K., C.P. Offord, S. Khanna, G.C. Ford, X.M. Perrson, P.A. Svingen, Y. Xiong, et al. (2013). Regulatory T cell kinetics in the peripheral blood of patients with Crohn's disease. *Human Immunology* 74, 145-150.

197. Akbas, F., E. Coskunpinar, E. Aynaci, Y.M. Oltulu & P. Yildiz. (2012). Analysis of serum micro-RNAs as potential biomarker in chronic obstructive pulmonary disease. *Experimental Lung Research* 38, 286-294.
198. Lewis, A., J. Riddoch-Contreras, S.A. Natanek, A. Donaldson, W.D. Man, J. Moxham, N.S. Hopkinson, et al. (2012). Downregulation of the serum response factor/miR-1 axis in the quadriceps of patients with COPD. *Thorax* 67, 26-34.
199. Donaldson, A., S.A. Natanek, A. Lewis, W.D. Man, N.S. Hopkinson, M.I. Polkey & P.R. Kemp. (2013). Increased skeletal muscle-specific microRNA in the blood of patients with COPD. *Thorax* 68, 1140-1149.
200. Soeda, S., J.H. Ohyashiki, K. Ohtsuki, T. Umezu, Y. Setoguchi & K. Ohyashiki. (2013). Clinical relevance of plasma miR-106b levels in patients with chronic obstructive pulmonary disease. *International Journal of Molecular Medicine* 31, 533-539.
201. Molina-Pinelo, S., M.D. Pastor, R. Suarez, B. Romero-Romero, M. Gonzalez De la Pena, A. Salinas, R. Garcia-Carbonero, et al. (2014). MicroRNA clusters: dysregulation in lung adenocarcinoma and COPD. *The European Respiratory Journal* 43, 1740-1749.

## APPENDIX

Hello Dr. Chatila,

Thank you for your interest in the American Thoracic Society journals. Your request is granted for no charge. Please be sure to include the below wording. Thank you.

Reprinted with permission of the American Thoracic Society. Copyright © 2015 American Thoracic Society.

Cite: Author(s)/Year/Title/Journal title/Volume/Pages.

*The American Journal of Respiratory and Critical Care Medicine* is an official journal of the American Thoracic Society.

Best,

**LanVay**

Journal Program Coordinator

American Thoracic Society

25 Broadway, 18th Floor

New York, NY 10004-1012

<http://www.atsjournals.org>

[lvay@thoracic.org](mailto:lvay@thoracic.org)

Phone: 212-315-6440

## NATURE PUBLISHING GROUP LICENSE TERMS AND CONDITIONS

Mar 03, 2015

---

---

This is a License Agreement between Wissam Chatila ("You") and Nature Publishing Group ("Nature Publishing Group") provided by Copyright Clearance Center ("CCC"). The license consists of your order details, the terms and conditions provided by Nature Publishing Group, and the payment terms and conditions.

**All payments must be made in full to CCC. For payment instructions, please see information listed at the bottom of this form.**

License Number	3581440604428
License date	Mar 03, 2015
Licensed content publisher	Nature Publishing Group
Licensed content publication	Nature Reviews Immunology
Licensed content title	Homeostatic control of regulatory T cell diversity
Licensed content author	Adrian Liston, Daniel H. D. Gray
Licensed content date	Jan 31, 2014
Volume number	14
Issue number	3
Type of Use	reuse in a dissertation / thesis
Requestor type	academic/educational
Format	print and electronic
Portion	figures/tables/illustrations
Number of figures/tables/illustrations	1
High-res required	no
Figures	Figure 1
Author of this NPG article	no
Your reference number	None
Title of your thesis / dissertation	microRNA expression in regulatory T cells in chronic obstructive pulmonary disease
Expected completion date	Mar 2015
Estimated size (number of pages)	170

Total 0.00 USD

Terms and Conditions

### Terms and Conditions for Permissions

Nature Publishing Group hereby grants you a non-exclusive license to reproduce this material for this purpose, and for no other use, subject to the conditions below:

1. NPG warrants that it has, to the best of its knowledge, the rights to license reuse of this material. However, you should ensure that the material you are requesting is original to Nature Publishing Group and does not carry the copyright of another entity (as credited in the published version). If the credit line on any part of the material you have requested indicates that it was reprinted or adapted by NPG with permission from another source, then you should also seek permission from that source to reuse the material.
2. Permission granted free of charge for material in print is also usually granted for any electronic version of that work, provided that the material is incidental to the work as a whole and that the electronic version is essentially equivalent to, or substitutes for, the print version. Where print permission has been granted for a fee, separate permission must be obtained for any additional, electronic re-use (unless, as in the case of a full paper, this has already been accounted for during your initial request in the calculation of a print run). NB: In all cases, web-based use of full-text articles must be authorized separately through the 'Use on a Web Site' option when requesting permission.
3. Permission granted for a first edition does not apply to second and subsequent editions and for editions in other languages (except for signatories to the STM Permissions Guidelines, or where the first edition permission was granted for free).
4. Nature Publishing Group's permission must be acknowledged next to the figure, table or abstract in print. In electronic form, this acknowledgement must be visible at the same time as the figure/table/abstract, and must be hyperlinked to the journal's homepage.
5. The credit line should read:  
Reprinted by permission from Macmillan Publishers Ltd: [JOURNAL NAME] (reference citation), copyright (year of publication)  
For AOP papers, the credit line should read:  
Reprinted by permission from Macmillan Publishers Ltd: [JOURNAL NAME], advance online publication, day month year (doi: 10.1038/sj.[JOURNAL ACRONYM].XXXXX)

**Note: For republication from the *British Journal of Cancer*, the following credit lines apply.**

Reprinted by permission from Macmillan Publishers Ltd on behalf of Cancer Research UK: [JOURNAL NAME] (reference citation), copyright (year of publication) For AOP papers, the credit line should read:  
Reprinted by permission from Macmillan Publishers Ltd on behalf of Cancer Research UK: [JOURNAL NAME], advance online publication, day month year (doi: 10.1038/sj.[JOURNAL ACRONYM].XXXXX)

6. Adaptations of single figures do not require NPG approval. However, the adaptation should be credited as follows:

Adapted by permission from Macmillan Publishers Ltd: [JOURNAL NAME] (reference citation), copyright (year of publication)

**Note: For adaptation from the *British Journal of Cancer*, the following credit line applies.**

Adapted by permission from Macmillan Publishers Ltd on behalf of Cancer Research UK: [JOURNAL NAME] (reference citation), copyright (year of publication)

7. Translations of 401 words up to a whole article require NPG approval. Please visit <http://www.macmillanmedicalcommunications.com> for more information. Translations of up to a 400 words do not require NPG approval. The translation should be credited as follows:

Translated by permission from Macmillan Publishers Ltd: [JOURNAL NAME] (reference citation), copyright (year of publication).

**Note: For translation from the *British Journal of Cancer*, the following credit line applies.**

Translated by permission from Macmillan Publishers Ltd on behalf of Cancer Research UK: [JOURNAL NAME] (reference citation), copyright (year of publication)

We are certain that all parties will benefit from this agreement and wish you the best in the use of this material. Thank you.

Special Terms:

v1.1

Questions? [customercare@copyright.com](mailto:customercare@copyright.com) or +1-855-239-3415 (toll free in the US) or +1-978-646-2777.

Gratis licenses (referencing \$0 in the Total field) are free. Please retain this printable license for your reference. No payment is required.

## 1. Frontiers Terms and Conditions

### Post - Publication

Under the Frontiers Terms and Conditions, authors retain the copyright to their work. All Frontiers articles are Open Access and distributed under the terms of the **Creative Commons Attribution License**, (CC-BY 4.0), which permits the use, distribution and reproduction of material from published articles, provided the original authors and source are credited, and subject to any copyright notices concerning any third-party content.

<https://frontiers.zendesk.com/hc/en-us/articles/202026301-What-is-the-Frontiers-Copyright-Policy->

(March 3, 2015)

(197-198-199-200-201)